

HYDROLOGY OF THE UPPER-GARONNE BASIN (VALLE DE ARÁN, SPAIN)

BY

H. RIJCKBORST

ABSTRACT

The runoff in the Valle de Arán, which is a steep and high mountain basin in the Pyrenees, consists essentially of baseflow, and fast runoff is only a minor phenomenon.

The baseflow is related to areas of scree and forest, and the percentage of the precipitation which contributes to the fast runoff, is related to the area of barren rocks.

The orographic precipitation pattern has been statistically determined for eight valleys. It was found, that orographic precipitation increases linearly with altitude, while the maximum increase occurs perpendicular to the slopes of the steep mountain ranges. The expected errors, due to measurements of rainfall at 1.50 m above ground level, showed as a 10—15 percent error in the water balance. The Penman evaporation values were corrected for snow evaporation and they subsequently gave reliable results.

CONTENTS

Illustrations 2; Tables 3; Tables 1—45 Appendices 4; List of symbols 4; Abbreviations.	5	5.4 Wind	23
1. Introduction	7	5.5 Cloud cover	24
1.1 The project.	7	5.6 Relative air humidity	25
1.2 Acknowledgments	7	6. Precipitation analysis	25
1.3 Location	7	6.1 Introduction	25
1.4 History of the Valle de Arán	7	6.2 Precipitation regime	25
1.5 Stream system	9	6.3 Variations in the annual precipitation 1946—1966.	26
2. Morphometry	9	6.4 Relation of precipitation, wind direction and cloud cover	28
2.1 Morphometric data	9	6.5 The precipitation map	28
2.2 Influence of basin morphology on hypsometric curves	11	6.6 Height of the rain gauge orifice	29
2.3 Specific degradation	12	6.7 Regression analysis	30
2.4 Hypsometric integral.	12	6.8 Major topographic features, which affect precipitation	31
2.5 Erosion models	13	6.9 Precipitation on steep valley slopes	31
2.6 Origin of the Garonne River	13	6.10 Snowfall	33
2.7 The Miocene planation level	14	6.11 Snow duration	33
2.8 Quaternary developments of the Valle de Arán	17	6.12 Water content of fresh snow.	35
2.9 Slopes	17	7. Runoff	35
3. Available meteorological data	18	7.1 Introduction	35
3.1 Introduction	18	7.2 Available data	35
3.2 Precipitation and snowfall	18	7.3 Stage-discharge relations	36
3.3 Temperature, wind direction, wind velocity and cloud cover	19	7.4 Land classification map and morphological analysis	37
3.4 Air pressure and air humidity	19	7.5 Introduction to runoff characteristics	39
3.5 Unused records	19	7.6 J-values of the Pontet de Rius basin	41
4. Climatology of the Valle de Arán	21	7.7 Relation of runoff, land classification and morphology in Pontet de Rius.	42
4.1 Introduction	21	7.8 J-values of the Aigüestortes basin	43
4.2 Classification of the climates	21	7.9 J-values of the Upper Negro basin	43
4.3 The effect of the Pyrenees on the Valle de Arán climate	21	7.10 Monthly runoff variation coefficients of eight representative drainage basins	45
5. Climatic elements	21	7.11 Relation of variation coefficients, morphology and land classification in eight drainage basins	45
5.1 Air pressure	21	7.12 Flood frequency	45
5.2 Temperature	22	7.13 Flood routing through fourteen reservoirs in the Upper Aiguamoix	48
5.3 Vertical temperature gradients	22		

8. Evaporation	49	10.6 Groundwater flow through the ungrouted Aiguamoix dam foundations	61
8.1 Introduction	49	11. Karst systems	61
8.2 Evaporation estimations from meteorological data	49	11.1 Introduction	61
8.3 Evaporation estimations from the snow cover	50	11.2 Geology	62
8.4 Mountain shadow and orientation of the valleys	50	11.3 The Güells del Jueu system	62
8.5 Short wave radiation measurements	51	11.4 The Estua system	63
8.6 Actual evaporation estimations	53	11.5 The Ruda system	63
9. Glaciers of the Aneto group	54	11.6 The Bó system	64
9.1 Introduction	54	11.7 The Pila system	64
9.2 Precipitation on the glaciers	54	11.8 Tracer experiments	64
9.3 Monthly increase of the 0° C-isotherms	55	11.9 Chemical analyses	65
9.4 Snow depth and snow density	55	11.10 Runoff analysis	66
9.5 Evaporation from the glaciers	56	11.11 Infiltration into limestones	67
9.6 Long term variations of the glaciers	56	12. Water balance	67
10. The Aiguamoix dam	57	12.1 Water balance of two selected basins	67
10.1 Introduction	57	12.2 Water balance of eight basins	67
10.2 Topography and geology	58	12.3 Water balance of the Valle de Arán	68
10.3 Development of the project	58	12.4 Runoff of the Valle de Arán	69
10.4 Watertight screen and drainage of the foundations	58	Conclusions	70
10.5 Water permeability tests	60	References	71

ILLUSTRATIONS

1.1 Location of the Valle de Arán.	3.3 Mougín rain gauges.
1.2 The medieaval church of Bossost.	5.1 Mean monthly air pressure (mb) of Arties and Viella, compared with the Naca standard atmosphere.
1.3 Tombstone of an Aranese nobleman (church of Las Bordas) 12th century.	5.2 Monthly temperature of the valley station Viella and the mountain station Bonaigua.
1.4 Stream system of the Garonne River.	5.3 Annual fluctuation of temperature gradients during the period 1955—1965.
1.5 The karst spring Güell del Garona where the Garonne River originates.	5.4 Wind roses from meteorological stations during the period 1955—1965.
2.1 Hypsometric histograms of thirty-three basins.	5.5 Morning valley slope wind in the Valarties valley.
2.2 Hypsometric histogram and slope-altitude distribution of the Valle de Arán.	6.1 Monthly precipitation coefficients for the valley stations and mountain stations.
2.3 Hypsometric histogram and slope-altitude distribution of the Jueu- and Aiguamoix-River.	6.2 Maximum daily rain precipitation and rain duration for Viella and Restanca (1955—1965).
2.4 Maps of three simplified valley cross sections.	6.3 Precipitation map of the Valle de Arán (1946—1966).
2.5 Hypsometric histograms of three simplified valley cross sections for a rectangular-, elliptic- and circular-drainage basin.	6.4 Double mass curve of the Bonaigua precipitation measured in a mougín gauge (y) and in a daily rain gauge (x).
2.6 Hypsometric integral of the Valle de Arán, showing the volume of eroded material per 100 m altitude.	6.5 Accumulated precipitation values of Bonaigua, showing the 44 percent error in the measurements 4.40 m above ground level.
2.7 Results of the model analysis of the Valle de Arán.	6.6 Relation of the average annual precipitation (mm) and altitude (m) during the period 1946—1966.
2.8 Structure-contour map of the top Devonian in the Valle de Arán.	6.7 Relation of the average annual snowfall (cm) and altitude (m) during the period 1946—1966.
2.9 Morphometric analysis of the Iñola basin, showing the dip of the Miocene planation level in the direction of the present river.	6.8 Snowfall map of the Valle de Arán during the period 1946—1966.
2.10 Glaciation of a Tertiary planation level.	6.9 Snow to total precipitation ratio map of the Valle de Arán during the period 1946—1966.
2.11 Cross section of the Toran valley at the Lower Toran damsite.	7.1 Distribution of runoff gauging stations and catchment areas, showing the effect of karst systems.
2.12 Cross section of the Toran valley at the Upper Toran damsite.	7.2 Bar graph, showing runoff records during the period 1946—1966.
2.13 Distribution of the weighted average slope per 100 m altitude in ten drainage basins.	7.3 Stage-discharge curves for runoff gauging station 13 (Negro River) and 16 (Barrados River).
2.14 Frequency of weighted average slopes.	7.4 Area-altitude distribution and hypsometric integral of the Pontet de Rius- and Aigüestortes basins.
2.15 Length profiles of the Valle de Arán rivers and increase of drainage area in a downstream direction of the Garonne River.	
3.1 Location of meteorological stations.	
3.2 Bar graph, showing precipitation records from 1946—1966.	

- 7.5 Weir at station 20 and 3 and its stage-discharge rate relation.
- 7.6 Areas of land classification units in thirty-three drainage basins.
- 7.7 Runoff analysis of the Pontet de Rius basin.
- 7.8 Relation of baseflow and percentage of the precipitation, contributing to the fast runoff of the Pontet de Rius basin.
- 7.9 Length profile of the Valarties River upstream from station 20.
- 7.10 Average monthly runoff variation coefficients for eight basins.
- 7.11 Relation of maximum runoff variation coefficients to land classification units.
- 7.12 Flood frequency at four stations in the Valle de Arán.
- 7.13 Relation of magnitude of floods and drainage basin.
- 7.14 Reservoirs of the Upper Aiguamoix area.
- 7.15 Relation of the inflow and storage in the Upper Aiguamoix area.
- 7.16 Flood routing through the Aiguamoix west branch.
- 8.1 Average monthly temperatures during the period 1955—1965.
- 8.2 Average monthly wind velocity during the period 1955—1965.
- 8.3 Average monthly Penman-evaporation values and combined Penman-Dalton evaporation values.
- 8.4 Monthly decrease in outer atmosphere shortwave radiation ($oaHsh$) on a valley bottom and error in the monthly Penman evaporation values due to mountain shadow (1965).
- 8.5 Shadowed areas in the Valle de Arán during the winter solstice at 12.00 h.
- 8.6 Relation of the percentage shadowed area during the winter solstice and the average weighted slope of 31 basins.
- 8.7 Comparison of calculated and measured shortwave radiation (Hsh).
- 8.8 Average height of the monthly 0°C-isotherm during the period 1955—1965.
- 9.1 Position of the glaciers of the Aneto group during the summer of 1958.
- 9.2 Average monthly rainfall and snowfall in the Aneto area.
- 9.3 Position of the 0°C-isotherm in the Aneto area during the summer months.
- 9.4 Snow cover in the Lago Mar area (elev. 2200—3000 m) in June 1965.
- 9.5 Estimation of the average annual snow accumulation on the Aneto glacier.
- 9.6 Areal extent of the Aneto glaciers in various periods (1810, 1928, 1948 and 1958).
- 9.7 Long term precipitation measurements (1922—1965) from Lés.
- 10.1 Topographical map of the Aiguamoix dam.
- 10.2 Fluvio-glacial material in the left Aiguamoix bank at the dam axis (elev. 1400 m).
- 10.3 Fluvio-glacial material in the left Aiguamoix bank, 700 m south from the dam.
- 10.4 Geological profile of the left Aiguamoix bank at the damsite.
- 10.5 Hydrogeological section along the Aiguamoix dam axis.
- 11.1 Structures of the Devonian limestones related to the Güells del Jueu system.
- 11.2 Outcrops of karstified limestones, catchment areas of karst systems and surficial water divides in the Valle de Arán.
- 11.3 Two geological profiles of the Pila-karst system.
- 11.4 Discharge measurement of the Pila-karst spring.
- 11.5 Map, showing the situation of the Güells del Jueu karst spring.
- 11.6 Relation of the fast runoff and baseflow of the Güells del Jueu karst system.
- 11.7 Runoff analysis of three hydrographs of the Güells del Jueu karst system.
- 12.1 Graphical correlation of the runoff of the Pontet de Rius- and Aigüestortes-basin.
- 12.2 The "roche moutonnée" landscape in the Pontet de Rius basin.
- 12.3 Hypsometric integrals for eight basins.
- 12.4 Runoff of the entire Valle de Arán during the calendar year 1956.

TABLES

- 2.1 Specific degradation values of twelve rivers (mm/1000 year).
- 2.2 Volume (km^3) of rock, discharged out of the Valle de Arán during successive erosion phases.
- 5.1 Monthly average air pressures (mb) in Arties (elev. 1138 m) and Viella (elev. 935 m).
- 5.2 Monthly average daily fluctuation in air pressure (mb) for Arties (elev. 1138 m) from 1959—1965.
- 5.3 Monthly average wind velocity ($m.s^{-1}$) in Restanca during the period 1957—1965.
- 5.4 Non ventilated relative air humidity values (percent) of Arties (08.00 h and 18.00 h) and Viella (08.00 h).
- 6.1 Seasonal precipitation coefficients for five stations (1946—1966).
- 6.2 Fluctuations in the annual precipitation for five stations.
- 6.3 Frequency and humidity of winds (percentage).
- 6.4 Frequency of cloud cover (percentage) during different winds.
- 6.5 Regression analysis of monthly precipitation values.
- 6.6 Average annual precipitation values (mm) during the period 1946—1966.
- 6.7 Increase of the precipitation from the valley station Arties to six mountain stations in $mm.100 m^{-1}.year^{-1}$.
- 6.8 Average annual snowfall (cm) for eleven stations during the period 1946—1966.
- 6.9 Water content of fresh snow (percentage), measured at three stations during the period 1956—1966.
- 7.1 New drainage areas (km^2) after the construction of hydropower systems.
- 7.2 Areas (km^2) of units of the land classification map for thirty-three drainage basins.
- 7.3 Distribution of land classification units in the Pontet de Rius basin.
- 7.4 Distribution of land classification units in ten drainage basins of the Valle de Arán.
- 7.5 Characteristics of fourteen lakes in the Upper Aiguamoix area.
- 8.1 Penman monthly evaporation values (mm) during the period 1955—1965.
- 8.2 Comparison of Penman-, Penman-Dalton-, Thornthwaite-, and Turc-annual evaporation values (mm) during the period 1955—1965.

- 8.3 Short wave radiation measurements in Restanca and Viella during 1965 with Gun Bellani pyranometers (in cal. cm⁻².day⁻¹).
- 8.4 Average monthly percentage of the Valle de Arán covered with snow during the period 1955—1965.
- 8.5 Dalton monthly evaporation values (mm) from a snow cover at Restanca and Bonaigua.
- 8.6 α -values, estimated for the Valle de Arán.
- 9.1 Average monthly snowfall (cm) on the glaciers of the Aneto group during the period 1955—1965.
- 9.2 Estimated vertical monthly temperature gradients (°C/100 m) and average monthly temperatures (°C) at an elevation of 3000 m.
- 9.3 Average monthly evaporation and sublimation values (mm) for the Aneto area.
- 11.1 Sinkholes in the karst systems.
- 11.2 Results of color tracer experiments in the karst systems.
- 11.3 Chemical analyses of the Cambro-Ordovician- and Devonian limestones.
- 12.1 Water balance of the Pontet de Rius- and Aigüestortes-basin (1959—1963).
- 12.2 Ten year water balance of eight basins (1946—1956).
- 12.3 Water balance of the Valle de Arán of 1956, 1957, 1962 and 1963.

APPENDICES TABLES 1—45

- 1. Monthly precipitation (mm) at Cledes (st. 1)
- 2. Monthly precipitation (mm) at Viella (st. 2)
- 3. Monthly precipitation (mm) at Arties (st. 3)
- 4. Monthly precipitation (mm) at Puerto de Bonaigua (st. 4)
- 5. Monthly precipitation (mm) at Benos (st. 5)
- 6. Monthly precipitation (mm) at Camara Barrados (st. 6)
- 7. Monthly precipitation (mm) at Tunnel Viella North (st. 7)
- 8. Monthly precipitation (mm) at Restanca (st. 8)
- 9. Monthly precipitation (mm) at Camara Arties (st. 9)
- 10. Monthly precipitation (mm) at Moncasau (st. 10)
- 11. Monthly snowfall (cm) at Cledes (st. 1)
- 12. Monthly snowfall (cm) at Viella (st. 2)
- 13. Monthly snowfall (cm) at Arties (st. 3)
- 14. Monthly snowfall (cm) at Puerto de Bonaigua (st. 4)
- 15. Monthly snowfall (cm) at Benos (st. 5)
- 16. Monthly snowfall (cm) at Camara Barrados (st. 6)
- 17. Monthly snowfall (cm) at Tunnel Viella North (st. 7)
- 18. Monthly snowfall (cm) at Restanca (st. 8)
- 19. Monthly snowfall (cm) at Camara Arties (st. 9)
- 20. Monthly snowfall (cm) at Moncasau (st. 10)
- 21. Monthly snowfall (cm) at Bossost (st. 11)
- 22. Average monthly temperatures in °C (1955—1965)
- 23. Average monthly maximum temperatures in °C (1955—1965)
- 24. Average monthly minimum temperature in °C (1955—1965)
- 25. Average monthly temperature amplitudes in °C (1955—1965)
- 26. Average monthly temperature gradients in °C/100 m (1955—1965)
- 27. Average monthly number of frost days, with minimum temperatures below 0° C (1955—1965)
- 28. Average monthly number of ice days, with maximum temperatures below 0° C (1955—1965)
- 29. Average monthly number of precipitation days (1955—1965)
- 30. Average monthly number of snow days (1955—1965)
- 31. Average monthly cloud cover in percentage (1955—1965)
- 32. Average monthly number of cloudless days (0—1/10) 1955—1965
- 33. Average monthly number of clouded days (9/10—10/10) 1955—1965
- 34. Average monthly number of clouded days (1/10—9/10) 1955—1965
- 35. Average monthly number of days with northern winds (1955—1965)
- 36. Average monthly number of days with eastern winds (1955—1965)
- 37. Average monthly number of days with southern winds (1955—1965)
- 38. Average monthly number of days with western winds (1955—1965)
- 39. Average monthly number of days with unknown wind direction (1955—1965)
- 40. Average monthly wind velocity m/sec (1955—1965)
- 41. Average monthly runoff (mm) of the Iñola river (st. 6)
- 42. Average monthly runoff (mm) of the Barrados river (st. 16)
- 43. Average monthly runoff (mm) of the Negro river (st. 13)
- 44. Average monthly runoff (mm) of the Garona de Ruda river (st. 2)

LIST OF SYMBOLS

		Dimensions			
A	area	m ²	E _o	evaporation from a wet plant cover	mm.day ⁻¹
A _i	cross section of horizontal layer	m ²	E _q	evaporation characteristic in Penman's formula	mm.day ⁻¹
b	duration of rainfall	day	h	water stage height	m
B ₁₁	average horizontal distance from the reservoir to bedrock	m	h _o	original snow depth	cm
B ₁₂	average horizontal distance from the downstream exposure of the horizontal layer to bedrock	m	H _{ra} ^{ne}	net radiation	J.m ²
D _i	average thickness of the horizontal layer	m	H _{sh}	short wave radiation	J.m ²
E	evaporation from a free water surface	mm.day ⁻¹	oaH _{sh}	outer atmosphere short wave radiation	J.m ²
E _{ac}	actual evaporation	mm.day ⁻¹	h _t	snow depth after the elapse of t days	cm
			j	storage coefficient	day
			k _i	permeability coefficient	m.day ⁻¹

List of symbols

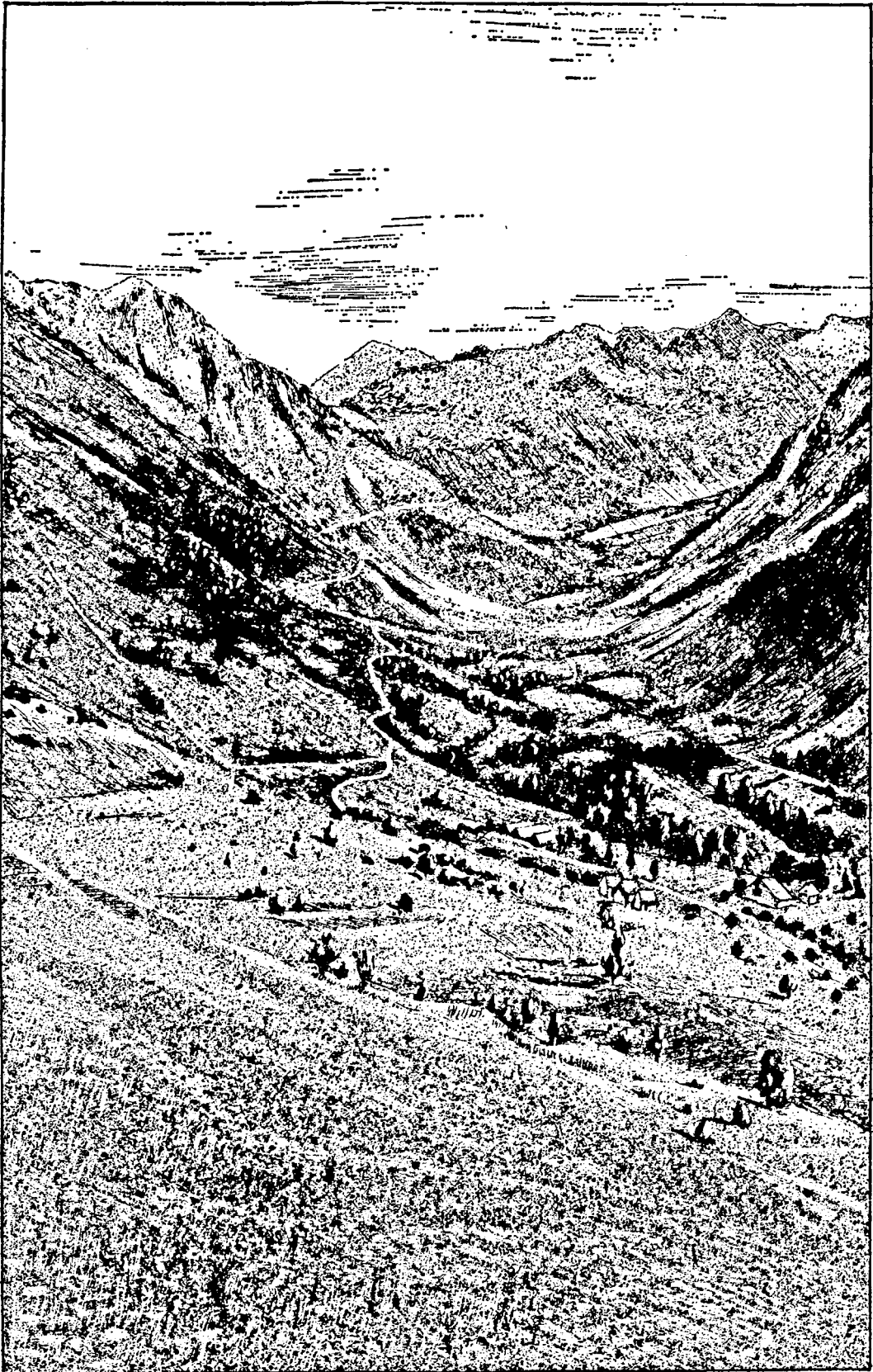
L	latent heat of vaporization	J·kg ⁻¹ ·°C ⁻¹		u ₂	wind velocity at 2 meter above ground level	
L _i	length of horizontal layer	m		z	length	m·s ⁻¹
p	slope of the stage-discharge curve	—		Z _i	vertical distance of the centre of gravity of the horizontal layer to the impermeable bedrock	m
P	rainfall intensity	mm·day ⁻¹		α	actual evaporation coefficient	—
p _z ^{wa}	vapour pressure of water at height z	mb		γ	psychrometer constant	mb·°C ⁻¹
p _z ^{wa}] _{sa}	maximum vapour pressure of water at height z	mb		Δ	slope of the temperature-vapour pressure curve at air temperature at 2 m height	mb·°C ⁻¹
q	runoff	m ³ ·day ⁻¹		Φ ₀	hydraulic head	m
Q	runoff	m ³ ·s ⁻¹		ρ	density of water	kg·m ⁻³
Q ₂₋₃₃	mean annual flood	m ³ ·s ⁻¹				
Q _t	groundwater flow	m ³ ·day ⁻¹				
t	time	s or day				

ABBREVIATIONS

Cbf, Dcf, EF: Köppen classification of climates

G.L.: ground level

MSL.: mean sea level



1. INTRODUCTION

1.1 *The project*

This study of the hydrogeology of the Valle de Arán in the High Pyrenees of Spain is a continuation of the geological work, which has been carried out under the guidance of Dr. L. U. de Sitter, professor in structural and applied geology at Leiden University. This geological survey was started in 1952 and completed in 1960 by Kleinsmiede.

The hydrogeological project of the Valle de Arán started in July 1964 and the results of the work have been compiled in this comprehensive report. It is an appraisal of the hydrology of a drainage basin, covering an area of 572 square kilometers. The basic data, hydrological techniques and results are discussed. Part of this work has been carried out by students as master in science thesis projects.

1.2 *Acknowledgments*

The assistance of the students A. J. Brugman, B. van Hoorn, H. D. F. Leniger and D. A. Zeilmaker have been very beneficial for this study.

The numerous inspiring discussions with prof. Dr. L. U. de Sitter during my study at Leiden University, are gratefully acknowledged. The assistance of Dr. C. Voûte is also much appreciated.

The active cooperation of the research department of the "Koninklijke Nederlandsche Heidemaatschappij" is most sincerely appreciated. Especially the scientific guidance of Dr. L. Wartena and Mr. A. D. Kusse has been of great value.

Sincere appreciation is extended to Mr. A. A. Ruitenberg (M.Sc.) for his assistance in the preparation of the English text of this thesis.

The management of the Fuerzas Electricas de Cataluña gave readily permission for the use of their archives. M. A. Würth (P.Eng.) director of the constructora Pirinaica S.A., has materially supported and encouraged this study. Messrs Gomez Rivera, Pena Deo, Colon, Vidal, Sanmartí, Vila and Torrijos gave valuable information about the hydrology of the Valle de Arán.

Miss C. P. J. Roest displayed great skill in the drawing of the enclosed land classification map and Mr. F. J. Fritz expressed fine artistic ability in the preparation of the plates. Miss T. W. Terpstra typed the manuscript.

Financial assistance towards the expenses of the field work was received from the "Molengraaff-Fonds" and the "Ministerie van Onderwijs en Wetenschappen".

1.3 *Location*

The Valle de Arán (= valley of Arán) is a small drainage area in the central and highest part of the Pyrenees. It has a range in altitude of 3000 meters. The valley is located at the French side of the mountain chain and its southern limit coincides with the main water divide. Except for the Valle de Arán, the east-west drainage divide constitutes the frontier

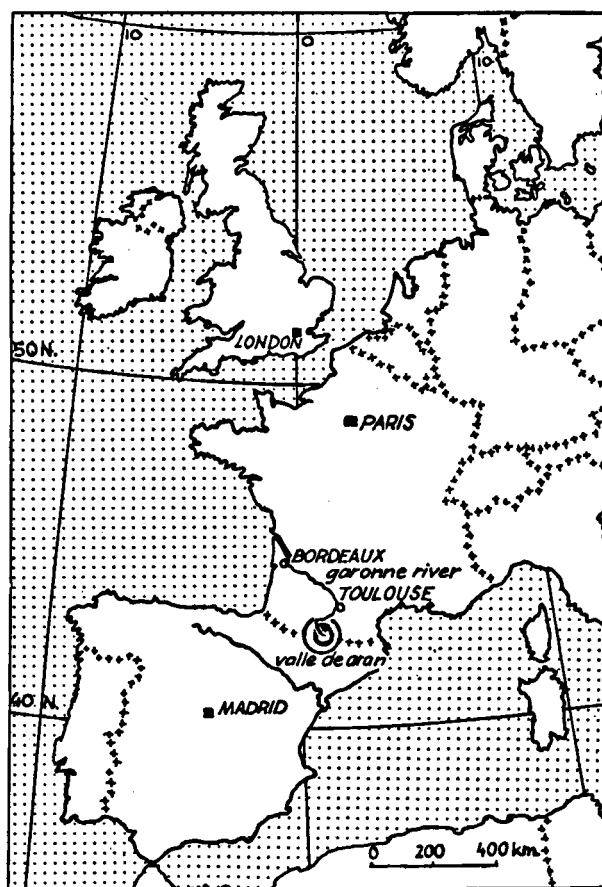


Fig. 1.1 Location of the Valle de Arán.

between France and Spain (fig. 1.1). The valley is situated at latitude 42° N and departure 1° east of Greenwich, corresponding to a distance of 180 km from the Mediterranean Sea and 150 km from the Atlantic Ocean. The Garonne, which is one of the important French Atlantic rivers, has its headwaters in the Valle de Arán. Since the valley is the only Spanish territory (since 1659) at the French side of the Pyrenean water divide, this beautiful rich and strategic area has been the object of numerous wars. Three percent of the Spanish electric power production is generated in this valley (1964).

1.4 *History of the Valle de Arán*

The north Pyrenean valleys were populated in the Upper Paleolithicum (Pericot, 1934). Descendants of these people continued to live there during the Neolithicum (Campistol, 1960).

In the Roman era, the valley was a part of the Civitas Convenarum (Lizop, 1931) and a Roman road, which connected Toulouse (south France) with Portugal, led through the Valle de Arán. We still can find Roman inscriptions in churches of some villages and until recently also in the two balnearios, which were built

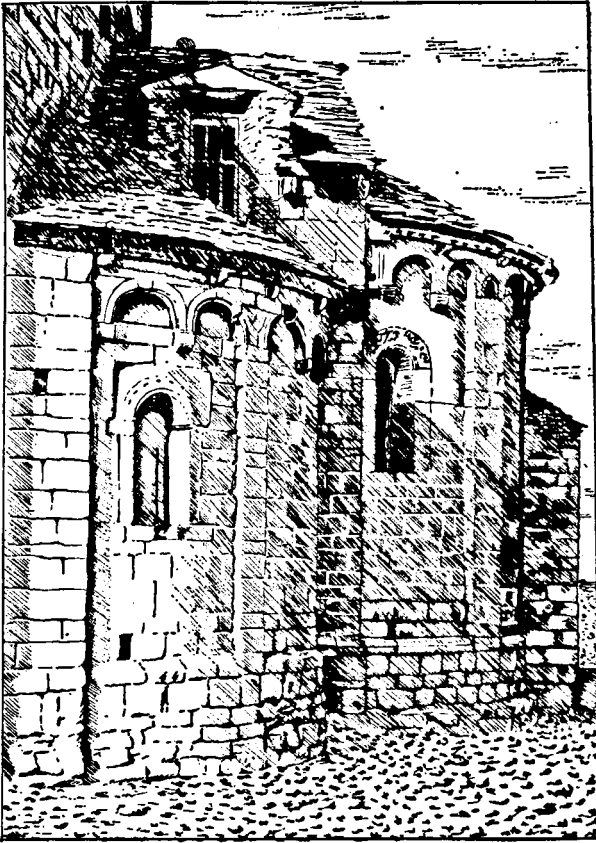


Fig. 1.2 The medieaval church of Bossost.

by the Romans around thermal springs. At about 410 A.C. the Roman empire disappeared and people of the Valle de Arán returned to their isolated existence. In the tenth century the valley formed part of the duchy of French Commingues. In 1036 it turned to the Kingdom of Aragon. The church of Bossost (fig. 1.2) dates from this period.

The French occupied the valley from 1283 until 1298 and subsequently it was transferred to the kingdom of Mallorca. Since 1313 the Valle de Arán is definitively a Spanish outpost, and it has been frequently attacked by the French, and finally in 1950 by a group of Spanish exiles. Fig. 1.3 shows a sculpture on a tombstone of an Aranese nobleman.

Since about 1900 the Valle de Arán has been selected by tourist as the 'Spanish Switzerland'. The valley forms now a part of the Province of Lerida and it is connected with the remainder of Spain through a five kilometer long tunnel (elev. 1450 m) under the main water divide and along the Bonaigua pass. The Bonaigua pass (elev. 2072 m) is inaccessible during the winter because of snow. Before the Viella tunnel was completed in 1948, the Valle de Arán was isolated in the winter half year from the rest of Spain. The name of Arán has been explained in different ways. Soler Santalo (1906) supposes a Basque origin, whereas Caro Baroja (1946), Cenac Moncaut (1873), and Moner y de Siscar (1898), emphasize a Celtic origin.

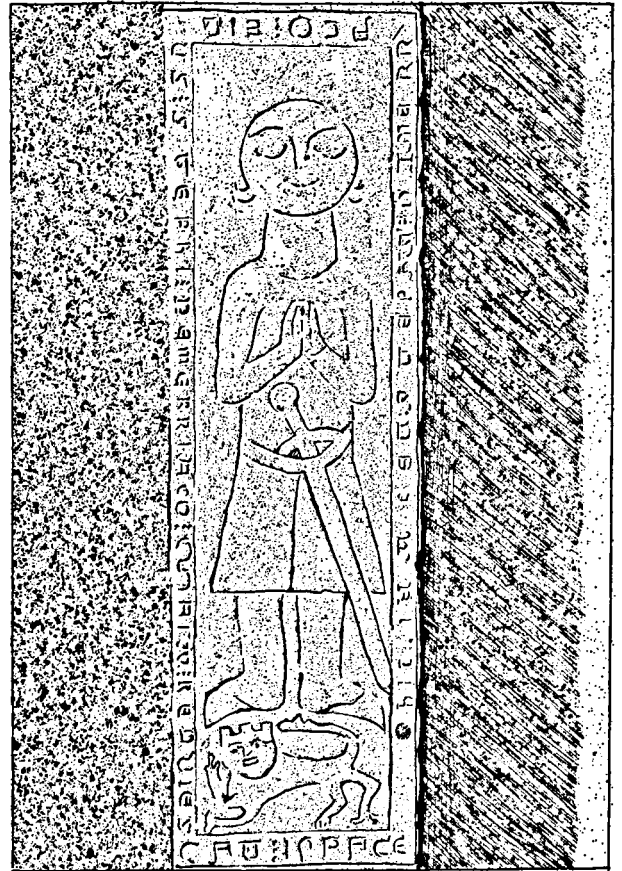


Fig. 1.3 Tombstone of an Aranese nobleman (church of Las Bordas) 12th century.

The young villages in the valley have Roman names while the others have ancient Celtic names. Since mediaeval times, seven villages have disappeared and only one new village has been built. The villages with Celtic names are situated at the sunside slopes of the Garonne valley.

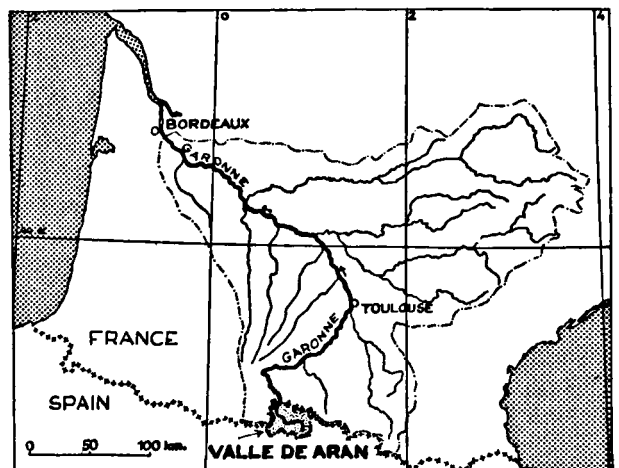
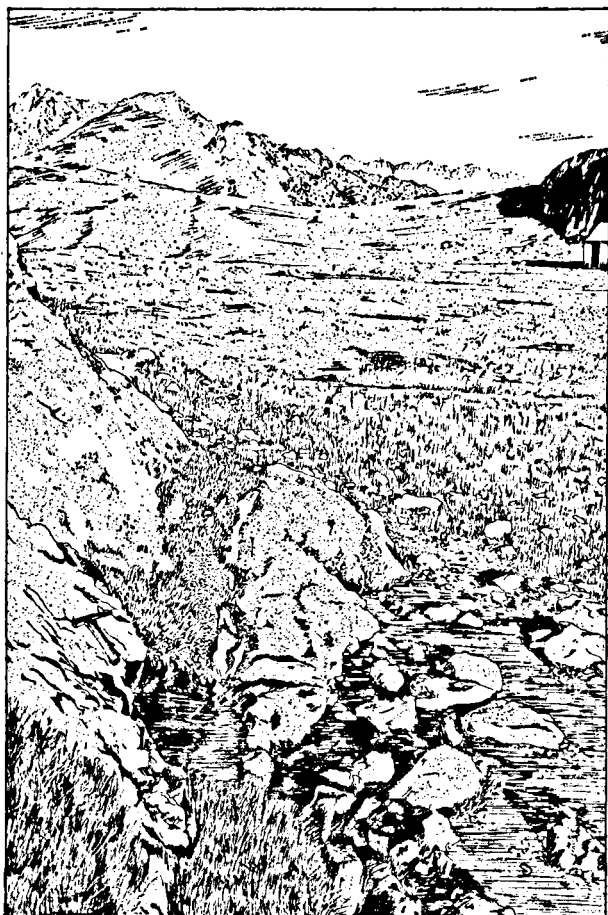


Fig. 1.4 Stream system of the Garonne River.



1.5 Stream system

The valley constitutes about one percent of the total drainage basin of the Garonne River, which covers about 53.000 km² (fig. 1.4). The Garonne River in the Valle de Arán has a length of 36 km, while the entire river, from the Pyrenees to the Atlantic Ocean, is 360 km long. The Garonne has its headwaters in the Valle de Arán on the slopes of the Cabeza des Portans (elev. 2240 m) in a small karst spring (fig. 1.5). The river, after leaving the Valle de Arán, flows generally northwestward into France and via Toulouse and Bordeaux into the Atlantic Ocean.

Fig. 1.5 The karst spring Güell del Garona where the Garonne River originates.

2. MORPHOMETRY

2.1 Morphometric data

Hypsometric curves are required for a precipitation analysis of the Valle de Arán. In this chapter, however, they are used as morphometric data. The hypsometric curve is a frequency curve of area/altitude (Scheidegger, 1958). Hypsometric histograms of thirty-three drainage basins and of the entire Valle de Arán are plotted on linear paper in fig. 2.1. The hypsometric curve of the Valle de Arán has afterwards been drawn on double logarithmic paper (fig. 2.2) because parabols show as straight lines and as Nye (1965) demonstrated: a parabolic cross section has smallest resistance for a flowing valley glacier. Indeed, the glacial valleys of the Valle de Arán are step-shaped superpositions of two or three parabolic channels (fig. 2.3). Consequently, the hypsometric curves of glacial valleys show step shaped superpositions of straight lines, if plotted on logarithmic paper. Valley steps are clearly distinguishable (fig. 2.3).

In the Valle de Arán a hypsometric curve is essentially asymmetric, because the horizontal area bound by and above the longest contour lines is smaller than the underlying area. The lower parts of fig. 2.2 and fig.

2.3 are slightly curved because the parabolic channels are deformed by scree and recent river erosion. The frequency of area-altitude of thirty-three basins of the Valle de Arán (fig. 2.1) is irregular and partly coinciding with the denudation levels, which have been described by many authors (see Kleinsmiede, 1960). In the entire Valle de Arán, four areas of low relief can be distinguished by morphometric analysis as points that do not fit into the hypsometric curve (fig. 2.2):

1. From 3500—3100 m
2. From 2800—2700 m
3. From 2500—2000 m
4. From 1100— 900 m

Only the area between 2500—2000 m elevation can be called a real planation level in the Valle de Arán. The others show as minor deviations from the hypsometric curve. The frequency of area versus altitude can be compared with the average slope between two contour lines on fig. 2.2. The combination of both curves permits a description of the morphology of the Valle de Arán:

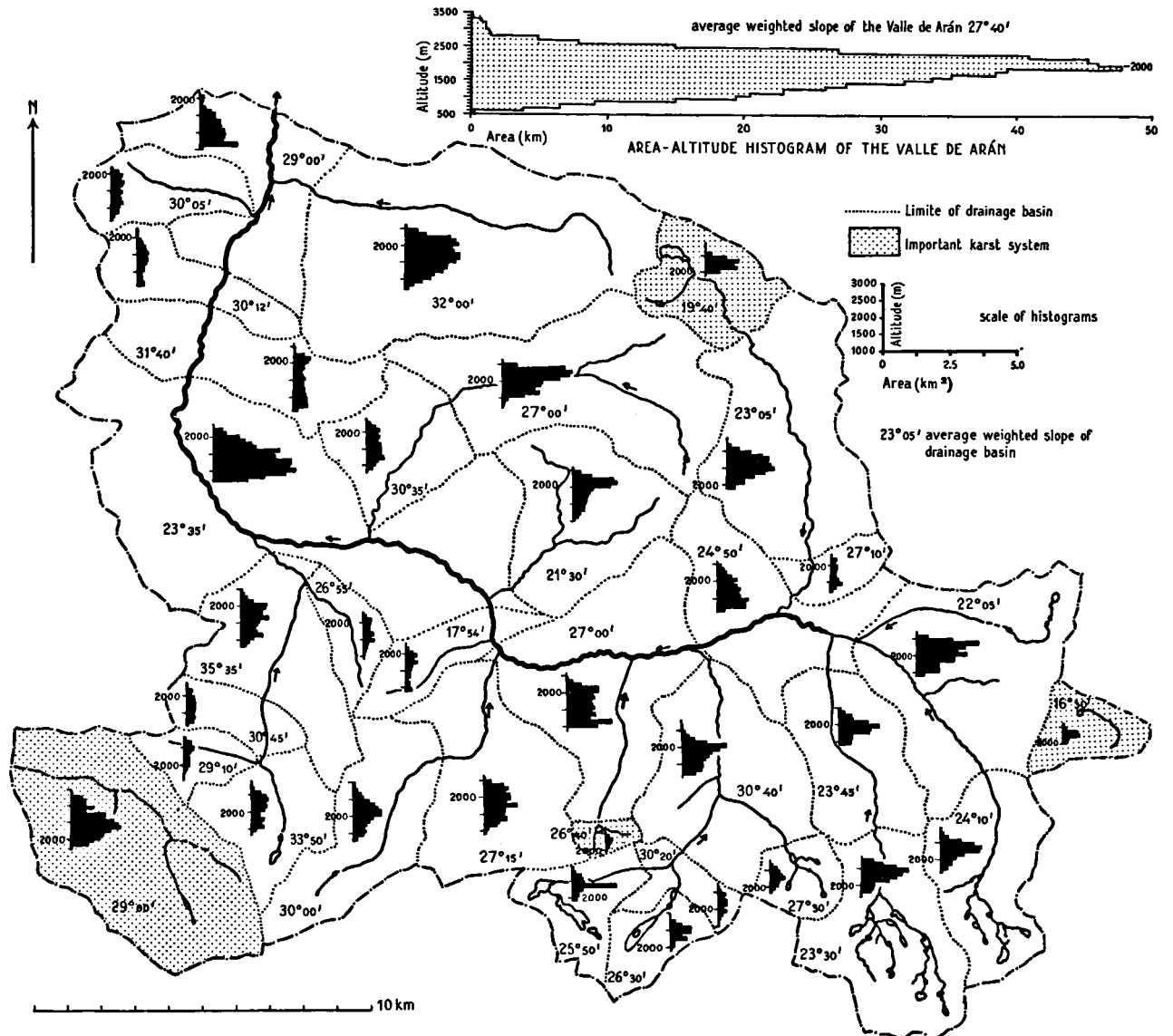


Fig. 2.1 Hypsometric histograms of thirty-three basins.

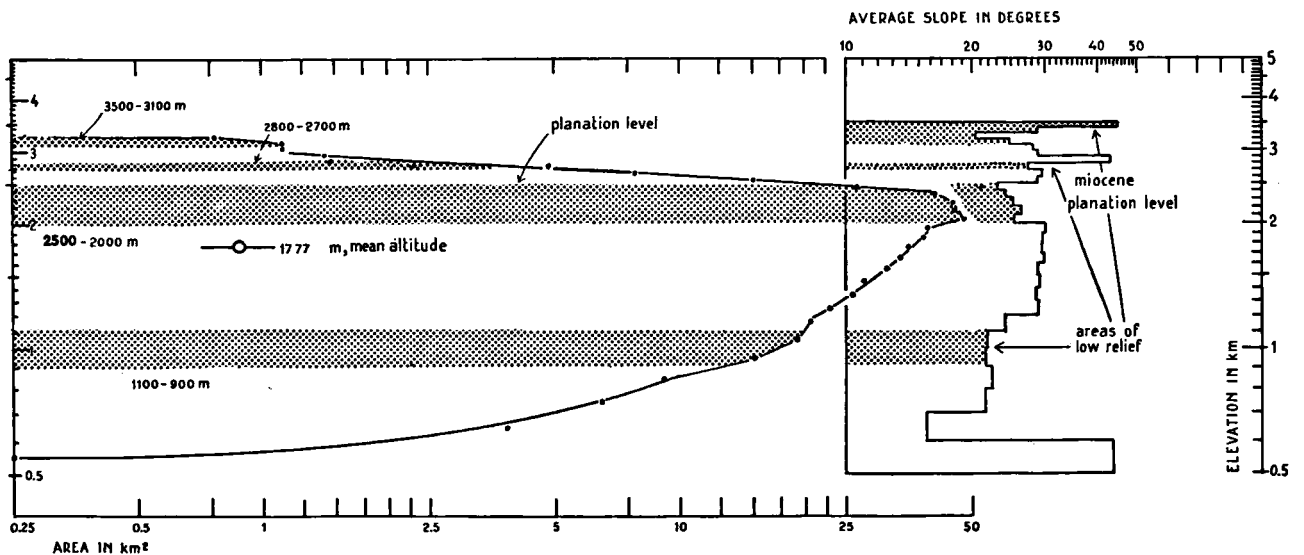


Fig. 2.2 Hypsometric histogram and slope-altitude distribution of the Valle de Arán.

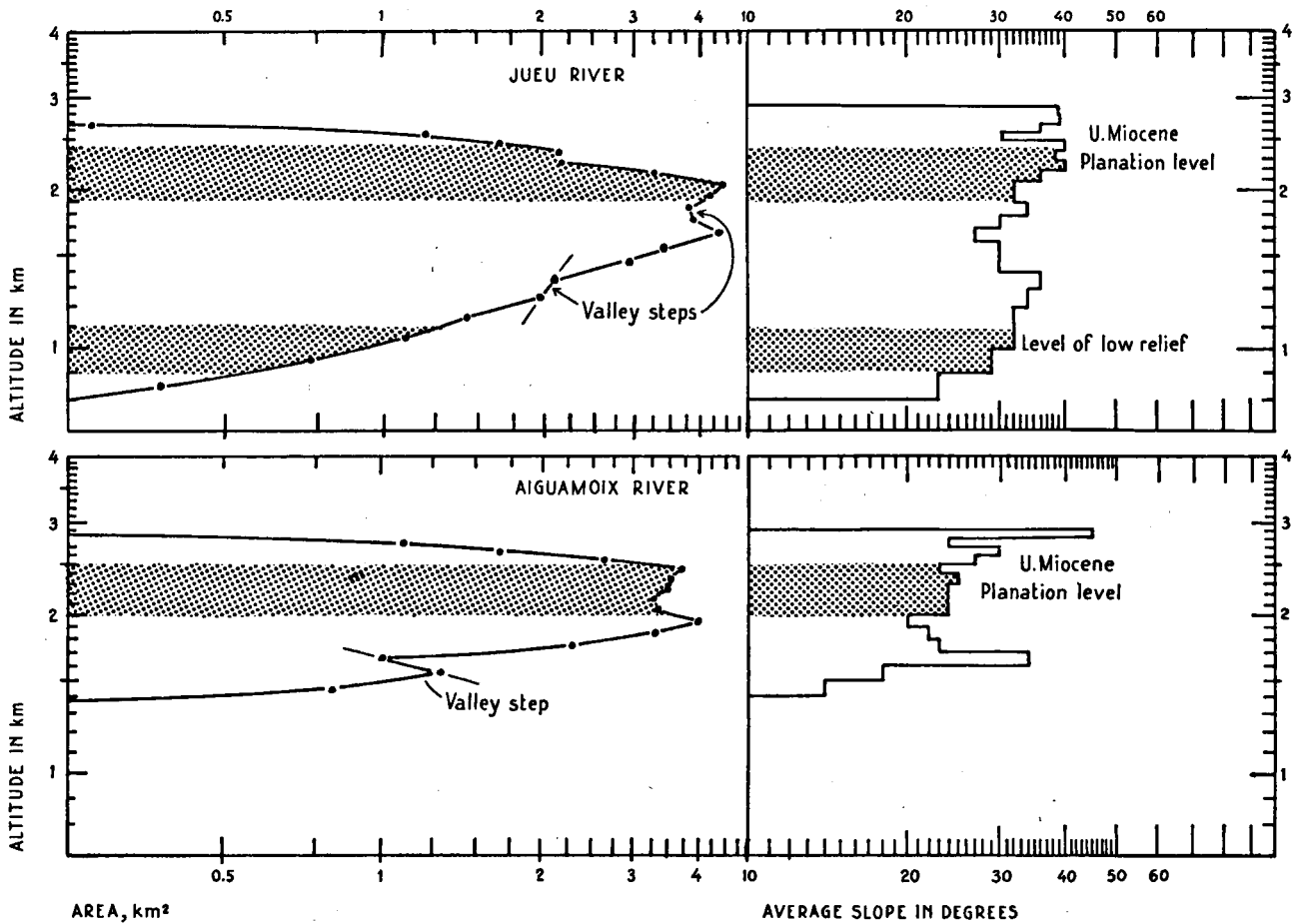


Fig. 2.3 Hypsometric histogram and slope-altitude distribution of the Jueu- and Aiguamoix-River.

The high and steep cirque landscape (elev. 3500—2500 m) contains two areas of moderate relief. An area of low relief is situated between altitudes 2500—2000 m, which served as an area of snow accumulation where numerous Pleistocene glaciers originated. They descended from this planation level into eight beautiful valleys (elev. 2000—1100 m) which merge into the main Garonne valley (1100—563 m), which contains the lowest area of moderate relief (1100—900 m).

2.2 Influence of basin morphology on hypsometric curves

For the determination of low relief areas in the valley from the hypsometric curves, it was required to study the effect of the shape of drainage basins and of the valley cross sections on the curves. Three simplified valley cross sections (parabolic-, V-shaped-, and elliptic), were tested for various types of basin shapes (fig. 2.4). Results are shown in fig. 2.5 for a rectangular, an elliptic and a circular drainage basin. It can be concluded, that parabolic valleys can be distinguished as straight lines on logarithmic paper, independent of the basin shape. It is not possible to distinguish elliptic- from V-shaped-valleys, although the V-shaped types show steeper curves. The circular basins show steeper

MAPS OF SIMPLIFIED VALLEYS

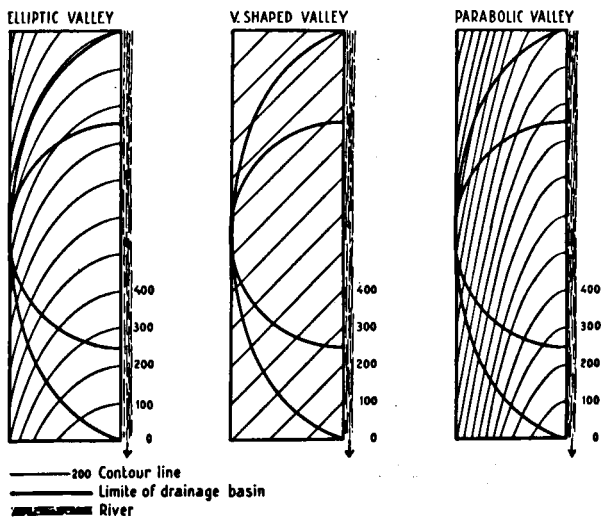


Fig. 2.4 Maps of three simplified valley cross sections.

hypsothetic curves than the elliptic or rectangular types. It should be emphasized, that the three ideal cross sections of fig. 2.4 are simplifications.

All valleys of the Valle de Arán are parabolic channels of glacial origin, and therefore hypsothetic curves plotted on logarithmic paper offer a possibility to determine the four areas of low relief as points that do not fit into the hypsothetic curve. Valley steps, which are in general situated below the 2200 m elevation, can be mistaken for planation levels (fig. 2.3). The low relief type in the Jueu glacial valley (1100—900 m) was found, because the hypsothetic curve does not correspond to a steep drainage basin. An area of similar relief was found in the Barrados- and Toran valley from 1100—900 m.

2.3 *Specific degradation*

The specific degradation of a drainage basin can be defined as the total mass, expressed in terms of thickness (in mm) of a sheet, distributed over the entire basin, which is discharged out of a drainage basin in one thousand years. From the literature (Water Supply Papers 1251, 1351, 1401, 1450, 1451, 1520 and 1547) specific degradation has been estimated for twenty-eight Atlantic slope basins in the U.S.A. between latitudes 38°—45° N. Those basins have areas, comparable to that of the Valle de Arán (572 km²). Because of the short time-range of the data, no reliable results were obtained for a period of one thousand years. In general, specific degradation during a flood is 20—1500 times the average annual degradation. The arithmetic mean of specific degradation values for twenty-eight basins was 110 mm/1000 year. Recent measurements of the specific degradation of the Garonne basin near Toulouse indicate values 150—200 mm/1000 year. Table 2.1 shows specific degradation values of twelve rivers.

TABLE 2.1. *Specific degradation values of twelve rivers (mm/1000 year)*

River	Area km ²	Specific degradation mm/1000 year
Rhone	64,700	265
Rhone	90,000	200
Po	70,000	480
Po	77,700	548
Rio Grande	77,700	25
Irrawaddy	323,000	451
Upper Ganges	370,000	486
Uruguay	388,400	22
Danube	606,000	59
Danube	829,000	59
Indus	940,000	225
Hwango	1,812,000	268
Nile	2,848,000	10
Mississippi	3,221,000	63
Amazone	5,594,000	200—270

The degradation for the Pleistocene has been calculated to be 100 mm/1000 year in the Valle de Arán. If continuous erosion is assumed during the Upper-Miocene, Pliocene and Quaternary (20 million years), which started at the 2500 m level, an average specific degradation of only 33 mm/1000 year is required to reach the present level. It can be concluded that in general, erosion in the Valle de Arán during part of the Tertiary was not great.

2.4 *Hypsothetic integral*

Scheidegger (1958) advocates the use of the hypsothetic integral curve in order to define drainage patterns at various stages. In this thesis it was used to calculate the mass, which has been discharged out of

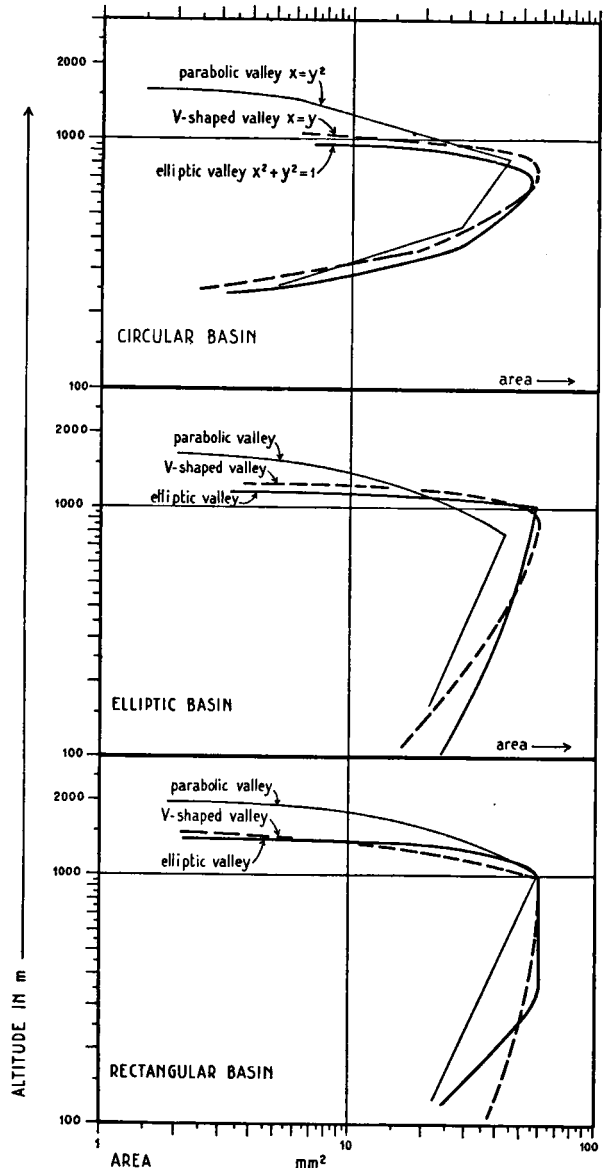


Fig. 2.5 Hypsothetic histograms of three simplified valley cross sections for a rectangular-, elliptic- and circular-drainage basin.

the Valle de Arán. Volumes were computed by applying a trapezium formula. Fig. 2.6 shows the hypsometric integral for the area. A mass of 391 km^3 has been discharged out of the valley since Miocene time, if the Miocene base level is assumed to be 2500 m. This is equivalent to 35 percent of the block between the elevations 2500 and 563 m. In order to get an idea, of what 391 km^3 represents, the volume of the huge Adour-Lannemezan piemont of the adjacent Neste River has been estimated to be only 94 km^3 from data of Taillefer (1951). An average thickness of 60 m of the piemont has been used. Apparently the Adour-Lannemezan piemont, if compared with the material discharged out of the Valle de Arán, is very small indeed. With 391 km^3 material derived from the Valle de Arán, a large part ($3,250 \text{ km}^2$) of the entire Garonne molasse basin could be covered with a

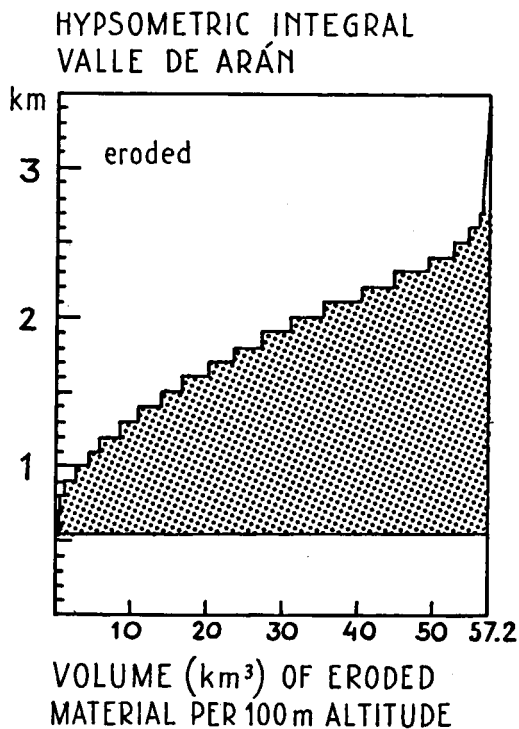


Fig. 2.6 Hypsometric integral of the Valle de Arán, showing the volume of eroded material per 100 m altitude.

sediment of an average thickness of 120 m, as measured in the field.

2.5 Erosion models

Four areas of low relief occur in the Valle de Arán. If erosion is assumed to start at the present maximum elevation of 3500 m and to continue to the present base level of 563 m, three erosion models can be devised. Four "planation" phases, corresponding to the four areas of low relief in the valley (see 2.1) and four intermediate erosion phases are assumed:

1. In model 1 the assumption has been made, that 75 percent of the available volume is removed during the four planation phases, whereas only 50 percent during the four intermediate phases is removed.
2. In model 2 the assumption has been made, that in both phases 50 percent is removed. Model 1 and 2 represent a discontinuous uplift in eight steps.
3. Model 3 is a refinement of model 2, because it is calculated for 100 meter intervals rather than for the total interval during the erosion phase. This model represents a continuous uplift in thirty-five steps.

Table 2.2 and figure 2.7 show the results of the model analysis. Two graphs (fig. 2.7) show the removed volume per 100 meter lowering of the base level, and the accumulated volumes, which were eroded during the eight erosion phases. Model 3 can probably be applied to the Pyrenees. Some information about specific degradation during the Tertiary should make it possible to estimate the required time for each erosion phase.

2.6 Origin of the Garonne River

Hercynian structures were studied to determine their effect on the present position of the Garonne River. Fig. 2.8 shows the relief above a horizontal plane, which is at present situated at an elevation of 3000 m. Data from the profiles and maps of Kleinsmiede (1960) were used. The structure-contour map (fig. 2.8) of the top of the Devonian shows, that the Bossost dome and the late Carboniferous intrusions underlie

TABLE 2.2. Volume (km^3), discharged out of the Valle de Aran during successive erosion phases

3500— 3100 m	3100— 2800 m	2800— 2700 m	2700— 2500 m	2500— 2000 m	2000— 1100 m	1100— 900 m	900— 563 m	Increase erosion range
1		2		3		4		Number erosion phase
172.031	114.182	99.495	90.939	212.440	130.082	71.452	67.185	Model 1
114.695	142.857	99.700	105.176	163.903	161.472	84.344	86.831	Model 2
228.097	112.762	56.541	111.776	239.535	190.586	11.421	7.175	Model 3

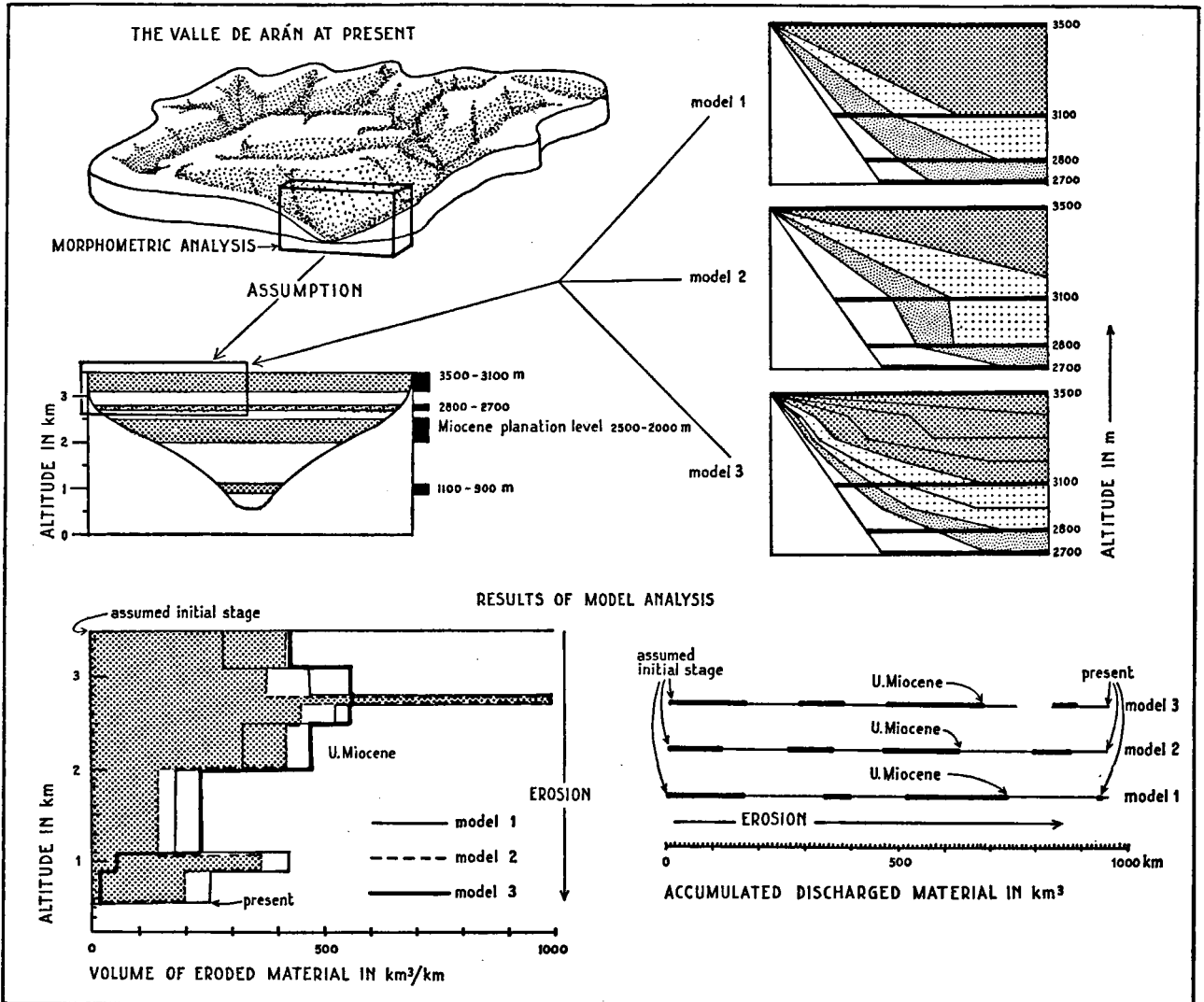


Fig. 2.7 Results of the model analysis of the Valle de Aragón.

high areas which both reached elevations of 6000 meters. It can be concluded that the position of the Garonne River from Las Bordas to Salardu appears to be controlled by the Hercynian structures. During the Cretaceous, a small part of the axial zone of the Pyrenees rose above sea level. Therefore the present Garonne River, and certainly its S-N part which crosses the Bossost dome, is of Tertiary age. The fault pattern has not affected the position of the main rivers. Many tributaries, however, are situated along fault lines.

Although it is not certain that the Garonne River is partly a Permian or Triassic feature, an old erosion phase is required to explain certain features in the Valle de Aragón. In the Aiguamoix valley, at an elevation of 2000 m, a patch of Triassic- (de Sitter, 1953a—1956b; Kleinsmiede, 1960) or Permian-sedimentary rock (Mattauer, 1966) has been found. From the map and profiles of Kleinsmiede it can be concluded, that there has been an erosion phase before the deposition

of the latter sediments, even if preservation in a fault zone is assumed. This erosion phase is partly responsible for the removal of a mass of 530 km³, which was situated above the 3100 m level (fig. 2.8) and partly for the removal of a mass of 567 km³, which was situated between the elevations 3100 m and 2500 m. The rest of the mass, which was not eroded during the Permian- or Triassic-phase, has been removed during the Tertiary, together with the Mesozoic sediments. Taillefer (1951) considers the Garonne River as one of the oldest features of the Pyrenees because it follows along the northern border of the Pyrenees a fault zone of pre-Miocene age.

2.7 *The Miocene planation level*

De Sitter (1956-b), Jelgersma (1958) and Kleinsmiede (1960) date the planation level of 2500—2000 m as Upper-Miocene. By hypsometric analysis we could trace this level in each river of the Valle de Aragón

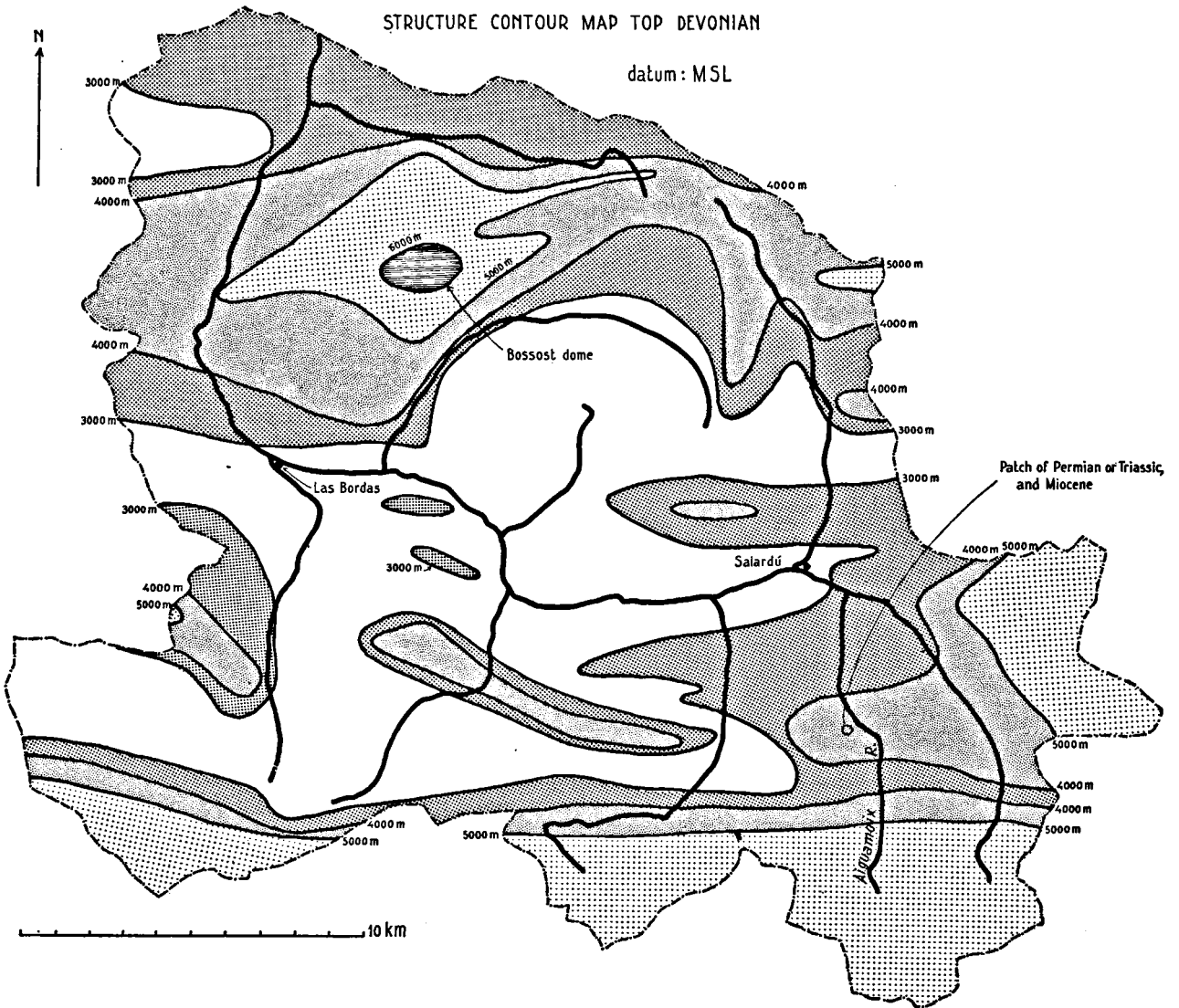


Fig. 2.8 Structure-contour map of the top Devonian in the Valle de Arán.

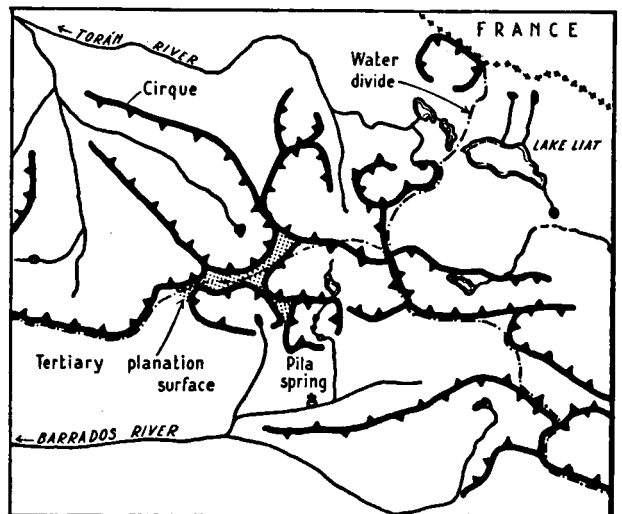


Fig. 2.10 Glaciation of a Tertiary planation level.

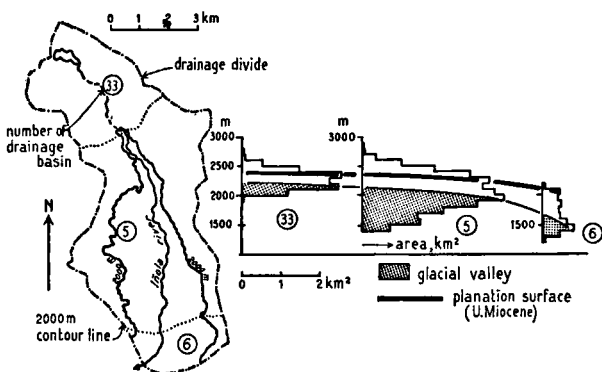


Fig. 2.9 Morphometric analysis of the Iñola basin, showing the dip of the Miocene planation level in the direction of the present river.

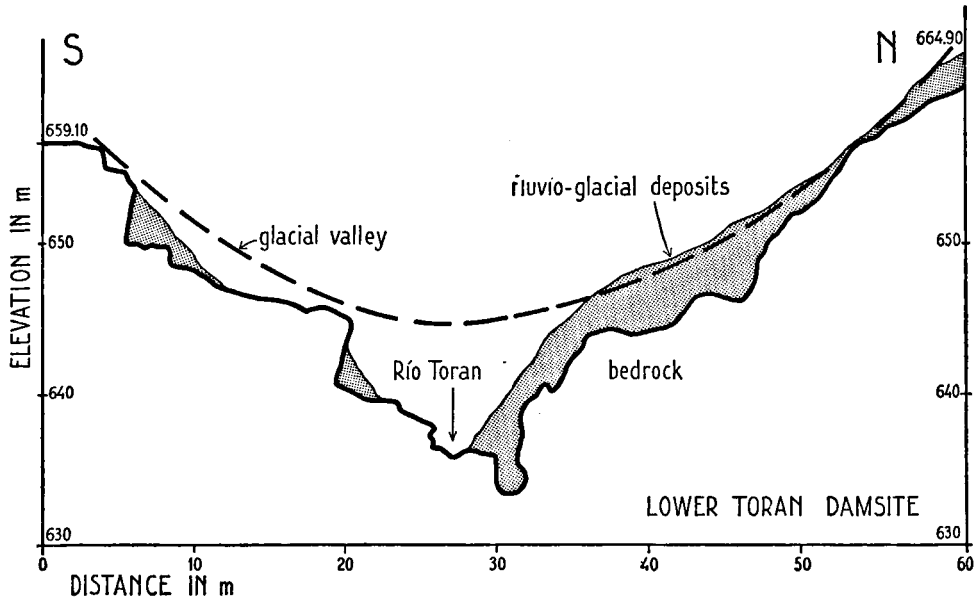


Fig. 2.11 Cross section of the Toran valley at the Lower Toran damsite.

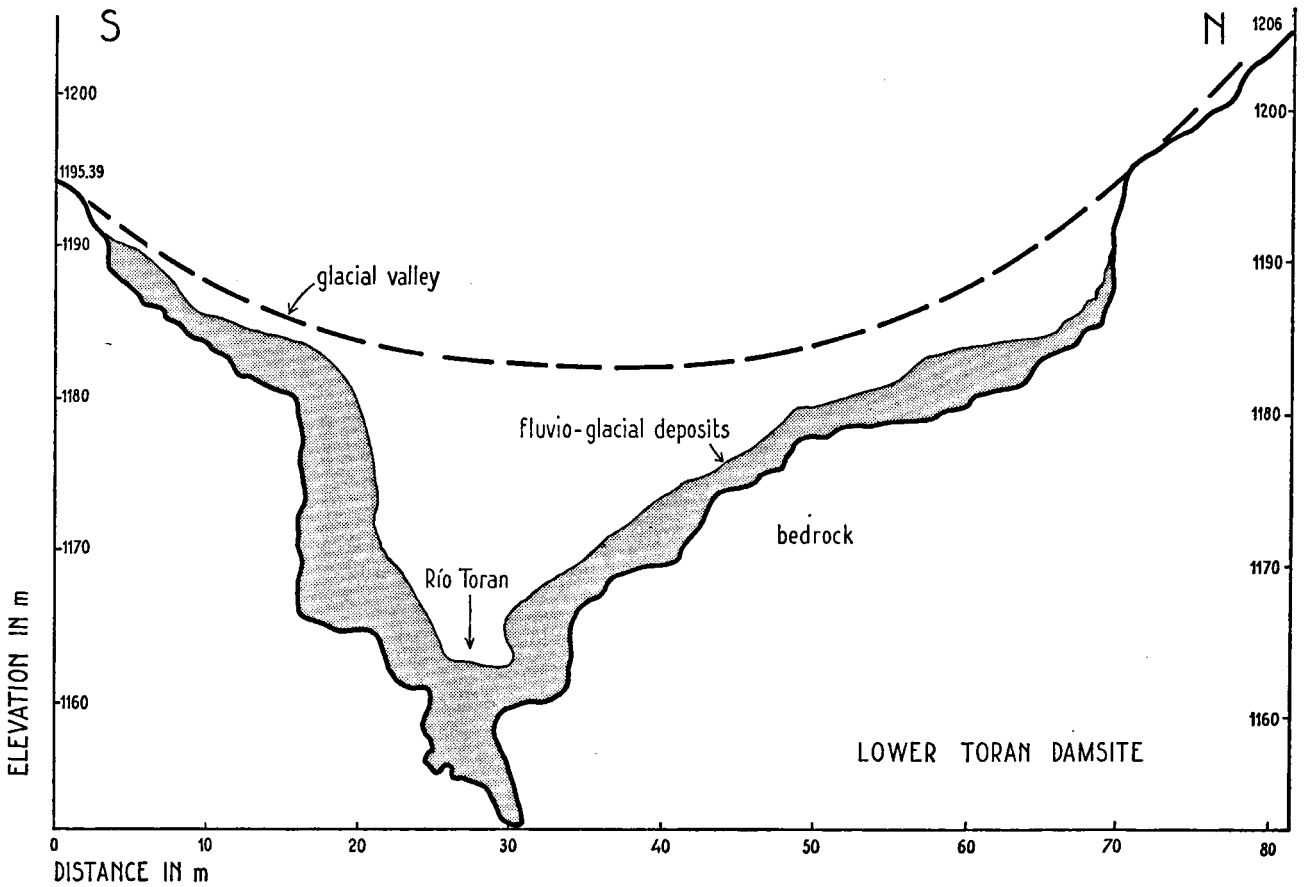


Fig. 2.12 Cross section of the Toran valley at the Upper Toran damsite.

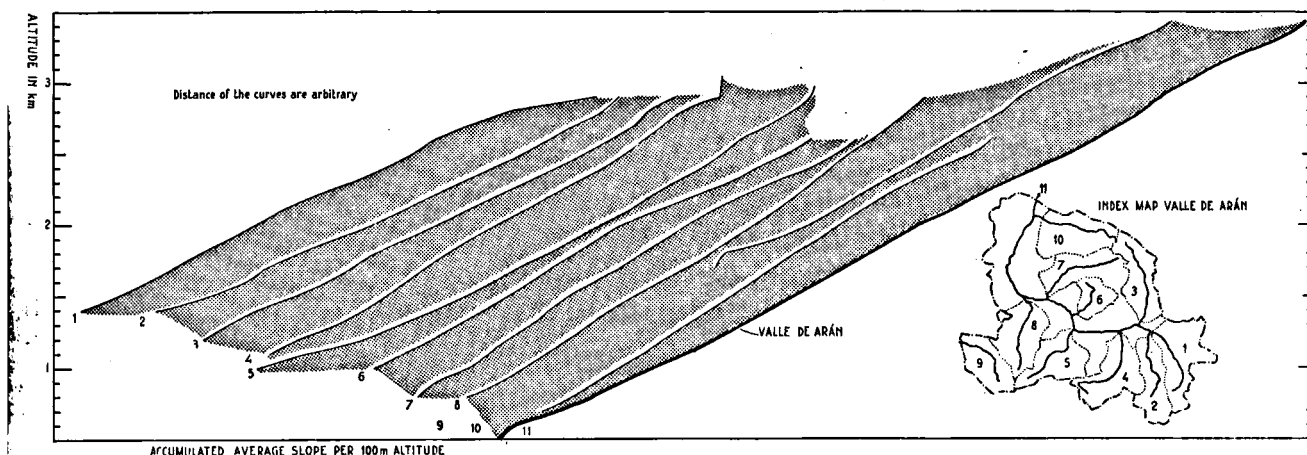


Fig. 2.13 Distribution of the weighted average slope per 100 m altitude in ten drainage basins.

(fig. 2.1). It can be concluded, that the planation level constitutes the remains of a Miocene landscape, which showed a significant residual relief of at least 1000 meters. The regional slope of the Miocene erosional surface dips in the direction of the present rivers, for instance in the Iñola River (fig. 2.9). A hypsometric analysis by Liezenberg (1967) in the adjacent Capdella area shows, that the Miocene main water divide was situated at the same position as the present main water divide.

2.8 Quaternary developments of the Valle de Arán

After the hot and moist Miocene and the dry Pliocene (Flohn, 1965 — Taillefer, 1951) cold and dry climates followed in the Pyrenees (Fairbridge, 1965). Glaciers descended into the Garonne valley, and reached even

St. Gaudens (50 km). The glaciation of the Miocene planation level gave rise to typical glaciers, which flowed in all directions into the steep valleys (fig. 2.10). Recent erosion has dissected the glacial valley bottoms, for instance in the Toran River (figs. 2.11 and 2.12). The observations are derived from numerous FECSA drill hole data.

2.9 Slopes

Average slopes were determined for all drainage basins in the Valle de Arán. The average slope was obtained by dividing the area between two successive contour lines by the arithmetic mean of the length of those contour lines. The relation of the average slope to altitude is cumulatively plotted in fig. 2.13 for ten river basins. The average slope of the entire Valle de Arán is shown in fig. 2.2. The frequency of the average slopes is shown in fig. 2.14. Slopes between 28° and 31° are very frequent. The areas of low relief in the Valle de Arán are not apparent on fig. 2.13 because many steep slopes at the same elevation as the areas of low relief predominate. The regular increase of drainage area in a downstream direction of the Garonne River is shown in fig. 2.15.

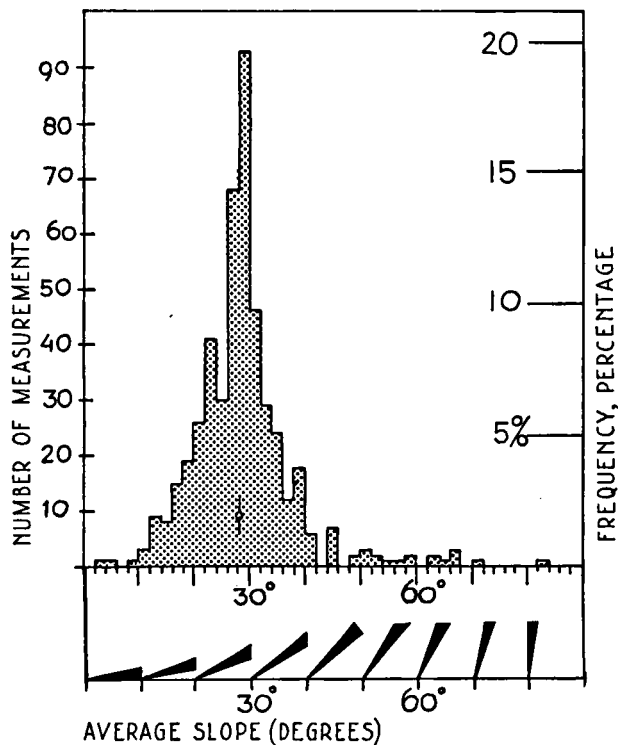


Fig. 2.14 Frequency of weighted average slopes.

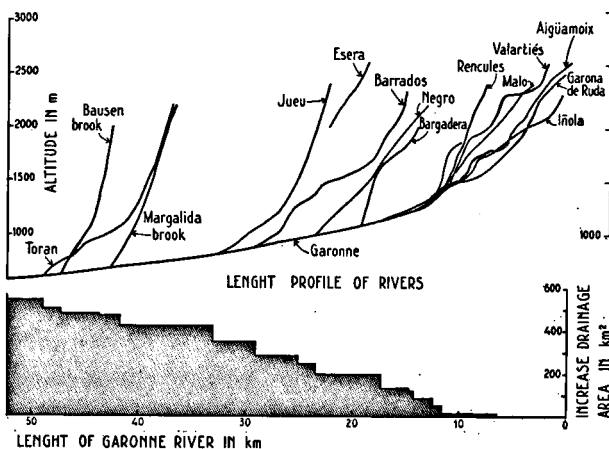


Fig. 2.15 Length profiles of the Valle de Arán rivers and increase of drainage area in a downstream direction of the Garonne River.

3. AVAILABLE METEOROLOGICAL DATA

3.1 Introduction

The three temporary and seven permanent meteorological stations in the Valle de Arán are managed by the Spanish hydroelectrical company FECSA. The permanent meteorological stations are situated at power stations while temporary posts are mostly situated near important construction sites of the FECSA. FECSA has commenced with the recording of meteorological observations in 1946. All the available data over the period 1946—1966 were placed at our disposal. The meteorological information is stored in the Viella head office. Except for the precipitation, all other climatic elements have been analysed over the period 1955—1965 using data from the Cledes, Viella, Arties, Restanca and Bonaigua meteorological stations.

3.2 Precipitation and snowfall

The Upper-Garonne basin has been well equipped with 10 daily measured rain gauges. They are distributed throughout the entire basin of 572 km². In addition to these gauges, 10 accumulating rain gauges of the Mougín type have been mounted high in the mountains of the Valle de Arán. The Mougín gauges are measured 1—3 times a year.

In figure 3.1 the position of the 20 rain gauges is indicated. In order to show the periods of precipitation records the bar graph figure 3.2 has been drawn for all gauges from 1946—1966.

Data of self recording rain gauges are not available in the Valle de Arán.

The 10 daily observed rain gauges have a height of

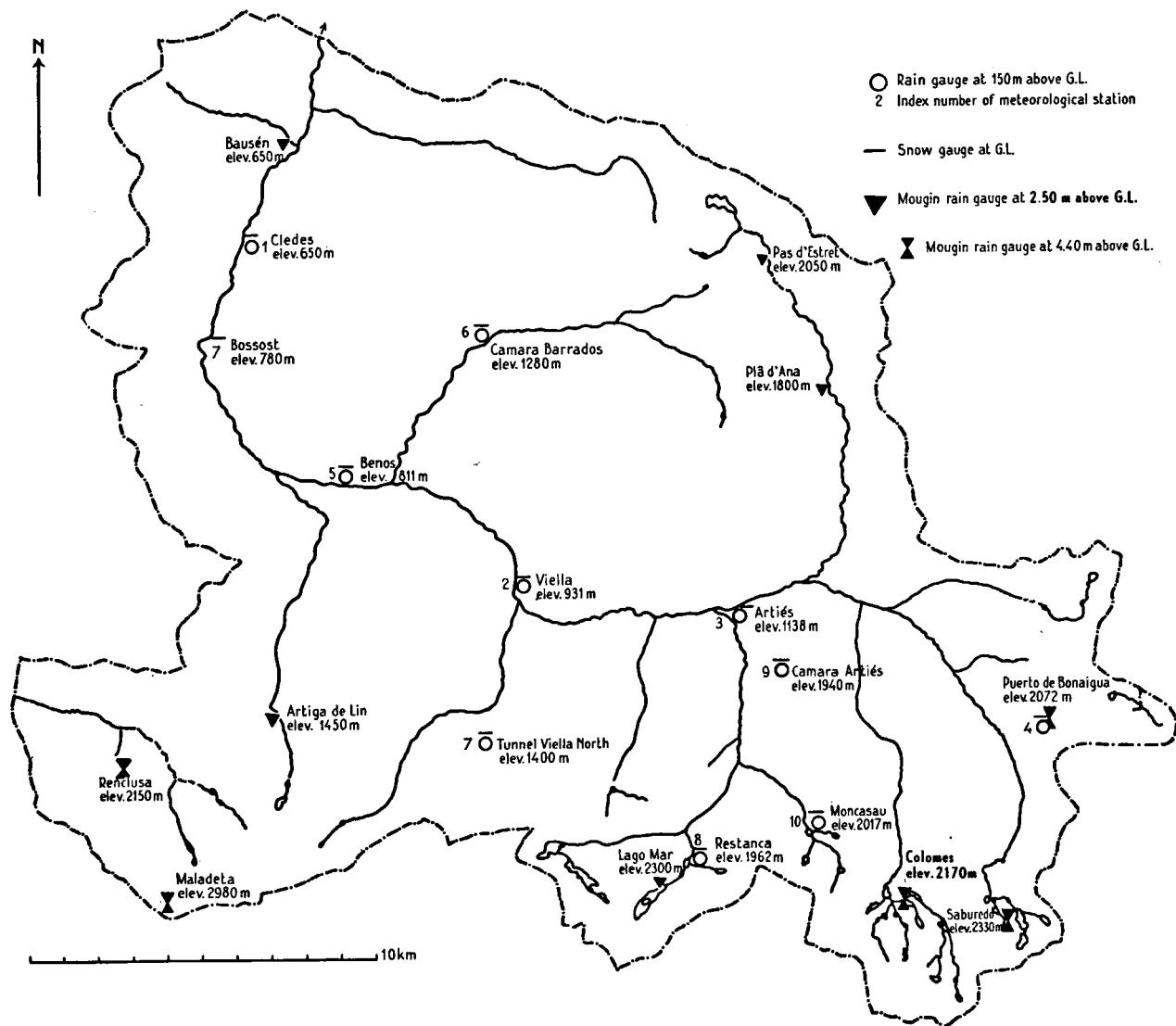


Fig. 3.1 Location of meteorological stations.

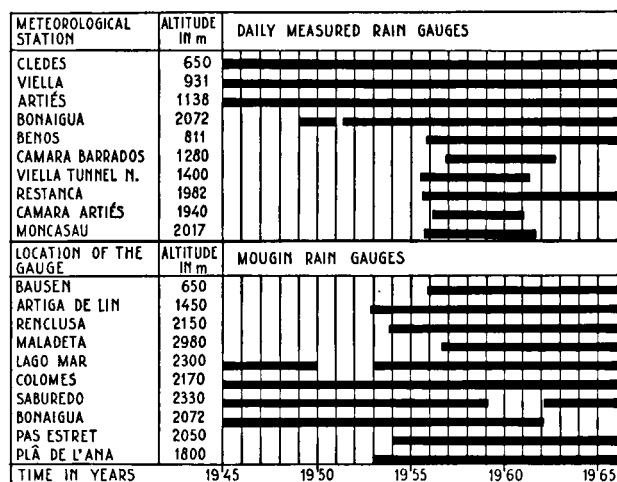


Fig. 3.2 Bar graph, showing precipitation records from 1946—1966.

1.45 m above GL (ground level) and an orifice surface of 200 cm². These gauges are daily read at 08.00 h. All Mougin accumulating rain gauges have an orifice of 200 cm² while their heights reach to 2.50 m above GL or to 4.40 m above GL. In fig. 3.3 the latter type of gauge is shown. Whether a height of 2.50 m or 4.40 m is maintained, depends on the snow height at the gauging site. After measuring the accumulated precipitation in a Mougin gauge, the apparatus is filled again with 1 liter water, vaseline and calciumchloride. The anticongealing CaCl₂, attacks however the zinc catchment basin of the Mougin gauge. This results in losses of precipitated water during a period of measurement, which are not very frequent, but difficult to detect and to evaluate.

Near the 10 meteorological stations and also in Bossost, the daily snowheight on GL is measured at 08.00 h. Most data include total snow height and the height of the fresh fallen snow at ground level.

3.3 Temperature, wind direction, wind velocity and cloud-cover

At the meteorological stations Cledes (650 m), Viella (932 m), Arties (1138 m), Restanca (1982 m) and Bonaigua (2072 m) the temperature, wind direction, wind force and cloud-cover are observed daily. Temperature measurements at 08.00 h. include maxi-

imum, minimum and actual temperature in °C. These variables are measured at a height of 1.50 m above GL. Calibration of the Six-maximum-minimum thermometers used at the stations, showed small systematic errors for all thermometers.

The daily wind direction at a height of 3 m above GL is registered at 08.00 h. as north, east, south or west. Wind force is estimated simultaneously and registered as Fuerza (force) 1, 2, 3 and 4. Wind force estimations can be converted to Beaufort with Fuerza n = Beaufort 2n. This equation has been derived from control measurements in Restanca with a rotation anemometer at 2.00 m above GL. Wind velocity is not measured.

Cloud-cover is estimated every day at 08.00 h, which are sometimes accompanied by a cloud description. These cloud types are not defined according to W.M.O. standards (International Cloud Atlas). The observed cloud types in the Valle de Arán data are described in the Atlas reducido de nubes, publ. C.12 (1943) of the Servicio Meteorologico Nacional de España.

3.4 Air pressure and air humidity

In the power station Viella (1956—1966) and Arties (1959—1966) the air pressure is registered with barographs. At the same stations air humidity measurements are carried out at 08.00 h and at 18.00 h using ventilated dry and wet bulb psychrometers. The air humidity data have been available from Viella since 1960 and in Arties since 1963. The air humidity measurements represent the situation at 1.50 m above GL, but they are not recorded during the winter time.

3.5 Unused records

Pre-1946 meteorological information from the meteorological stations Cledes, Viella and Bonaigua have not been analysed because they show interruptions during the Civil War and during World War II. For our analysis of the climatology of the Valle de Arán the period 1946—1966 was the only one with continuous precipitation observations coinciding with an equal period of continuous hydrological records. The old records are stored in the archives of the Centro Excursionista de Cataluña (Barcelona); Servicio Meteorologico Nacional (Zaragoza) and Fuerzas Electricas de Cataluña S.A. (Barcelona).

4. CLIMATOLOGY OF THE VALLE DE ARAN

4.1 Introduction

An evaluation of the climatic elements of the Valle de Arán is essential for the determination of the terms evaporation and precipitation in the water balance. For that purpose the meteorological data over the period 1955—1965 have been analysed for the stations Cledes, Viella, Arties, Restanca and Bonaigua. The analysed data are summarized in tables 1—45.

The Valle de Arán has an almost endless variety of local climates, because it is a high mountain basin. It is difficult to give a complete idea of all those local climates with the data from only five meteorological stations distributed over an area of 572 km². The atmospheric conditions in the Valle de Arán vary markedly with exposure and rapidly with variations in height. The climate of the broad Garonne valley is very different from that of an exposed high peak. The climate of the windward slopes differs greatly from that of the leeward slopes, and the flanks inclined towards the sun are dissimilar from those which are shaded slopes. The 10 years observation period is statistically not long enough for an evaluation of a certain climatic type. The description of the "climates" in the Valle de Arán is only based upon ten years of continuous observations (1955—1965), which is insufficient to comply with the international accepted period of 30 years (1930—1960).

4.2 Classification of the climates

The classification of Köppen (1922) has been applied to the meteorological data 1955—1965 of the Valle de Arán. It has to be emphasized that the Köppen classification attempts to classify highland climates, by employing the same system of climatic types and their limiting boundaries as for a hypothetical continent of low and uniform elevation.

The Köppen classification gives the main Garonne valley with the stations Cledes (650 m), Viella (932 m) and Arties (1138 m) a Cbf climate. This means that the broad Garonne valley is characterized by a maritime moderate climate with precipitation in all seasons. At least four months have average temperatures exceeding 10° C.

The higher parts of the Valle de Arán have a Dcf climate. This implies a mountain climate with precipitation in all seasons. In such a climate two months have average temperatures higher than 10° C. The Dcf climate is determined by using the data

from Restanca (1982 m) and Bonaigua (2072 m). The Köppen classification can also be applied to the highest peaks of the Valle de Arán which are situated near the Pyrenean water divide. Those high mountains, ranging from 2300 to 3400 m, have an EF climate with abundant annual precipitation ranging from 2000 mm to more than 3000 mm. The precipitation is evenly distributed in all seasons. The high peaks above 3000 m are characterized by nine frost months whereas three months have an average temperature higher than 0° C.

4.3 The effect of the Pyrenees on the Valle de Arán climate.

The Valle de Arán is situated at 180 km from the Mediterranean Sea and at only 150 km from the Atlantic Ocean (fig. 1.4).

The climates in the Valle de Arán in the centre of the High Pyrenees are therefore strongly influenced by the presence of those extensive bodies of water.

The exceptional climate of the Pyrenees can be attributed to its peculiar geographic position: the East-West direction of the mountain chain and its great altitude, which exceeds the average altitude of the Alps by 100 meters (Dominy, 1965). Most of the northern side of the Pyrenees contrasts sharply with the dry Spanish side of the mountain chain, which is strongly affected by the Iberian continent and the Mediterranean Sea.

The climate of the western Pyrenees, near the Atlantic coast, is strongly influenced by the Atlantic Ocean and especially the Gulf Stream. The zone of maximum precipitation near the maritime northwestern border of the western Pyrenees is situated at a very low altitude. This zone rises along the northwestern face of the mountain chain in an eastward direction until it reaches the Valle de Arán, which is situated in the central Pyrenees. Those central or high Pyrenees consist of a 220 km long continuous range of summits exceeding 2500 m elevation. The passes across the high Pyrenees have altitudes ranging from 1600 to 2300 m. In the intramontane Valle de Arán, in the centre of the high Pyrenees, the zone of maximum precipitation coincides with the highest peaks on the main water divide, which range in altitude from 2300 to 3400 m. In the eastern Pyrenees, eastward from Andorra, the precipitation diminishes greatly due to the proximity of the Mediterranean Sea (Solé Sabaris 1962, Lautensach, 1964).

5. CLIMATIC ELEMENTS

5.1 Air pressure

In figure 5.1 the mean monthly air pressure of Arties (1138 m) and Viella (932 m) is compared with the Naca standard atmospheric pressures for those two stations. The Naca atmosphere for the two stations has been calculated according to the Smithsonian meteorological tables (1951). This has not been done

with the ideal vertical temperature gradient of 0.0065° C.m⁻¹, but with the measured gradients of 0.0054° C.m⁻¹ (Viella) and 0.0053° C.m⁻¹ (Arties). The ideal Naca atmospheric pressures for Viella (906,2 mb.) and Arties (884,3 mb.) appear to be superior to the measured values.

In the same figure the summer air pressure increase,

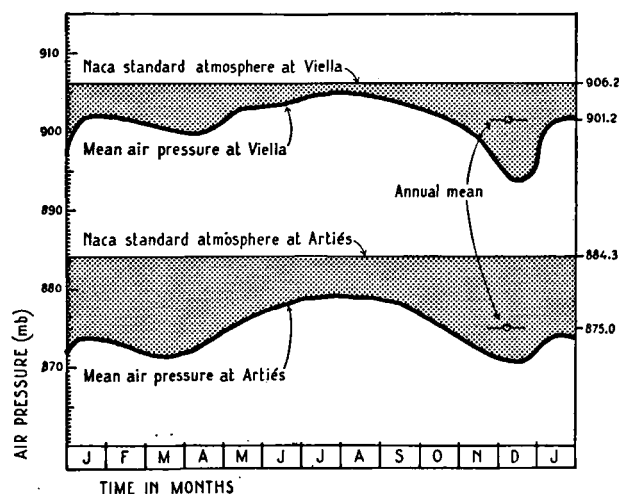


Fig. 5.1 Mean monthly air pressure (mb) of Arties and Viella, compared with the Naca standard atmosphere.

due to the shifting position of the Azores high pressure ridge, is clearly demonstrated for both stations. The monthly average air pressures for Arties and Viella are summarized in table 5.1. For the station Arties the monthly average daily variation in air pressure has been determined (table 5.2). The daily variation

appears to be considerable; it is the greatest during the winter time and the smallest in the summer months.

TABLE 5.1. *Monthly average air pressures (mb) in Arties (elev. 1138 m) and Viella (elev. 935 m)*

	Viella mb	Arties mb
J	901.9	873.8
F	901.8	873.1
M	900.5	871.4
A	899.3	872.7
M	903.1	876.2
J	903.7	878.2
J	904.9	879.3
A	904.9	879.0
S	903.8	878.3
O	902.1	875.4
N	899.0	872.1
D	893.4	870.5
Year	901.5	875.0
Naca	906.2	884.3

TABLE 5.2. *Monthly average daily fluctuation in air pressure (mb) for Arties (elev. 1138 m) from 1959—1965.*

J	F	M	A	M	J	J	A	S	O	N	D	Year
2.8	2.8	3.2	2.4	2.0	2.0	2.0	2.4	2.0	2.0	2.8	2.8	2.4

5.2 Temperature

In the Valle de Arán, marked variations occur during the various seasons. The daily air temperature fluctuations at 1.50 m above GL are also considerable. In fig. 5.2 the mean monthly temperatures of a typical valley station such as Viella (932 m) and of a typical mountain station such as Bonaigua (2072 m) are compared. In the same figure the average monthly as well as the absolute maximum- and minimum-temperatures are indicated. The figure shows that the average monthly amplitude in Viella amounts to 12° C, while the amplitude in Bonaigua is only 8° C. This is due to the more important influence of the free atmosphere at Bonaigua. The monthly temperature fluctuations are greater during the summer than during the winter, in both Viella and Bonaigua. In figure 5.2 it is shown that the difference between the warmest and coldest month is 15.6° C in Viella, whereas in Bonaigua it has a value of 14.1° C. The average annual temperature for the Garonne valley has a high value of 10° C. The highland stations on the contrary have a low value of only 3° C. The coldest month is not the same for the Garonne valley and the highland stations Restanca and Bonaigua. In

the Garonne valley January is the coldest and driest month (−4° C), whereas for the mountain stations February is the coldest month. For all stations, July is the warmest month, which indicates the strong influence of the Atlantic Ocean.

The annual number of days with freezing temperatures in the Valle de Arán ranges from 80 in the Garonne valley to 200 at the altitude of 2000 m. At the 3400 m level this number increases probably to 360.

The temperature data of the period 1955—1965 are compiled in appendix-tables 22—28.

5.3 Vertical temperature gradients

In order to compare the gradients between the meteorological stations, the annual fluctuations for the period 1955—1965 have been plotted in fig. 5.3. Vertical gradients on the Garonne valley floor are extremely small, variable and in some months even inversed. On the steep valley slopes, however, temperature gradients can be as high as the Naca gradient and they are constant throughout the year. The gradients between the two high mountain stations are extremely steep and variable. Very steep vertical temperature gradients have also been observed between

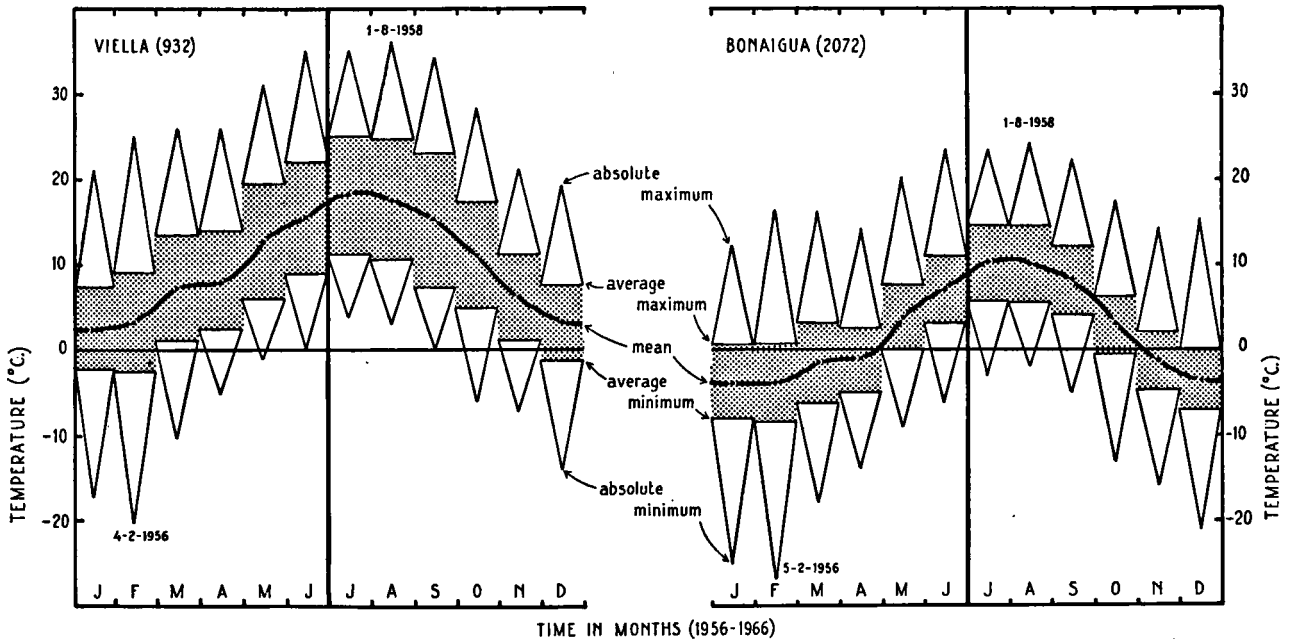


Fig. 5.2 Monthly temperature of the valley station Viella and the mountain station Bonaigua.

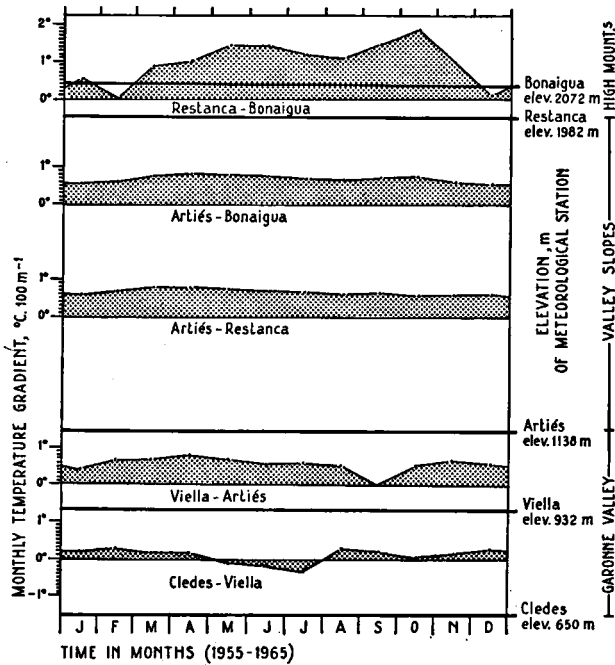


Fig. 5.3 Annual fluctuation of temperature gradients during the period 1955-1965.

Lago Restanca and Lago Mar during the summer. Maximal vertical temperature gradients occur in the Valle de Arán from March to April and October to November, whereas minimum gradients can be observed in December to January and also in August. This is largely due to the presence or absence of snow in certain parts of the Valle de Arán. In March to

April and October to November the lower parts of the valleys are free of snow while the area at the 2000 m elevation is deeply covered. In August the Valle de Arán is completely free of snow, whereas in December to January it is entirely covered.

5.4 Wind

The valley topography controls largely the movement of the air masses, in a steep mountainous terrain such as the Valle de Arán, with a weighted average slope of 27°. The rough valley topography and the slopes explain in part the great variation in wind directions. The latter are measured only at 08.00 h. The results of the observations give therefore very incomplete information about the daily mountain-valley air-circulations. The wind roses from all meteorological stations in the Valle de Arán show a maximum parallel to the trend of the valleys (fig. 5.4).

A typical morning valley slope wind, observed in the Valarties valley during the summer of 1965, is drawn in fig. 5.5. In this case the north-south oriented valley shows cold air flowing downside the shaded east slope and rising warmer air on the sunny west slope.

Results of wind velocity measurements, with a rotation anemometer, showed that at Restanca the wind velocity is low when the wind is blowing in a direction at right angles to the Valarties valley. Wind velocity appears to be higher when the wind is blowing more or less parallel to the Valarties valley. Average monthly wind velocities for Restanca are listed in table 5.3 for the period 1957-1965. From May to October, the average wind velocity is 3.8 m.s⁻¹, whereas from November to April the average wind velocity has a value of 4.3 m.s⁻¹.

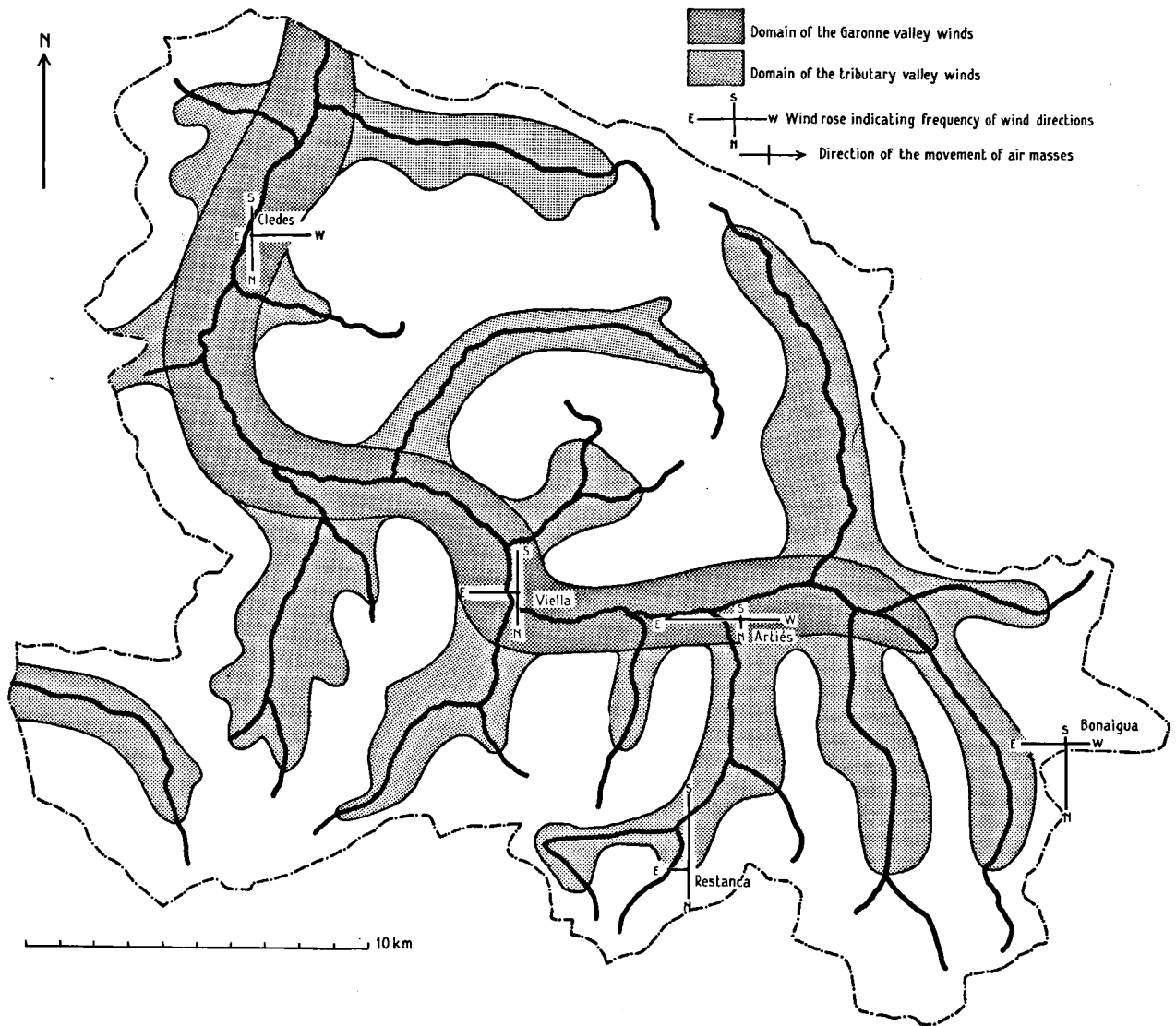


Fig. 5.4 Wind roses from meteorological stations during the period 1955–1965.

TABLE 5.3. *Monthly average wind velocity ($m.s^{-1}$) in Restanca during the period 1957–1965*

J	F	M	A	M	J	J	A	S	O	N	D	Year
4.7	4.5	4.3	3.9	3.3	3.1	3.3	3.6	3.5	3.8	4.2	4.3	3.9

5.5 Cloud cover

The cloud cover varies little over the entire Valle de Arán. The average annual percentage of clouded days amounts to 46 at all stations. April has the most clouded days (60 %) whereas January has the smallest percentage (41 %).

Cloudless days are more frequent during the winter than during the summer months. Since cloud cover observations are only carried out at 08.00 h, daily variations are not recorded.

According to our observations (1965), cloud cover in the Valle de Arán increased during the afternoon and reached a maximum at about 16.00 h. In the valleys, radiation fog has often been observed in the early morning and evening. Most cloudy days coincide with northerly winds. Persistent northern wind forces the fog up against the high water divide. A subsequent reversal from northern to southern wind results in a rapid transport of the clouds downstream. Near the high water divide, which forms the southern limit of

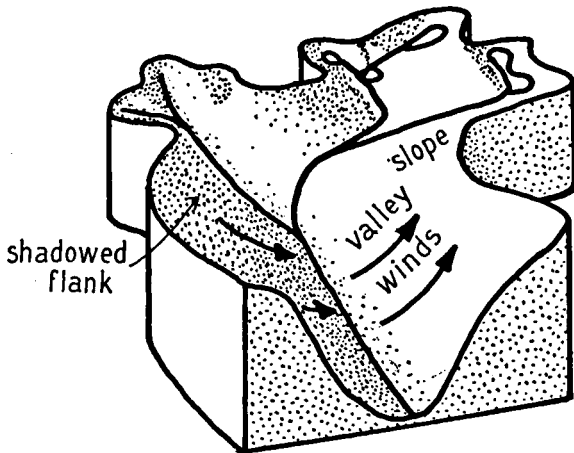


Fig. 5.5 Morning valley slope wind in the Valarties valley.

the Valle de Arán, the cloud cover appears to be slightly greater (about four percent) than in other parts of the basin.

5.6 Relative air humidity

Measurements of air humidity are restricted to the Viella-and Arties-meteorological stations. Dry- and wet-bulb psychrometers at these stations are placed in a ventilated housing at 1.50 m above GL. During measurements, carried out in the summer of 1965 (Brugman, 1965) it appeared that the non ventilated psychrometer vapor pressure values in Restanca (1982 m) had to be multiplied with a factor 0.75 in order to obtain the right values at that station. The factor 0.75 can be used to correct the non ventilated vapor pressure values of Arties (1138 m) as listed in table 5.4. In the same table, the non-corrected average monthly relative air humidity values at Viella are given. Relative air humidity data at Viella seem more reliable than in Arties, because the Viella station is better ventilated.

Relative air humidity in Restanca, with northern wind, is about 30 percent higher than with other wind directions. In Arties, there is little difference between the monthly average relative air humidity values measured at 08.00 h and those of 18.00 h (table 5.4).

TABLE 5.4. Non ventilated relative air humidity values (percentage) of Arties (08.00 h and 18.00 h) and Viella (08.00 h)

	J	F	M	A	M	J	J	A	S	O	N	D	Year
Arties 08.00 h	75.2	75.2	79.3	80.9	79.7	83.0	81.9	81.5	78.2	78.5	76.8	75.9	78.8
Arties 18.00 h	74.1	74.7	80.4	81.0	81.2	83.4	80.7	80.9	77.1	80.3	70.0	77.0	78.4
Viella 08.00 h	72.4	55.9	52.2	54.9	59.6	65.3	64.0	62.2	58.6	63.3	63.3	53.3	60.4

6. PRECIPITATION ANALYSIS

6.1 Introduction

The mean annual precipitation in the Valle de Arán increases from nearly 900 mm in the lower Garonne valley to more than 3000 mm on the highest peaks of the Maladetta massive. The weighted average of the annual precipitation for the period 1946—1966 has a value of 1325 mm.

The mean annual snowfall increases from 100 cm in the lower Garonne valley to more than 1000 cm in the Upper Esera valley. The weighted average annual snowfall amounts to 503 cm for the period 1946—1966. This means that with a water content of 10 percent of the fresh fallen snow, the average snowfall to total precipitation ratio has a value of 0.38.

6.2 Precipitation regime

The precipitation (1946—1966) in the Valle de Arán is evenly distributed throughout all seasons, but small variations are evident. There appear to be differences

between valley stations and mountain stations (Table 45).

In fig. 6.1 it is shown, that January, February, March, July and October are relatively drier months in the Garonne valley. The mountain stations do not show the dry October month. Maximum precipitation for the valley stations falls in December, except for the mountain stations in November. The minimum precipitation for all meteorological stations falls in February.

The seasonal precipitation coefficients for the Garonne valley stations Cledes (650 m), Viella (932 m) and Arties (1138) show only minor variations (table 6.1). The mountain stations Restanca (1982 m) and Bonai-gua (2072) have abundant autumn precipitation compared with the valley stations. The number of precipitation days is about the same for all months. The average annual number of precipitation days is 140 days for five stations. This corresponds to eleven to twelve monthly precipitation days (table 29).

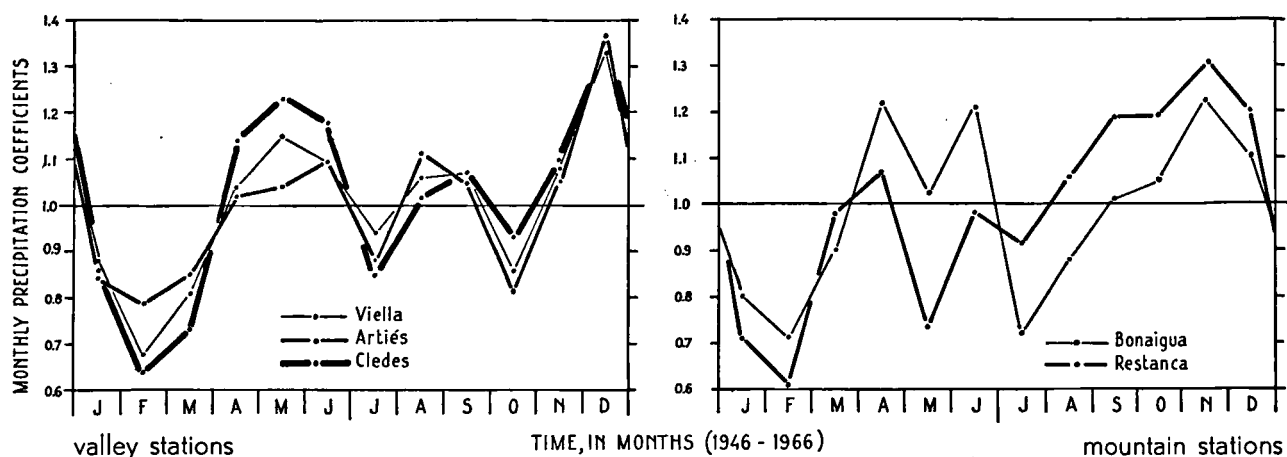


Fig. 6.1 Monthly precipitation coefficients for the valley stations and mountains stations.

TABLE 6.1. *Seasonal precipitation coefficients for five stations (1946—1966)*

Months	Cledes	Viella	Arties	Bonaigua	Restanca
M, A, M	1.03	0.99	0.98	1.05	0.94
J, J, A	1.02	1.03	1.04	0.94	1.00
S, O, N	1.02	1.01	0.98	1.09	1.24
D, J, F	0.94	0.96	1.00	0.91	0.82

6.3 Variations in the annual precipitation 1946—1966

The fluctuations in the annual precipitation for the period 1946—1966 are not great. The ratios of maximum and minimum precipitations for 20 years are all smaller than 2.0, while the average deviations of the average annual precipitation have a maximum value of 15 percent (table 6.2).

The highest monthly precipitation has been observed in Restanca in October 1960 (657 mm), and at the

same place the highest daily precipitation has been measured on November 15th (176 mm). Both precipitation maxima were measured as melted snow.

Figure 6.2 shows the 19 maximum daily rain precipitation values for Viella and Restanca. In the same figure, duration lines of (rain) precipitation periods in Viella and Restanca are indicated. Those lines are important in the runoff studies and flood analyses.

TABLE 6.2. *Fluctuations in the annual precipitation for five stations*

Station	Altitude	Average annual precipitation	Years	Maximum annual precipitation	Minimum annual precipitation	Ratio of maximum minimum	$\frac{n}{\sum_{t=0}^n} \frac{ N_t - \bar{N} }{n}$
Cledes	650 m	925 mm	1947—1966	1116 mm	694 mm	1.6	11 %
Viella	932 m	897 mm	1946—1966	1183 mm	635 mm	1.8	13 %
Arties	1138 m	937 mm	1947—1966	1273 mm	661 mm	1.9	15 %
Bonaigua	2072 m	1262 mm	1952—1966	1562 mm	1038 mm	1.5	10 %
Restanca	1982 m	1720 mm	1956—1966	2347 mm	1217 mm	1.9	11 %

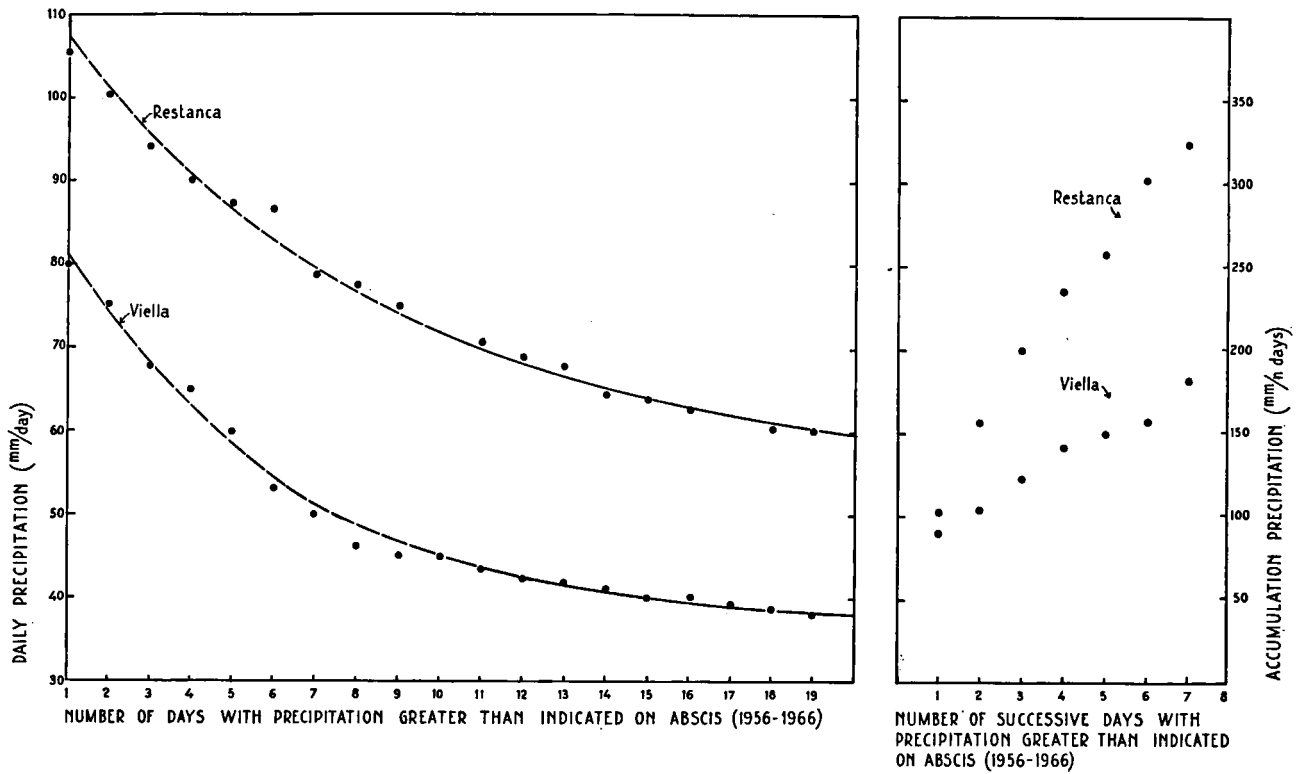


Fig. 6.2 Maximum daily rain precipitation and rain duration for Viella and Restanca (1955—1965).

TABLE 6.3. Frequency and humidity of winds (percentage)

Station	Wind direction				
	N	E	S	W	
Viella	27.2	37.6	33.2	2.0	frequency of winds (percentage)
Restanca	25.2	13.5	60.5	0.5	percentage of the total precipitation
Viella	35.8	39.8	23.2	1.2	
Restanca	29.8	18.3	51.6	0.3	percentage of the precipitation, exceeding 20 mm.day ⁻¹
Viella	36.7	42.2	19.3	1.8	
Restanca	19.1	22.8	57.8	0.2	

TABLE 6.4. Frequency of cloud cover (percentage) during different winds

Station	Wind direction				Percentage of days in cloud cover class	Frequency of cloud cover class
	N	E	S	W		
Viella	64.4	35.6	24.6	24.3	9/10—10/10	37.0
Restanca	72.8	33.4	19.7	62.5		
Viella	195.	21.3	22.4	25.7	1/10— 9/10	21.2
Restanca	16,4	28.2	56.9	25.0		
Viella	26.1	43.1	53.0	50.0	0— 1/10	41.8
Restanca	9.2	37.7	56.9	12.5		

6.4 Relation of precipitation, wind direction and cloud cover
For the stations of Viella (932 m) and Restanca (1982 m), the relations of precipitation, wind direction and cloud cover for the period 1955—1965 are summarized in tables 6.3 and 6.4.

As could be expected, moist northern and eastern winds bring most of the orographic precipitation and clouds in the Garonne valley. This is evident during the winter (November-April), when 58 percent of the northern winds bring rain or snow in Viella.

The “Balaguer”, a local name for southern wind, is much drier in Viella in all seasons, and it brings most unclouded days. Only 25 percent of the days with southern wind brings rain in Viella.

At Restanca (1982 m), which is situated at only 2 km from the main water divide, the relations of precipitation, wind direction and cloud cover are essentially the same as in Viella. However, in Restanca southern

winds predominate during all seasons (60.5 percent). During southern winds, only 25—35 percent of the days are rainy, while 53—57 percent are cloudless. On the other hand 47—49 percent of the northern winds bring rain and 84—91 percent of the days with northern winds are clouded days.

Important precipitation of a magnitude of 20 mm day⁻¹ or more falls in Viella during eastern and northern winds (79 percent) and in Restanca during southern and eastern winds (81 percent).

6.5 The precipitation map

Several problems were involved in the preparation of the Valle de Arán precipitation map (fig. 6.3).

- The systematic errors in the precipitation measurements in a steep mountainous terrain, due to the height of the rain gauge orifices above ground level and due to the location of the gauge.

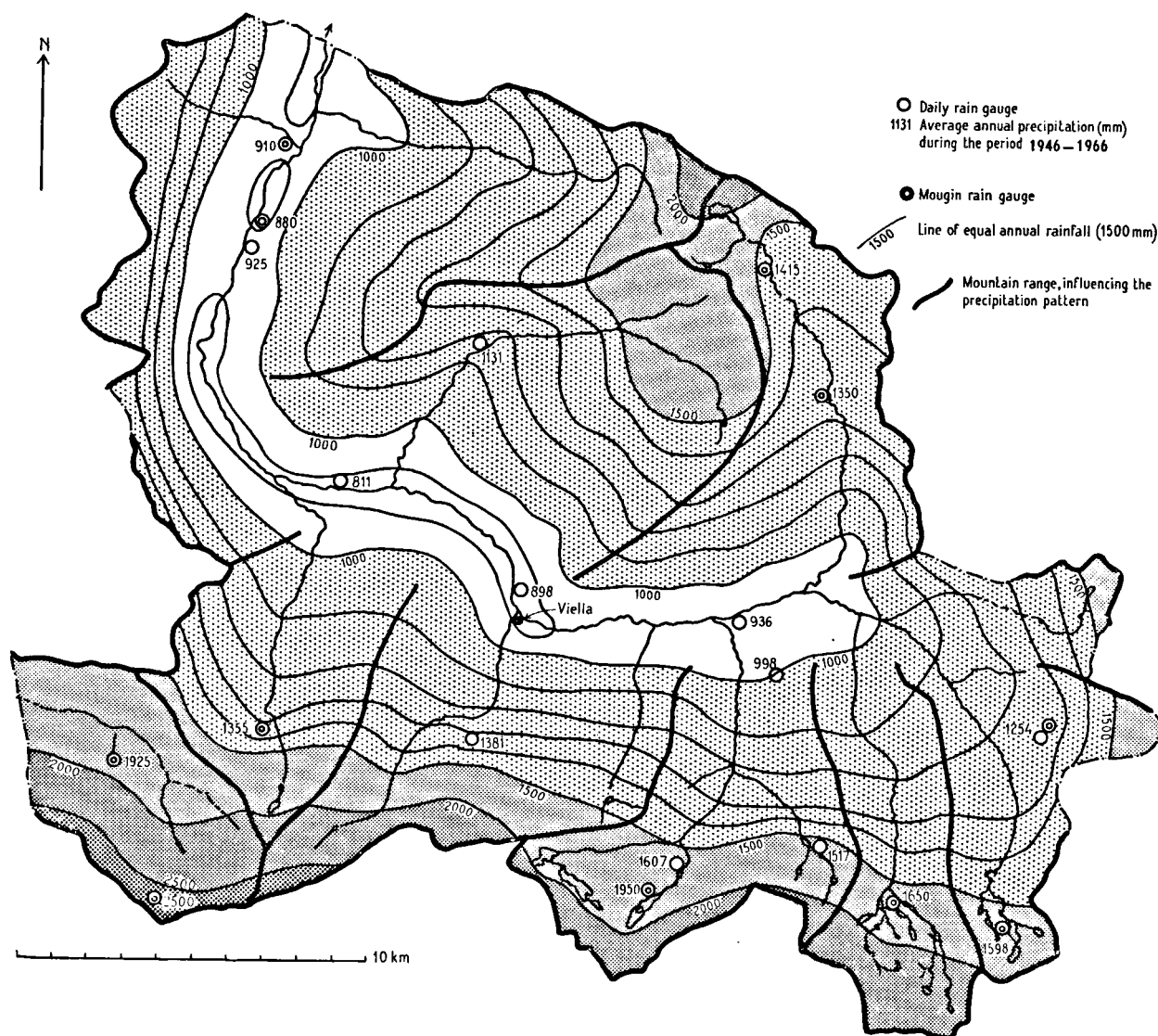


Fig. 6.3 Precipitation map of the Valle de Arán (1946—1966).

- b. The influence of the major and minor topographical features on the precipitation pattern.
- c. The augmentation of precipitation data of six short period stations with the data of four index stations by means of a correlation technique.

6.6 Height of the rain gauge orifice

From the literature there appears to be overwhelming evidence that the influence of the height of the rain gauge orifice on the results of precipitation measurements is considerable (Braat, 1945 — Bleasdale, 1959 — Bruce & Potter, 1957 — Colenbrander, 1965 — Gold, 1931 — Haver, 1951 — Kurtyka, 1953 — Lacy, 1951 — Nagel, 1954 — Poncelet, 1959 — Riesbol, 1940 — Stanhill, 1958 — Winter, 1962).

In the Valle de Arán, all daily rain gauges have their orifices at a height of 1.45 m above GL, while the accumulating Mougain rain gauges have their orifices at a height of 2.50 m or 4.40 m above GL. All these precipitation measurements are lower than could be expected from gauges with orifices situated at ground level. This can be illustrated with some examples:

- a. At the meteorological station Bonaigua (2072 m), two rain gauges are situated 10 m apart. The lower daily rain gauge (X) with its orifice at 1.50 m above GL receives 44 percent more precipitation than the

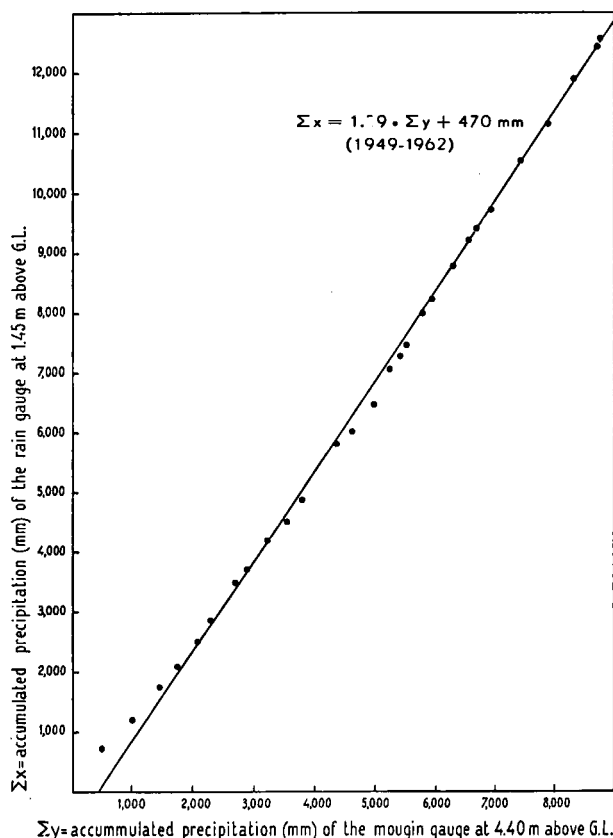


Fig. 6.4 Double mass curve of the Bonaigua precipitation measured in a Mougain gauge (y) and in a daily rain gauge (x).

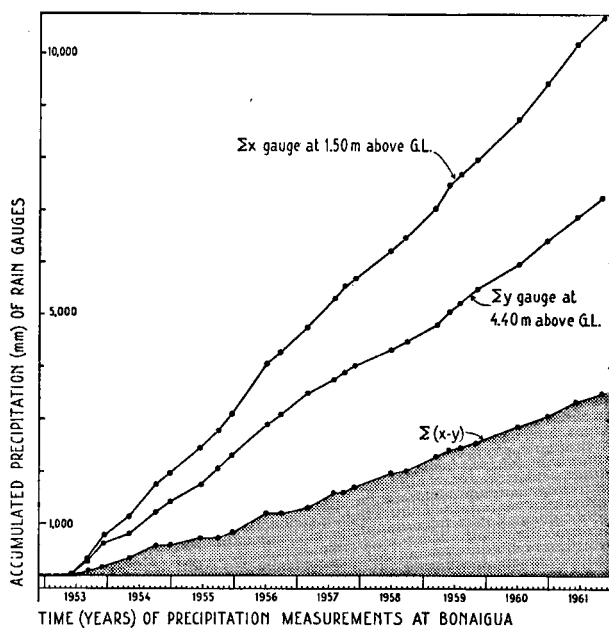


Fig. 6.5 Accumulated precipitation values of Bonaigua, showing the 44 percent error in the measurements at 4.40 m above ground level.

Mougain gauge (Y) with its orifice at 4.40 m above GL. The equation of the line, drawn through the accumulated precipitations of X and Y is: $X = 1.39 \cdot Y + 470$ mm (fig. 6.4). The relation of X and Y is not linear; in the winter half year the difference between X and Y is greater than in the summer half year. This is shown in fig. 6.5, where the broken line $\Sigma(X-Y)$ has been plotted for the period 1953—1961. The wind effects on snow precipitation measurements with a Mougain gauge are more important than on rain precipitation measurements.

- b. In Colomés (2170 m), in the high Aiguamoix valley, the Mougain precipitation, measured at 4.40 m above GL, is 45 percent less than the precipitation, measured at 1.45 m, in Moncasau (2017 m), although the Mougain gauge is situated 150 m higher above MSL. The horizontal distance between Colomés and Moncasau is two km and the measurements were taken over a five-year period.

- c. In Restanca (1982 m) and Lago Mar (2230 m), simultaneous precipitation measurements have been carried out as part of the Lago Mar project (Martinec, Wartena, Brugman & Zeilmaker — 1966). The rain gauge at Restanca has a height of 1.45 m, whereas the Lago Mar gauge was placed at 0.40 m above GL. The horizontal distance between Restanca and Lago Mar is one km and the measurements were taken over a two month's period. The results indicate, that the observed daily precipitation near Lago Mar in the 0.40 m gauge was 77 percent too high, compared with the measured daily precipitation near Restanca. A correction factor of 1.44, which has been found at Bonaigua (2072 m), has been used to correct the

results of the precipitation measurements for other Mougou gauges with their orifices at 4.40 m above G.L. In this manner the precipitation values at Saburedo (2330 m), Colomés (2170 m), Maladetta (2980 m), Renclusa (2150 m), Pas Estret (2050 m) and Plâ de l'Ana (1800 m) have been multiplied with 1.44.

For the Mougou gauges with their orifices at 2.50 m above G.L. different correction factors have been estimated. For Lago Mar (2300 m) a correction factor of 1.10 has been assumed and for Artiga de Lin (1450 m) a factor of 1.05. At Artiga de Lin the snow period is short. No correction has been applied for the Bausen gauge, because the precipitation values correspond with the values of Cledes.

Simultaneous snow measurements were taken at 1.45 m above G.L. and at G.L. The latter average reading exceeds the former by six percent (6.12).

6.7 Regression analysis

The supplementary data from the index stations (X_i) Cledes, Viella, Arties and Bonaigua have been used to provide a better estimate of the population parameters of the (Y_i) stations Benos, Camara-Barrados, Viella Tunnel North, Camara Arties, Restanca and Moncasau, whose records are shorter (fig. 3.2). By

applying the regression and correlation analysis the following assumptions were made:

1. The monthly precipitations are normally distributed.
2. A stable precipitation regime is known to exist so that significant correlation between the index stations (X_i) and the Y_i stations can be expected.
3. The rain gauge localities and methods of measurement have not been altered.
4. X_i and Y_i are linearly related.

With the 1620 IBM computer of the "RAET" computer centre of the Netherlands Land Development Consultants Ltd, Arnhem, 16 regression coefficients of Y_i on X_i and of X_i on Y_i have been calculated for the monthly precipitation values. The correlation coefficients and standard deviations have been computed. The results of the computations are listed in table 6.5. After testing the correlation coefficients, all values appeared to be highly significant. We can therefore conclude that there exists a linear relationship between the monthly precipitations measured in the Valle de Arán at various meteorological stations. This is in accordance with the results of Rubinstein (1956).

TABLE 6.5. *Regression analysis of monthly precipitation values*

Index station X_i	Altitude (m)	Station Y_i	Number of items	Standard deviations (mm)		Correlation coefficient r	Correlation equations	
				G_x	G_y		$X_i =$	$Y_i =$
Cledes	650	Benos	124	20.3	15.7	0.88	$0.96y + 7.33$	$0.80x + 11.35$
Cledes	650	Viella	232	25.2	23.4	0.82	$0.88y + 11.11$	$0.76x + 16.05$
Cledes	650	Camara Barrados	68	20.5	21.9	0.87	$0.78y + 2.84$	$0.97x + 20.43$
Viella	932	Benos	124	22.0	20.8	0.84	$0.90y + 10.69$	$0.79x + 13.19$
Viella	932	Camara Barrados	68	19.9	24.1	0.85	$0.70y + 9.69$	$1.03x + 15.91$
Viella	932	Viella Tunnel North	69	24.9	47.4	0.77	$0.41y + 27.53$	$1.47x + 9.08$
Viella	932	Viella Tunnel North*	68	21.8	31.7	0.82	$0.57y + 9.67$	$1.20x + 25.44$
Arties	1138	Camara Arties	45	20.4	20.0	0.86	$0.88y + 2.09$	$0.85x + 17.71$
Arties	1138	Viella	232	21.4	20.6	0.86	$0.90y + 9.8$	$0.83x + 10.70$
Arties	1138	Restanca	126	29.0	66.8	0.69	$0.30y + 35.50$	$1.60x + 15.14$
Arties	1138	Restanca**	124	27.3	49.3	0.72	$0.40y + 22.83$	$1.31x + 31.07$
Arties	1138	Moncasau	70	25.4	44.2	0.75	$0.43y + 20.65$	$1.31x + 24.41$
Arties	1138	Bonaigua	176	29.3	36.0	0.72	$0.58y + 16.36$	$0.89x + 36.55$
Bonaigua	2072	Camara Arties	45	30.6	23.9	0.80	$1.02y + 21.85$	$0.62x + 14.90$
Bonaigua	2072	Moncasau	70	37.9	44.8	0.74	$0.63y + 32.76$	$0.88x + 23.70$
Bonaigua	2072	Restanca	126	37.4	66.1	0.70	$0.40y + 52.14$	$1.24x + 6.03$

* September 1960 not included.

** October 1960 and November 1963 not included.

TABLE 6.6. Average annual precipitation values (mm) during the period 1946—1966

Meteorological station	Altitude (m)	Precipitation (mm)	Mougin rain gauge	Altitude (m)	Precipitation (mm)
Cledes	650	925	Pas Estret	2050	1415
Viella	932	898	Pla de l'Ana	1800	1350
Arties	1138	936	Saburedo	2330	1598
Bonaigua	2972	1255	Colomes	2170	1620
Benos	811	886	Artiga de Lin	1450	1355
Camara Barrados	1280	1131	Renclusa	2150	1925
Viella Tunnel North	1400	1381	Maladeta	2980	2500
Restanca	1982	1607	Lago Mar	2300	1950
Camara Arties	1940	998	Bausen	650	910
Moncasau	2017	1517			

The regression equations of table 6.5 have been used to compute the mean monthly precipitations over the periods without data for the Yi stations. By applying this procedure complete data of ten stations were obtained for the preparation of the precipitation map. The Mougin gauge records from the ten high mountain stations showed gaps. They have been calculated by applying the normal ratio method of the U.S. Weather Bureau (1952).

The results of all computations are given in table 6.6 and these data were used in constructing the precipitation map of the Valle de Arán.

6.8 Major topographic features, which influence precipitation

The Valle de Arán has a weighted average slope of 27°, which has an important effect on the movement and stability of the flowing air masses. The air flow in the Valle de Arán moves in the broad and slightly curved Garonne valley and in its nine tributaries. The watersheds, which affect the precipitation pattern and the air flow are indicated in figure 6.3 and 5.4.

The orographic precipitation in the Valle de Arán is largely induced by the air circulation from northern directions. Humid Atlantic air masses, which cross the Valle de Arán in a NW-SE direction, flow through the broad Garonne valley. The air flow is obstructed by the EW directed watershed of the Toran and Barrados valleys. The continuing air flow, funneling through the seven NS directed valleys, is blocked at the high and narrow upper stream valleys. Near the main water divide, air masses are forced to rise over a continuous EW range of mountain peaks, which vary in altitude from 2300—3400 meters which produces heavy orographic rainfall (fig. 5.4).

The relation of the annual precipitation and altitude is shown in figure 6.6 for nineteen stations. The important increase of the precipitation with height cannot without further data be applied to the area. In the Garonne valley for instance, a decrease of 10 mm . 100 m⁻¹.year⁻¹ in annual precipitation from Cledes (650 m) to Viella (1138 m) has been measured, which is the result of the broad valley near Viella. In the high mountains from Restanca (1982 m)

TABLE 6.7. Increase of the precipitation from the valley station Arties to six mountain stations in mm.100 m⁻¹. year⁻¹

Stations	Increase in mm.100 m ⁻¹ . year ⁻¹	Direction
Arties—Bonaigua	34	ESE
Arties—Bonaigua, corrected	52	ESE
Arties—Saburedo	54	SE
Arties—Colomes	66	SSE
Arties—Moncasau	69	SSE
Arties—Restanca	79	S
Arties—Lago Mar	88	SSW

to Lago Mar (2300 m), however, an increase of 110 mm . 100 m⁻¹.year⁻¹ has been observed. Therefore in the main Garonne valley a very uniform precipitation pattern exists; the situation changes completely near the main water divide. From table 6.7 it appears, that the increase in annual precipitation from the station Arties is largest in a N-S direction (orographic rainfall) and smallest in an E-W direction. Besides the precipitation pattern in the N-S valleys, diverging pattern exists in the E-W valleys of the Toran and Barrados rivers, because frequent western winds from the broad adjacent Pique valley produce orographic precipitation on the slopes of the Liat mountains.

6.9 Precipitation on steep valley slopes

For the study of the influence of minor topographical features, i.c. steep valley slopes, we used the data from three stations: Arties (1138 m), Camara Arties (1940 m) and Bonaigua (2072 m).

Camara Arties is situated at the top of the south Garonne valley slope, directly above the index station Arties. Arties is a valley floor station with an average annual precipitation of 936 mm. The average annual precipitation in Camara Arties amounts to 998 mm.

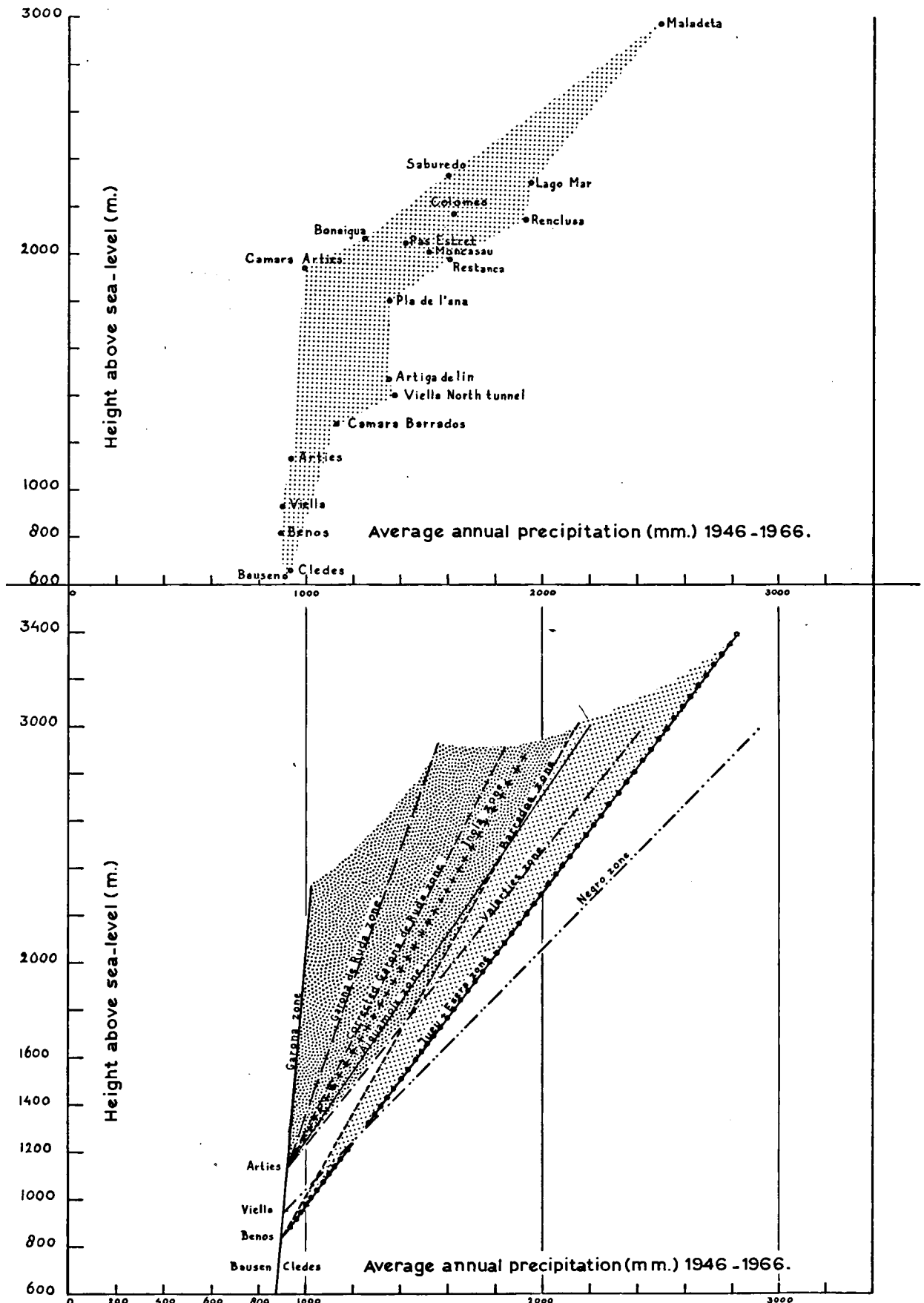


Fig. 6.6 Relation of the average annual precipitation (mm) and altitude (m) during the period 1946—1966.

In spite of its greater altitude (802 m), Camara Arties has only 62 mm more rainfall than Arties, corresponding with an increase of 8 mm.100 m⁻¹.year⁻¹. The increase in precipitation on the steep Garonne valley slope is apparently excessively small. It can therefore be concluded, that the precipitation pattern in the Garonne valley is very uniform. This is also demonstrated by the extremely small increase from Cledes (650 m) to Arties (1138 m), amounting to 5 mm 100 m⁻¹.year⁻¹ over a distance of 25 km along the Garonne valley bottom.

The second possibility to study the problem is offered by a comparison of the Arties and Bonaigua index stations. Despite the high elevation of Bonaigua (2072 m), its annual precipitation is low (1254 mm). The increase in precipitation has a value of only 34 mm 100 m⁻¹.year⁻¹. In order to correct the low value of 34 mm 100 m⁻¹.year⁻¹, we have used the computed factor of Arties-Camara to Arties (8 mm 100 m⁻¹.year⁻¹) for the valley slope near Bonaigua. The annual precipitation for the Garonne valley floor has been calculated to be 1225 mm, by adjusting the 1254 mm-value for Bonaigua. This value gives us a "corrected Arties-Bonaigua factor", which corresponds with an increase in average annual precipitation of 52 mm 100 m⁻¹.year⁻¹. This value fits much better in the general precipitation pattern of the N-S valleys and in the general trend of table 6.7.

During the preparation of the precipitation map for the Valle de Arán we allowed for valley wall- and orographic-effects. The precipitation map for the Toran valley (fig. 6.3) is only approximate.

6.10 Snowfall

A snowfall map, using the data of eleven stations, has been prepared. The snowfall data are listed in the appendix, tables 11—20 and 30.

The normal ratio (method U.S. Weather Bureau) has been determined for a number of stations and it has been used to complete the short range observations. The average annual snowfall for each of the eleven

TABLE 6.8. Average annual snowfall (cm) for eleven stations during the period 1946—1966

Meteorological Station	Altitude (m)	Snowfall (cm)
Cledes	650	58
Bossost	780	76
Benos	811	90
Viella	932	113
Arties	1138	175
Camara Barrados	1280	256
Viella Tunnel North	1400	252
Camara Arties	1940	606
Restanca	1982	575
Moncasau	2017	650
Bonaigua	2072	674

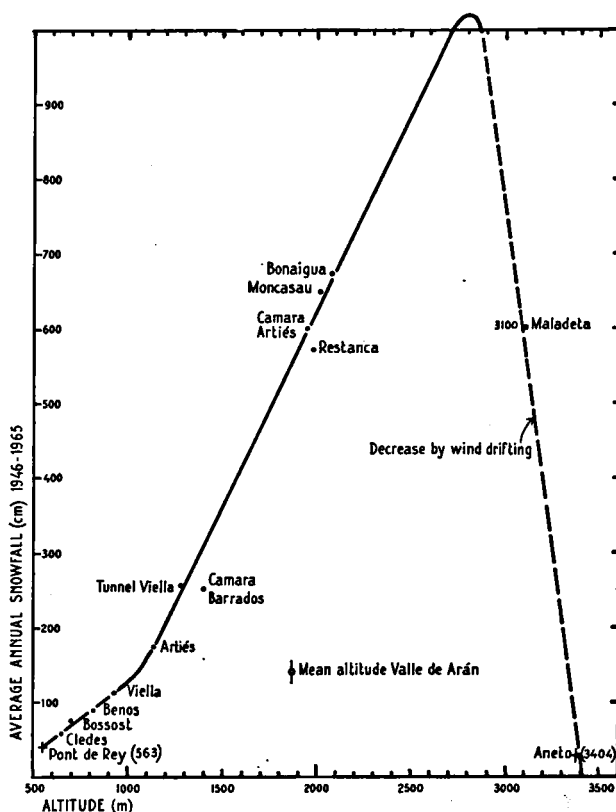


Fig. 6.7 Relation of the average annual snowfall (cm) and altitude (m) during the period 1946—1966.

stations is given in table 6.8. The relation of snowfall and altitude is shown in fig. 6.7.

The snowfall increases linearly with altitude and it is quite independent of valley effects. The valley effect from Cledes to Viella is only minor with a snowfall of only 23 cm.100 m⁻¹.year⁻¹, while the average increase in other parts of the Valle de Arán is 50 cm. 100 m⁻¹.year⁻¹.

On the snowfall map (fig. 6.8) the lines of equal snow height follow the contours of the topographical map. The map has been corrected for wind effects, because on steep cirque walls no important snow deposition is possible. The steep cirque ridges in the Valle de Arán are therefore indicated on the snowfall map as areas of non deposition. From the snowfall map and the precipitation map a snow versus total precipitation ratio map has been prepared for the period 1946—1966 (fig. 6.9).

6.11 Snow duration

In the lower parts of the Valle de Arán the average winter temperature is more than 0° C (appendix-tables 22—24). Periods of snowfall are short and irregularly distributed throughout the winter in the Garonne valley. The average temperature during the winter half year in Restanca and Bonaigua is, however, always below 0° C. From the average temperature of the winter half year at Restanca (—2.1° C) and Bonaigua (—2.7° C) and from the average tem-

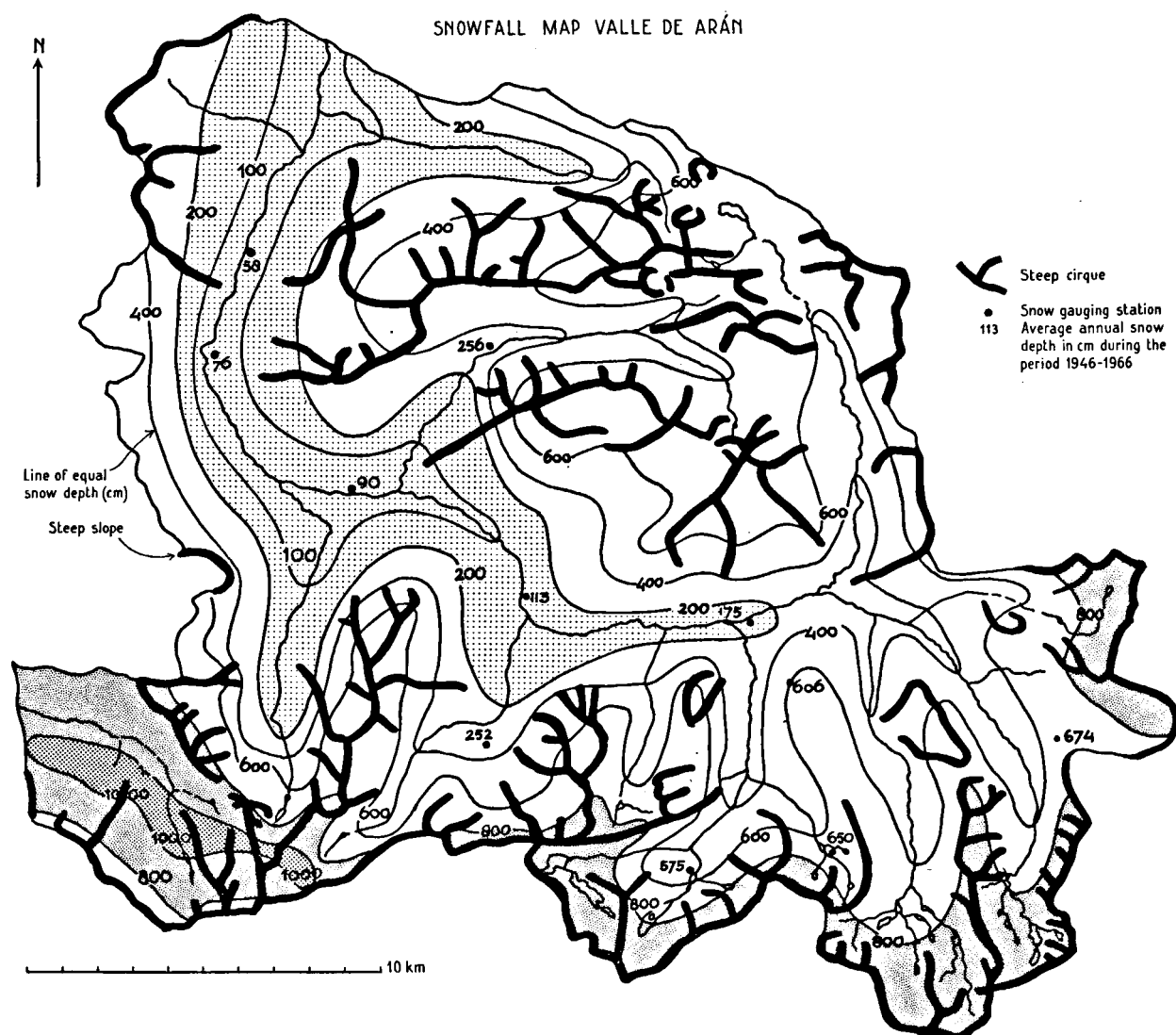


Fig. 6.8 Snowfall map of the Valle de Arán during the period 1946—1966.

perature gradients Arties-Restanca ($0.70^{\circ}\text{C}\cdot 100\text{ m}^{-1}$) and Arties-Bonaigua ($0.73^{\circ}\text{C}\cdot 100\text{ m}^{-1}$), it is possible to calculate the elevation of the winter 0°C isotherm. In the winter half year the 0°C isotherm appears to be situated at the 1700 m level, which corresponds with the 400 cm snow contour. Since 60 percent of

the Valle de Arán is situated above the 1700 m contour, the Upper Garonne basin has a tremendous water storage in the winter half year ($140\cdot 10^6\text{ m}^3$), equivalent to 18 percent of the total annual precipitation.

TABLE 6.9. *Water content of fresh snow, (percentage) measured at three stations during the period 1956—1965*

Meteorological station	Number of measurements	Total snow depth at G.L. (cm)	Total precipitation in rain gauge (mm) at 1.45 above G.L.	Water content % of fresh snow
Arties	282	1,945	1,831	9.4
Restanca	661	6,366	6,232	9.8
Bonaigua	724	7,583	6,863	9.1
Total	1,667	15,894	14,926	9.4

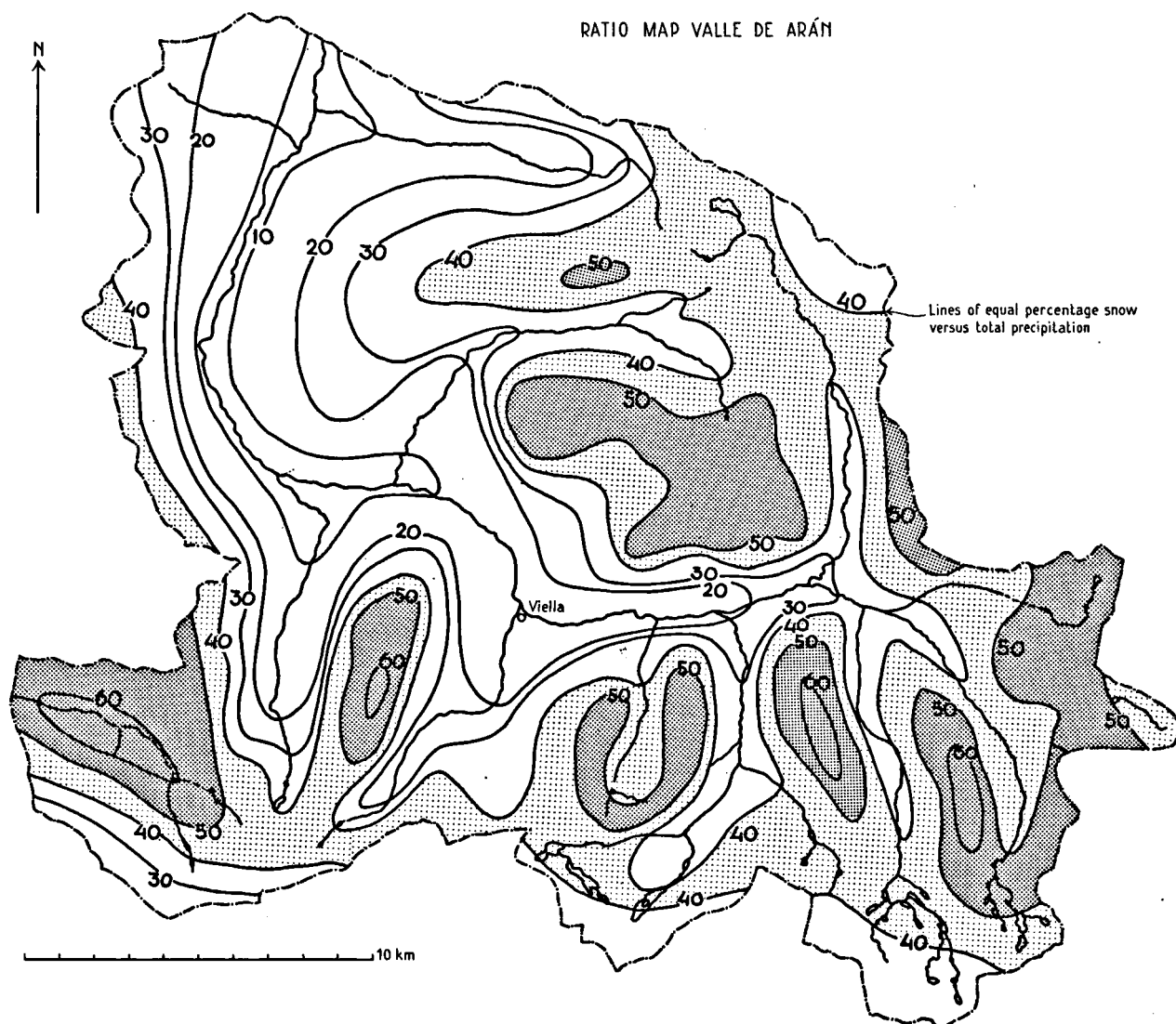


Fig. 6.9 Snow to total precipitation ratio map of the Valle de Arán during the period 1946—1966.

6.12 Water content of fresh snow

It was possible to calculate the water content of fresh snow by comparing the measured snow height at ground level with the snow precipitation in the rain gauges in the Valle de Arán. The results of the computations are listed in table 6.9.

From 1667 measurements the average water content of fresh fallen snow could be determined as 9.4 percent. Meinzer (1942), however, measured a water content of 10.0 percent. Our results show a 6 percent lower precipitation at a level of 1.45 m, compared with the precipitation of snow at ground level.

7. RUNOFF

7.1 Introduction

The purpose of this investigation was to apply the theory of De Jager (1965) on a steep mountain terrain as the Valle de Arán. The influence of vegetation, geology and morphology on runoff was also involved in this study. Finally the flood frequency and the effect of hydroelectric power generation on floods was investigated.

7.2 Available data

Some of the thirty-three runoff gauging stations in the Valle de Arán were designed and built as early as 1922 by the excellent Swiss engineer M. Würth. The entire distribution pattern of the streamflow stages, weirs and recording gauges is largely the result of his early and accurate studies concerning the hydrology of the Valle de Arán. Many old data, however, have been lost

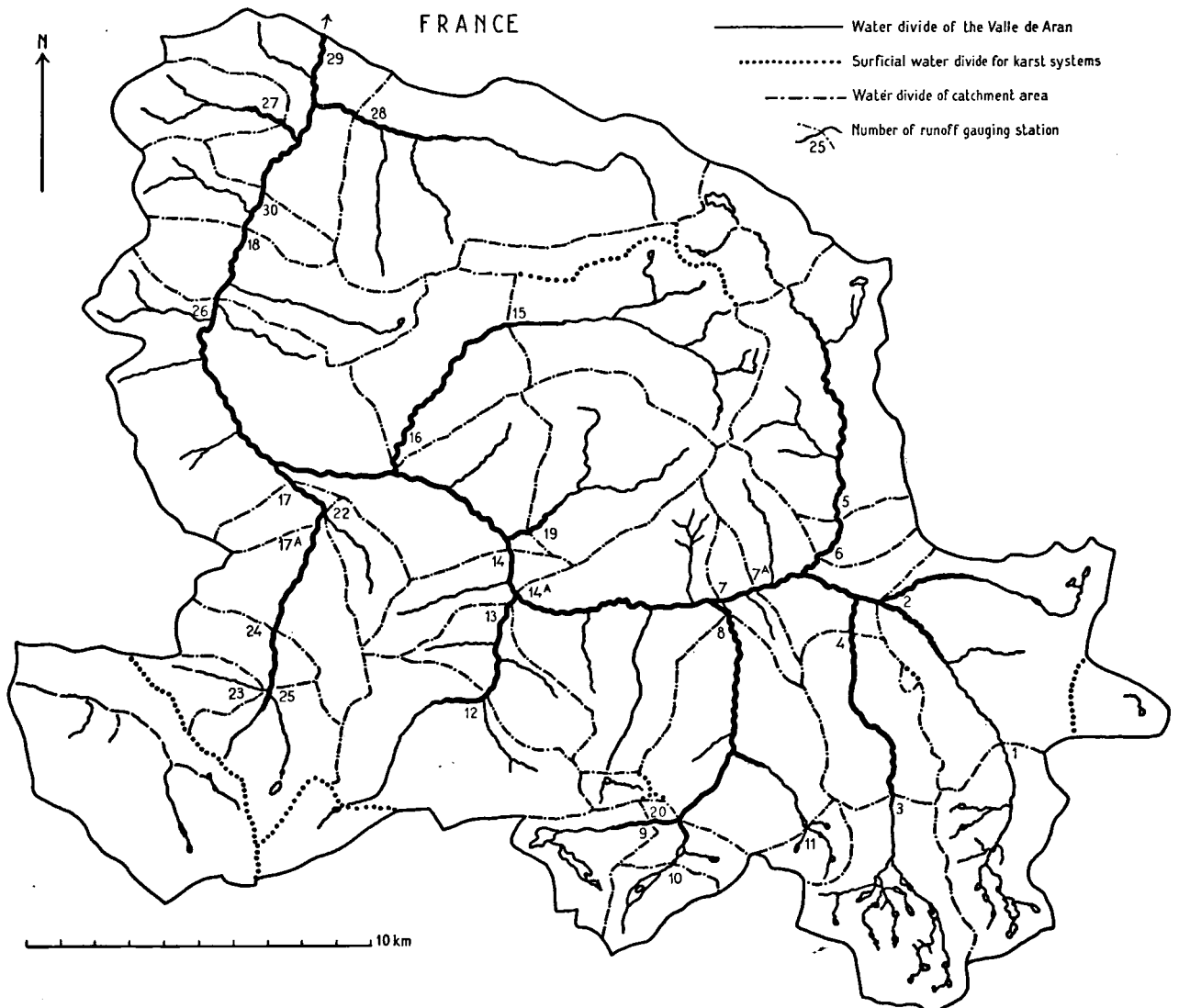


Fig. 7.1 Distribution of runoff gauging stations and catchment areas, showing the effect of karst systems.

during the Civil War and World War II. Figure 7.1 shows the distribution of the gauging stations, their catchment areas and the influence of the karst on some drainage basin areas. Figure 7.1 represents the situation before the construction of hydro power systems. In the bar graph of fig. 7.2 the available surface water data for 1945—1966 are shown, whereas in table 7.1 the new drainage areas after the construction of hydro power systems are indicated.

The daily stage data of the runoff gauging stations proved to be almost useless in analyzing the fast runoff characteristics of the catchment areas, because they are read only once a day. Only a few gauging stations are equipped with concrete weirs, which give reliable data for the flood frequency analysis, as well as for the calculation of the slow runoff characteristics or for the waterbalance. Almost all data could be used for the determination of the runoff regimes.

Of the twenty-six runoff stations twenty-one are read

once a day, three are read once every three days, and two every fourteen days.

The errors in the total annual discharge calculations, produced by this method of reading the stream flow stages cannot be estimated. Continuous recorded streamflow data over a restricted period were available from the stations 3, 20 and 25. The data of stations 3 and 20 have been used to compute the runoff characteristics of the Upper Aiguemoix- and Valarties-rivers. The data of station 25 were used in the computations of the karst reservoir of the Güells del Jueu system (see 11.10).

7.3 Stage-discharge relations

It is common practice in the FECSA, to determine the stage-discharge relations by measuring the water velocity, while the corresponding stage heights are read once or twice a month. Those measured values are plotted for a calendar year on linear paper.

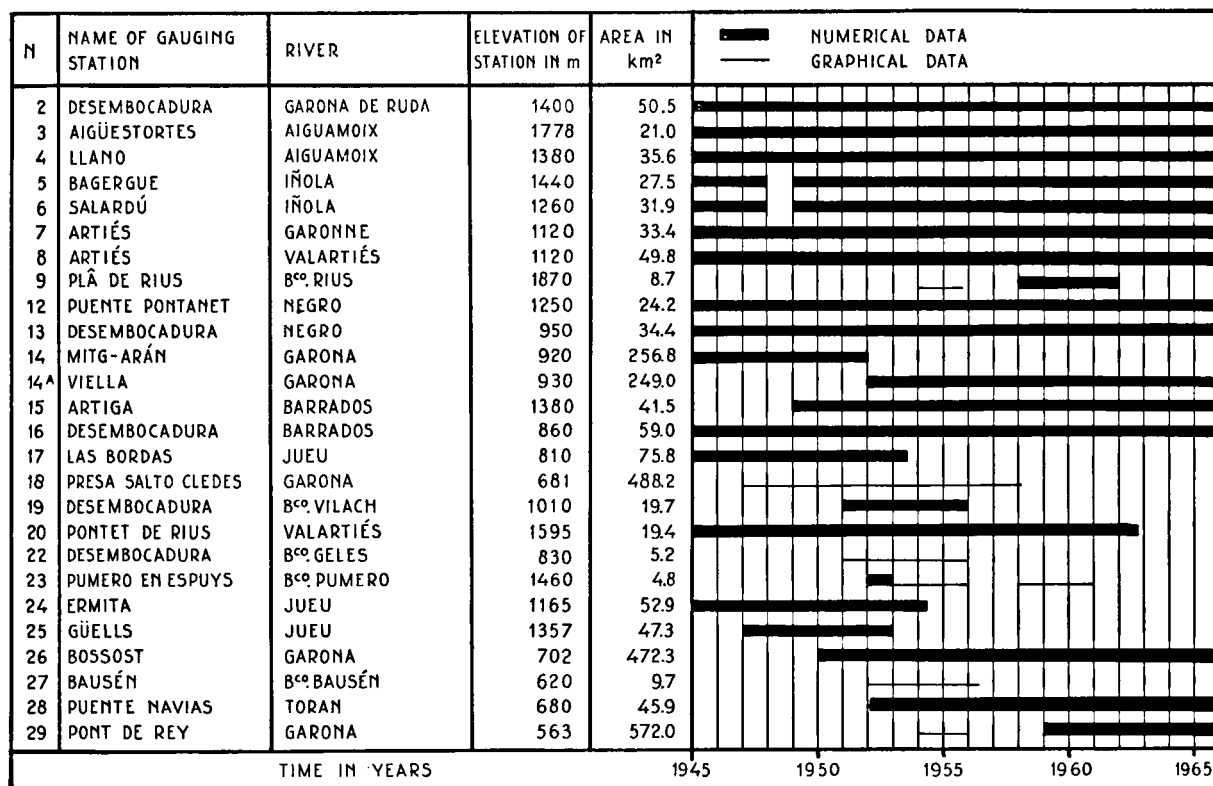


Fig. 7.2 Bar graph, showing runoff records during the period 1946—1966.

TABLE 7.1. *New drainage areas (km²) after the construction of hydropower systems*

Runoff gauging station number	Adjusted area (km ²)	Date of adjustment	Hydropower system
2	42.3	19-12-'54	Arties I
2	0.07	26- 8-'65	Arties II
3	6.10	19-12-'54	Arties I
4	20.4	19-12-'54	Arties I
5	2.6	26-12-'65	Arties II
6	7.0	26-12-'65	Arties II
7	112.7	19-12-'54	Arties I
7	23.7	26- 8-'65	Arties II
8	32.3	19-12-'54	Arties I
8	21.8	26- 8-'65	Arties II
9	3.7	19-12-'54	Arties I
14a	55.8	19- 3-'47	Viella
15	0.05	13-10-'56	Benos II
16	18.5	13-10-'56	Benos II
17	19.6	28- 4-'58	Benos III
17a	8.9	12- 1-'52	Benos I
20	6.1	19-12-'54	Arties
27	16.6	13- 1-'63	Toran

The obtained relation between stage and discharge (h/Q) is used by the FECSA for a calendar year in

order to convert daily stage data into discharge data. It is evident that this procedure is inefficient. The calculated errors in the total annual discharge, produced by this method, range from ten to twenty percent. In order to obtain better stage-discharge relations, a constant slope of the water surface was assumed and the formula of Krayenhoff van de Leur (1965) was applied:

$$2 \log Q = p \log h + \text{constant (1)} \quad (\text{see list of symbols}).$$

The available stage-discharge data were divided into stage-discharge curves from June to May (fig. 7.3). The following errors could not be eliminated: the tremendous snowmelt runoff in spring, the variable backwater, the aquatic vegetation, and the ice or variable channel storage.

From figure 7.3 an impression can be obtained on how some channels change in the course of two or three years.

7.4 Land classification map and morphometric analysis

The enclosed land classification map (scale 1:50,000) was prepared by B. van Hoorn and H. Rijckborst from sixty-two aerial photographs (24 × 24 cm) — 1:37,000 — from 1948, covering the Valle de Arán and the Upper Pallaresa. The total areas of the distinguished units such as scree, barren rocks etc. were measured for each of the thirty-three drainage areas. The average error in the measurements amounted to

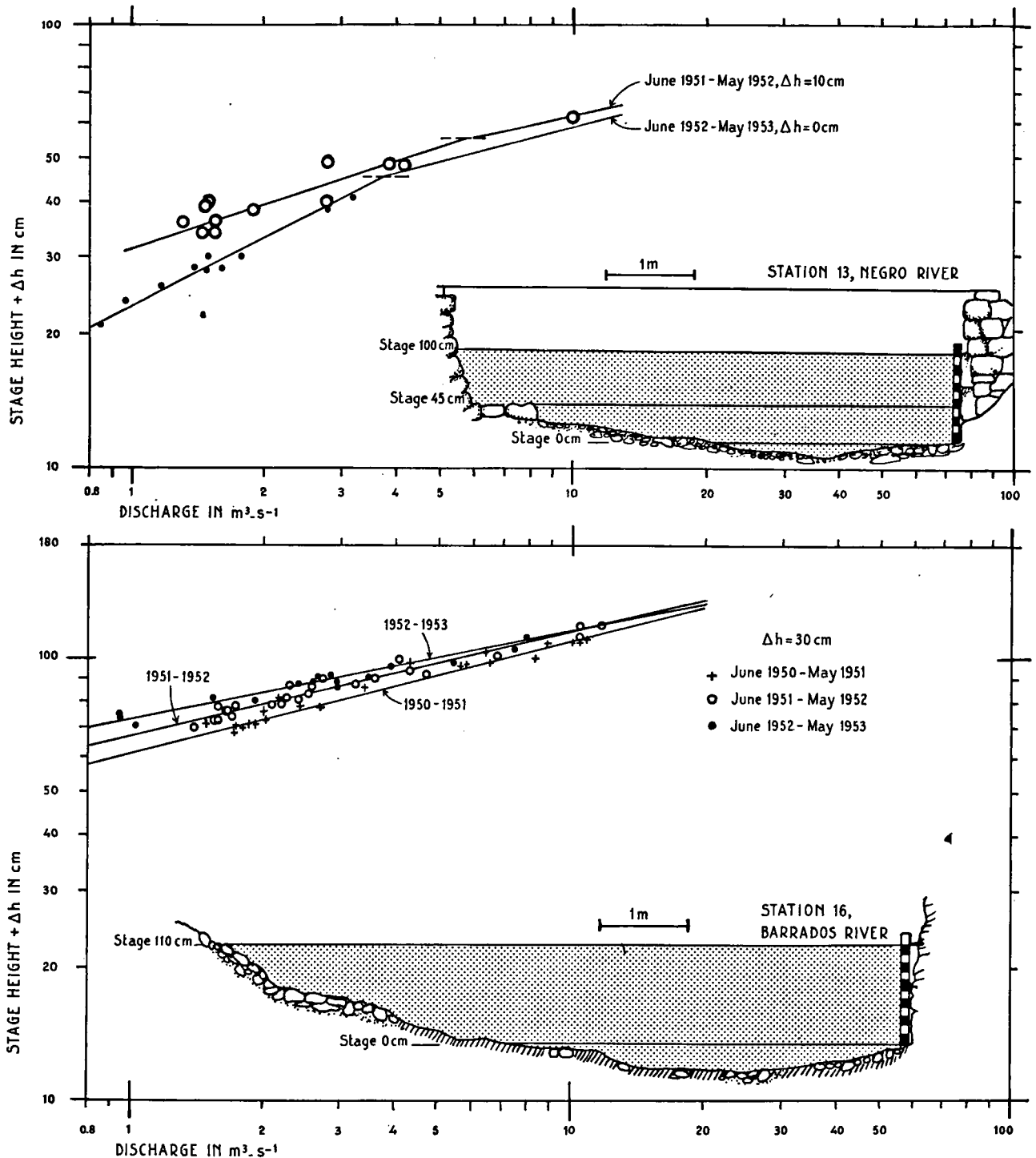


Fig. 7.3 Stage-discharge curves for runoff gauging station 13 (Negro River) and 16 (Barrados River).

six percent. The results of the computations are listed in table 7.2 and fig. 7.6.

The morphometric analysis involved the measurement of the area-altitude distributions for each of the thirty-three drainage areas (fig. 2.1). The weighted average slope for each basin was also determined (fig.

2.1). The accuracy of those measurements was within five percent, largely due to the good quality of the topographical map 1:50.000 of the Valle de Arán, prepared by FECSA. This topographical map was also used for the land classification map. The work of the Swiss engineer W. Würth, who prepared excellent

TABLE 7.2. Areas (km²) of units of the land classification map for thirty-three drainage basins

Number of basin	Scree	Grassland	Barren rocks	Lake	Village	Deciduous trees and brushwood	Conifers	Grass and scattered small groups of trees	Barren rocks and scattered small groups of trees	Arable land
1	1.62	4.05	6.81	0.50	—	—	—	2.72	0.52	—
2	6.49	11.76	2.34	0.25	—	—	1.00	5.71	3.07	—
3	2.33	1.25	12.26	1.36	—	—	1.70	0.41	1.23	—
4	1.86	4.25	0.03	—	—	—	1.45	6.76	0.70	—
5	3.23	18.15	4.51	—	0.05	0.13	—	0.52	0.52	0.37
6	0.53	3.22	0.04	—	0.06	—	—	0.16	0.35	0.09
7	2.35	10.97	1.08	—	0.45	—	3.12	0.69	0.62	—
8	4.35	2.21	0.95	—	0.01	—	8.95	5.07	1.80	—
9	2.07	—	5.08	0.70	—	—	—	—	0.83	—
10	0.79	—	4.32	0.53	—	—	—	0.06	0.27	—
11	0.91	0.21	1.82	0.30	—	—	—	0.57	0.82	—
12	5.17	13.85	1.63	—	—	0.48	2.15	0.35	1.13	—
13	1.05	4.93	—	—	0.03	0.50	2.25	0.10	—	0.90
14	4.35	15.01	1.56	0.07	0.50	1.10	3.65	1.66	0.55	4.35
15	4.13	17.20	5.82	0.19	0.04	1.05	2.22	1.67	0.45	—
16	1.05	4.32	0.07	—	0.06	2.20	2.85	1.66	—	0.22
17	1.02	7.20	0.25	—	0.10	2.78	6.00	0.15	—	0.23
18	0.80	7.46	0.03	0.04	0.17	1.62	3.35	1.40	1.00	0.10
19	2.59	9.53	2.30	—	—	—	3.71	0.57	0.92	0.35
20	1.21	0.44	0.90	0.90	—	—	0.30	—	1.26	—
22	0.12	0.94	0.21	—	—	1.40	1.18	1.27	—	—
23	1.30	2.62	0.50	0.04	—	0.08	0.20	—	—	—
24	0.39	2.90	—	—	0.01	0.90	1.40	0.07	—	—
25	1.59	4.77	2.59	0.06	—	1.10	0.54	—	—	—
26	1.65	12.43	0.37	—	0.93	8.63	19.90	7.70	—	9.15
27	0.03	7.20	0.15	—	0.03	1.24	1.17	0.70	—	0.27
28	5.00	12.62	4.85	0.29	0.46	7.78	9.40	4.32	3.10	1.25
29	0.62	1.23	0.72	—	0.32	3.46	2.90	8.76	0.80	2.10
30	0.20	1.67	—	—	0.08	2.82	2.35	1.35	—	0.20
31	5.34	6.93	13.10	0.20	—	—	0.02	4.97	0.90	—
32	0.67	2.11	0.85	0.05	—	—	—	—	—	—
33	1.82	4.51	4.11	0.40	—	—	—	—	—	—
Total	68.32	196.53	84.91	5.97	3.30	37.27	80.05	57.59	21.32	19.58
%	11.9	34.2	14.8	1.0	0.6	6.5	13.9	10.0	3.7	3.4

topographical maps at a scale of 1:20,000 for the high and inaccessible parts of the Valle de Arán, deserves special attention.

7.5 Introduction to runoff characteristics

The translation and transformation of a precipitation pattern into a runoff surge depends on the temporal water storage. The runoff intensity in this process is determined mainly by the rainfall intensity P during a time b ; the runoff q from an area A can be calculated for time $t > b$ with the formula:

$$q = \frac{8}{\pi^2} PA \sum_{n=1, 3, 5, \dots}^{\infty} \frac{1}{n^2} \left\{ e^{-n^2 b/j} - 1 \right\} e^{-n^2 t/j} \quad (2)$$

(see list of symbols)

The theory of the fluctuating groundwater flow is described by Krayenhoff van de Leur (1958—1962), De Jager (1965), Martinec, Wartena, Zeilmaker & Brugman (1966) and De Zeeuw (1966). According to this theory, the runoff characteristic of a certain catchment area comprises:

1. Percentage of the area contributing to a fast runoff.
2. The reservoir coefficient (j -value) of that fast runoff.
3. The base flow or the reservoir coefficient (j -value) of the slow runoff.

For example: 20 % $j = 3.0$ — 4 hours and 80 % $j = 90.0$ — 4 hours means, that during a short period 20 % of an area contributes to a fast runoff with $j =$

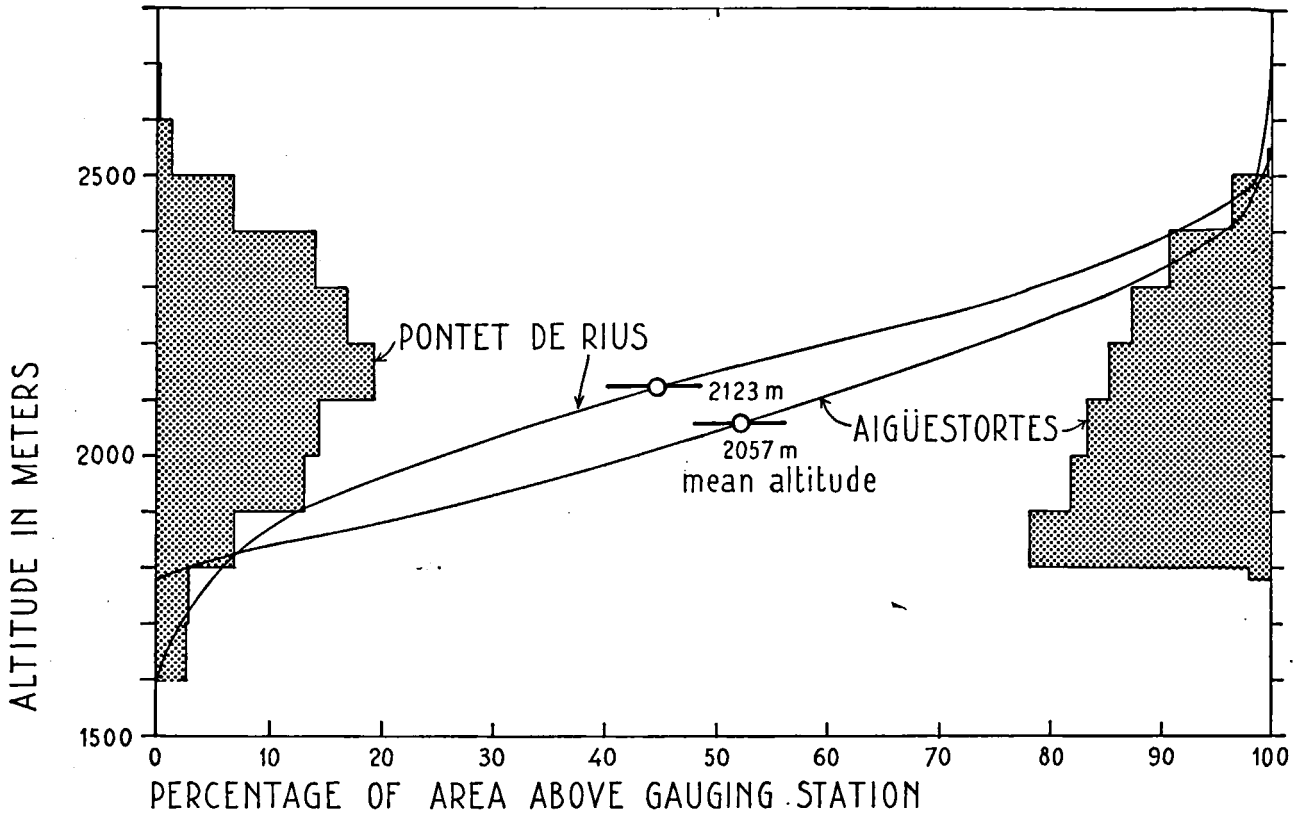


Fig 7.4 Area-altitude distribution and hypsometric integral of the Pontet de Rius- and Aigüestortes basins.

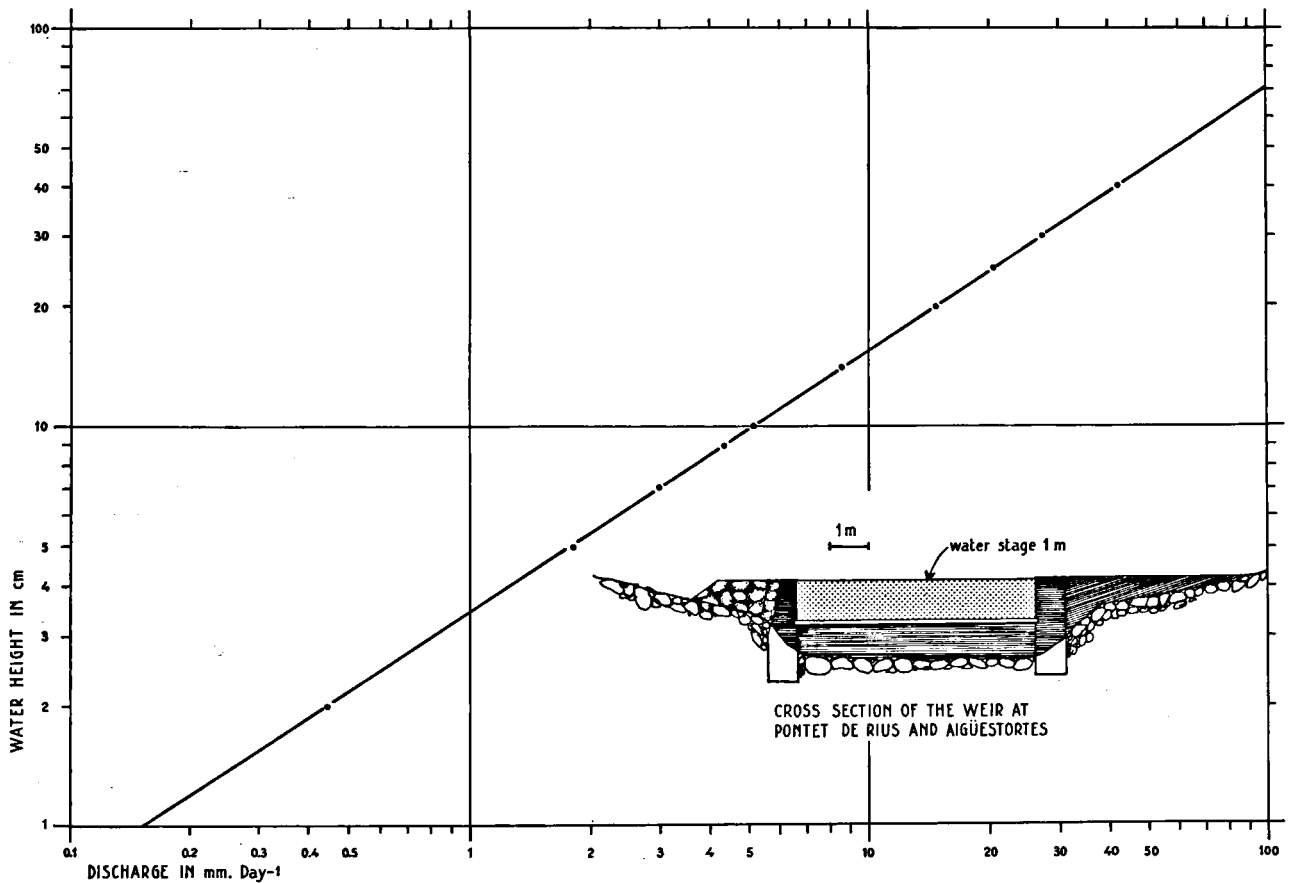


Fig. 7.5 Weir at station 20 and 3 and its stage-discharge rate relation.

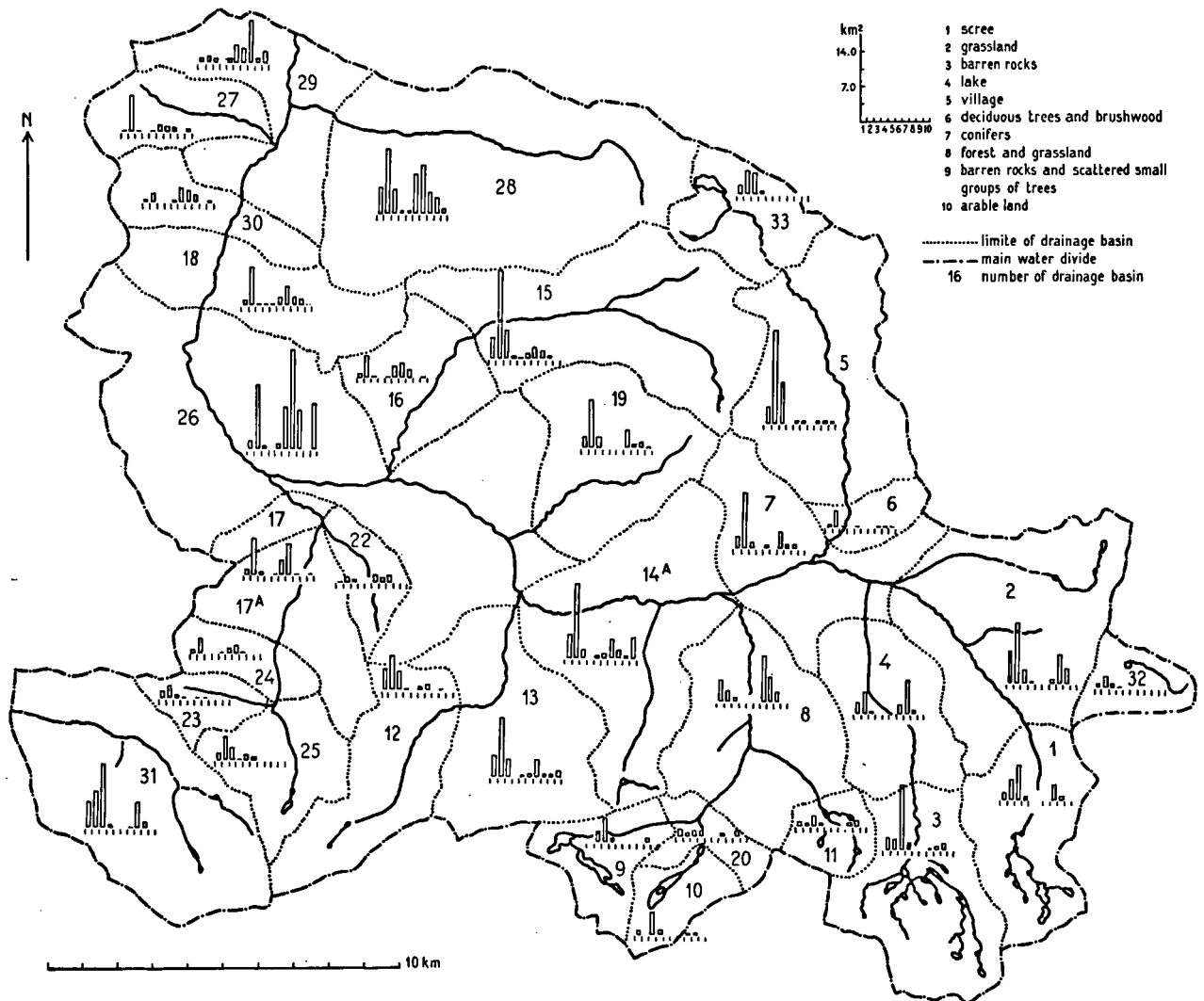


Fig. 7.6 Areas of land classification units in thirty-three drainage basins.

3.0 in 4 hours, whereas 80 % of that area contributes to a slow runoff with $j = 90$ in 4 hours (or $j = 15$ days).

7.6 J - values of the Pontet de Rius basin

Zeilmaker (1966) analyzed available hydrographs of the small Pontet de Rius catchment area (station 20), situated in the Upper Valarties river. This area has during the observation years 1961—1963 a surface of 6.1 km² while its altitude ranges from 1595 m to 2750 m above sea level. Pontet de Rius forms the upper part of a glacial valley. The area-altitude distribution and the hypsometric integral of the area are shown in fig. 7.4.

The enclosed land classification map shows 26% barren rocks (granite); 39 % scree; 7 % grassland and 28 % rocks with sparse trees. At a weir, equipped with a float activated water stage recorder, the discharges of the Pontet de Rius area were registered until the flood of August 3, 1963. In fig. 7.5 the weir is shown and

the stage-discharge relation is plotted as a relation of runoff intensity (mm.day⁻¹) to stage height (cm).

Since no hyetographs were available, daily rain precipitation, measured in Restanca (1982 m), which station is situated on the border of the Pontet de Rius area, had to be used. According to the area-altitude distribution of the Pontet de Rius area (fig. 7.4), the Restanca precipitation in the form of rain should be multiplied by 1.07 percent in order to obtain the correct precipitation value (fig. 6.6). The annual evaporation, however, is about 20—30 percent of the total precipitation at Restanca and since regional variations in precipitation intensity are unknown, the uncorrected Restanca value has been assumed to be representative for the Pontet de Rius area.

An approximate value for the slow runoff reservoir coefficient was obtained from 18 depletion curves during a number of successive dry days. The slow runoff can be characterized by $j = 15$ days. The exact fast runoff reservoir coefficient could only be

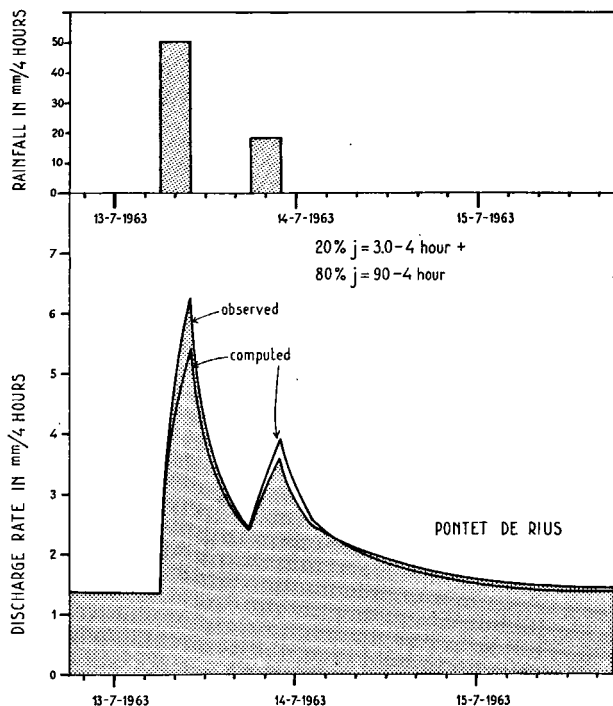


Fig. 7.7 Runoff analysis of the Pontet de Rius basin.

calculated by means of four precipitation values. Therefore the Restanca daily rain precipitation values had to be divided according to the registered precipitation hours of Viella. The distance Restanca-Viella is however 9,5 km and the daily precipitation distribution of Viella did usually not correspond with the runoff from the Pontet de Rius basin, except for the case shown in fig. 7.7. The runoff characteristics are: 20 % $j = 3,0-4$ hours and 80 % $j = 90,0-4$ hours. Instead of 80 % $j = 90,0-4$ hours, a constant base flow of 1.25 mm in 4 hours can be assumed. The observed runoff does not show a time-lag with respect to the calculated runoff.

7.7 Relation of runoff, land classification and morphology in Pontet de Rius

The analysis of twenty-three runoff peaks demonstrated that the percentages of the precipitation, contributing to the fast runoff in the Pontet de Rius area are a function of base flow (fig. 7.8). On logarithmic paper a broken line was obtained, indicating that the base flow and the percentage of the fast runoff have no linear relationship. After the snowmelt in June, an important base flow coincides with the maximum percentage of the precipitation as fast runoff (40 %). That percentage decreases suddenly in July (15 %) and in August-September (10 %). Figure 7.9 shows the explanation of this phenomena. The Upper Valarties valley is a glacial valley with a step-shaped river profile, in which three reservoirs, filled with glacial and torrential material, have been cut out by the glacier. Those reservoirs can reach depths of 25-40 m. They are all characterized by their bottle-

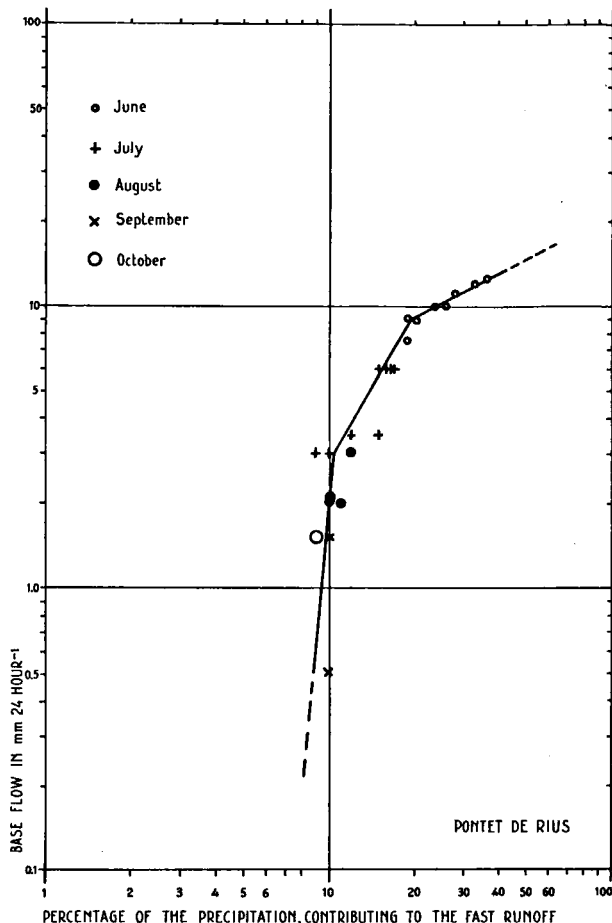


Fig. 7.8 Relation of baseflow and percentage of the precipitation, contributing to the fast runoff of the Pontet de Rius basin.

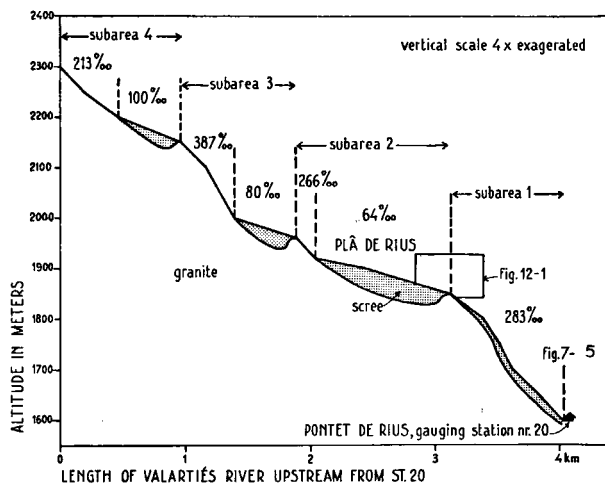


Fig. 7.9 Length profile of the Valarties River upstream from station 20.

neck shaped bottoms, damming up the water at the downstream ends in the summer after the snow melt period. If the Pontet de Rius area is divided according to its three glacial steps (table 7.3), it can be concluded

TABLE 7.3. *Distribution of land classification units in the Pontet de Rius basin*

Subarea	Percentage of total drainage basin	Barren rocks	Scree and disseminated trees
1	33	15	85
1 + 2	56	24	76
1 + 2 + 3	84	36	64
1 + 2 + 3 + 4	100	40	60

that the area of the barren and vegetated scree determines the percentage of the precipitation contributing to the base flow, whereas the barren granite rocks produce the fast runoff.

7.8 J - values of the Aigüestortes basin

The Aigüestortes catchment area is situated in the Upper Aiguamoix glacial valley. The area is 6.1 km² and the altitudes ranges from 1772—2545 m above sea level.

The area-altitude distribution and the hypsometric integral of the Aigüestortes basin are shown in fig. 7.4. The enclosed land classification map shows 31 % conifer forest; 30.5 % grassland; 16.5 % barren rocks (granite); 12 % scree; 9.5 % rocks with dispersed trees and 0.5 % lake.

Since the weir at Aigüestortes (station 3) is of the same construction as that near Pontet de Rius, fig. 7.5 can be used for this runoff analysis. No hyetographs corresponding to the hydrographs, were available

from the Aigüestortes basin and therefore the main problem concerned the precipitation data.

The nearest meteorological station to the Aigüestortes basin was Restanca and the problems, discussed in the Pontet de Rius analysis, appeared to be even more complicated, since Restanca was situated in another valley.

From the depletion curves 1961—1963 approximate j — values were calculated. The storage coefficient of the fast runoff appeared to be $j = 3,0$ —4 hours whereas the storage coefficient of the slow runoff has a value of $j = 72$ —4 hours.

Comparison of the results of Aigüestortes and Pontet de Rius shows that the fast runoff for both basins has the same j — values, independently of the differences in land classification characteristics (table 7.4). The total surface of barren rocks however, is for both basins almost equal.

The slow runoff is faster in Aigüestortes ($j = 12$ days) than in Pontet de Rius ($j = 15$ days). This is due to the three times greater scree volume of the Pontet de Rius basin and to the simpler river profile of Aigüestortes, which basin shows no valley steps.

It can be concluded that the steeper slope of the Pontet de Rius basin, compared with the Aigüestortes basin, does not affect the slow runoff, nor the fast runoff.

7.9 J - values of the Upper Negro basin

The Upper Negro catchment area has an area of 24.4 km². The altitudes range from 1250 m (gauging station 12) to 2623 m above sea level. The hypsometric integrals of the area are shown in fig. 12.2. The land classification map (see enclosed map) shows 56 percent grassland and 21 percent scree (table 7.4).

TABLE 7.4. *Distribution of land classification units in ten drainage basins of the Valle de Aran*

River and number of gauging station	Area, km ²	Percentage of area, contributing to				
		fast runoff	fast base flow		slow base flow	
		barren rocks	barren rocks + disseminated trees	barren rock + disseminated trees + grassland	scree	scree + forest
Iñola (6)	31.9	14	17	84	12	15
Negro (13)	34.4	5	8	63	19	36
Barrados (16)	59.0	18	19	65	13	34
Garona de Ruda (2)	50.5	21	28	63	17	35
Upper-Valarties (20+9+10)	19.4	53	62	65	22	23
Upper-Aiguamoix (3)	21.0	55	61	72	11	24
Upper-Negro (12)	24.4	7	11	67	21	31
Lower-Negro (13—12)	10.0	0	0	51	11	40
Aigüestortes (3)	6.1	17	26	49	12	43
Pontet de Rius (20)	6.1	26	53	53	39	40

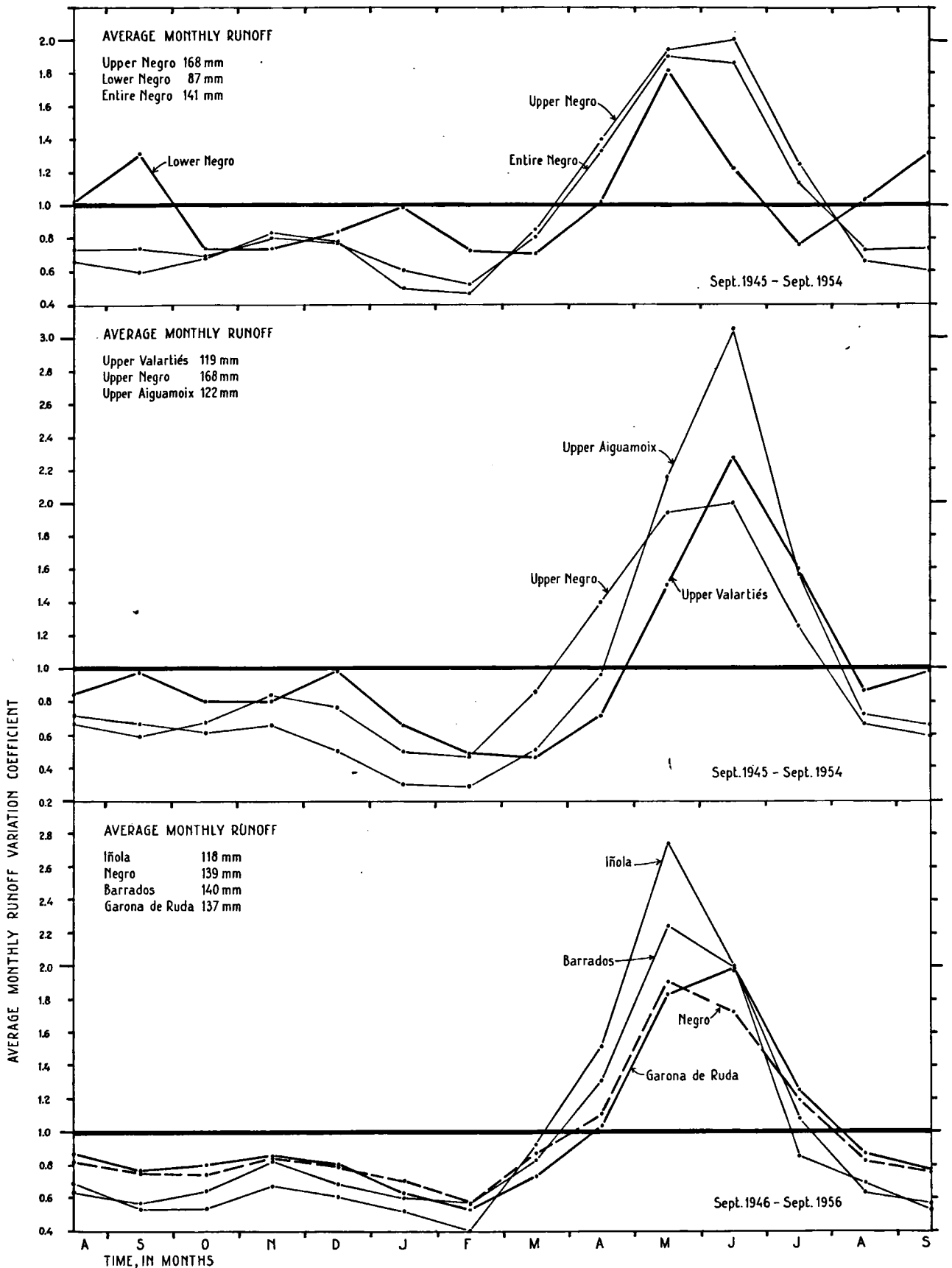


Fig. 7.10 Average monthly runoff variation coefficients for eight basins.

Since no hydrographs were available from station 12, a number of depletion curves during a sequence of dry days in 1962 had to be drawn by means of only one daily runoff observation. The reservoir coefficient of the fast runoff could not be calculated, but the j -value of the slow runoff amounted to $j = 16.5$ days. The j -value of the slow runoff of the Upper Negro basin ($j = 16.5$ days) is greater than the slow runoff value of the Aigüestortes basin ($j = 12$ days) and the Pontet de Rius basin ($j = 15$ days).

Since the Pontet de Rius basin has a larger scree area (39 percent) than the Upper Negro (21 percent), the runoff analysis seems to contradict former results. The average scree thickness of the Upper Negro however, has been calculated to be three times that of the Pontet de Rius basin. Moreover the Upper Negro River flows for a distance of three km under its own scree and the river profile shows five steps produced by the former glacier.

From the analysis of three small high mountain basins, it can be concluded that the percentage of the precipitation, which contributes to the fast runoff is related to the area of barren rocks, whereas the percentage slow runoff is related to the relative areas of scree and forest.

The reservoir coefficient of the fast runoff is approximately constant and small ($j = 0.5$ day), while the reservoir coefficient of the slow runoff ($j = 12$ — 16.5 day) is great, variable and largely determined by the scree volume.

7.10 Monthly runoff variation coefficients of eight representative drainage basins

The monthly runoff variation coefficient is defined as the ratio of the average monthly discharge (mm) to the average annual discharge (mm), divided by 12. Three groups of basins have been analyzed (fig. 7.10):

1. The Iñola- Negro- Barrados- and Garona de Rudabasins, ranging in area from 31.9—50.5 km².
2. The Upper Valarties- Upper Aiguamoix- and Upper Negro-basins, ranging in area from 19.4—24.4 km².
3. The Upper Negro- Lower Negro- and the entire Negro-basins, ranging in area from 10.0—34.4 km².

All rivers show the tremendous effect of the snow melt runoff during May or June, depending on the average altitudes of the basins. The second runoff maximum occurs in November or December under influence of the precipitation. The minimum runoff in February corresponds with the minimum precipitation. Each of the eight basins is representative for a certain kind of land classification, morphology and geology in the Central Pyrenees.

7.11 Relation of variation coefficients, morphology and land classification in eight drainage basins

In order to study the relation of variation coefficients and drainage basin characteristics, the enclosed land classification map at a scale 1:50,000 was prepared

and a morphological analysis was carried out. The results are summarized in tables 7.4 and in fig. 2.1 and fig. 7.6.

Since 43 %—93 % of the runoff of the eight analyzed drainage basins in the Valle de Arán consists of slow runoff or base flow, the monthly runoff variation coefficients give information about the annual progression in base flow variations.

We have analyzed the relation of maximum variation coefficients to land classification and morphology in fig. 7.11. It appears that the maximum base flow variation is determined by the total percentage of scree and forest area. Areas largely covered with scree and forest, have small base flow variations. On the other hand it can be shown that a greater area of barren rocks (with disseminated trees) produces a slight increase in base flow variation. No relation exists between base flow variations and the average weighted slope. These results confirm the conclusions of sections 7.6—7.9.

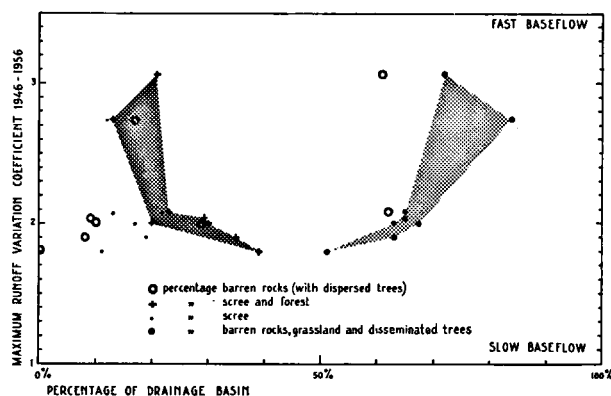


Fig. 7.11 Relation of maximum runoff variation coefficients to land classification units.

7.12 Flood frequency

From four representative runoff gauging stations (3, 7—7a, 8—8a, 13) in the Valle de Arán the frequency of annual floods have been studied according to the method described by Powell (1943) Dalrymple (1960) and Benson (1962). It should be emphasized that the method provides a measure for the recurrence interval for floods of given size. The curves shown in fig. 7.12 are discharge curves, derived from momentary peak rates of flow. Plotting positions for the frequency scale were obtained by applying the "California method". (Calif. Dept. Public Works, 1923; Jarvis and others, 1936). The logarithmic ordinate scale, as shown on form 9—179b of the U.S. Geol. Survey, was used and straight lines have been drawn through the plotted points. A bar graph showing graphically the length of records in the Valle de Arán which were used for the preparation of fig. 7.12, is presented in the same figure. A set of curves, showing the variation of the mean annual flood ($Q_{2.33}$) and of the 10, 25, 50 and 100 year floods with drainage area is shown as fig. 7.13. The homogeneity test of Langbein (1949) was

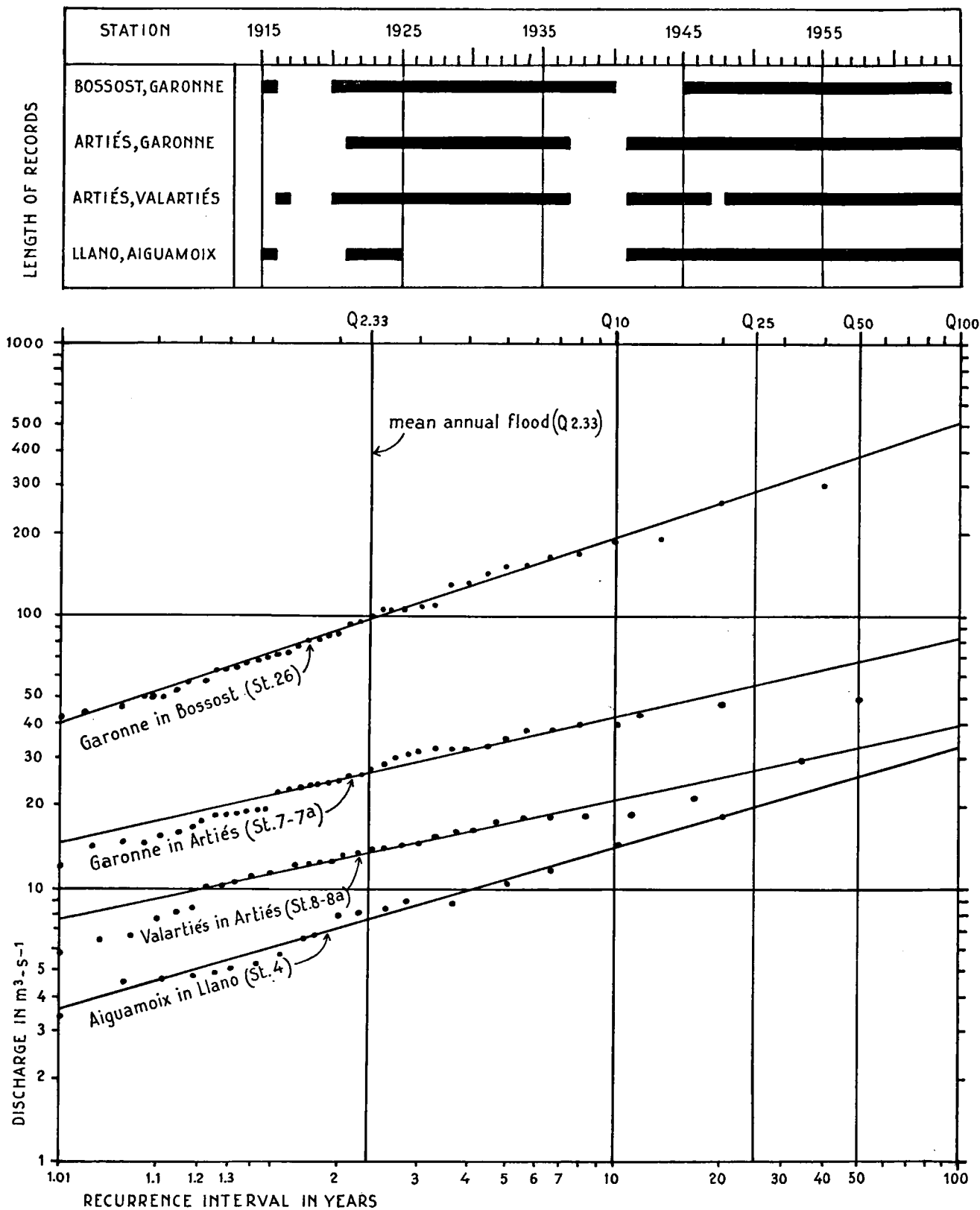


Fig. 7.12 Flood frequency at four stations in the Valle de Arán.

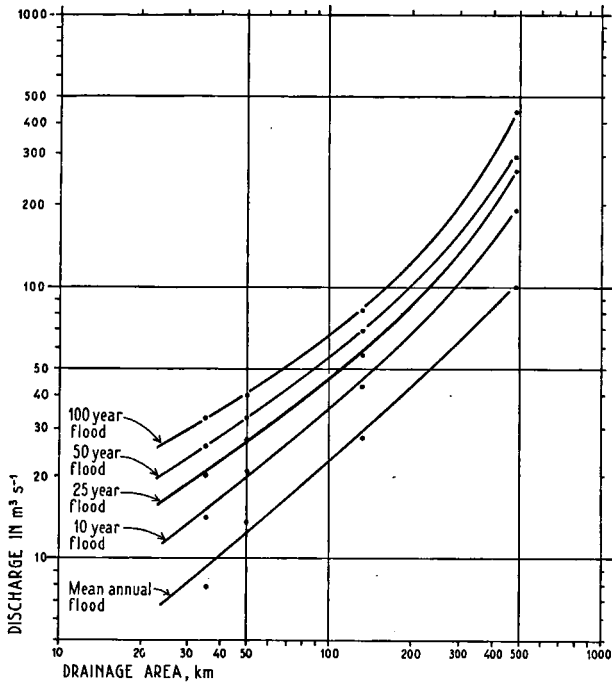


Fig. 7.13 Relation of magnitude of floods and drainage basin.

applied to the records and it was found that the data are reasonably homogeneous. The flood analysis in the Valle de Arán shows that floods are frequent but local phenomena. Destructive floods tend to increase in relative size in a downstream direction.

The influence of the generation of hydroelectric power on the destructive power of floods is a serious point of discussion in the Valle de Arán. Before it started, a certain equilibrium between transported sediment mass and discharged water mass existed. The energy distribution within the stream system has changed fundamentally as a result of the energy withdrawal. In 1947 for instance, 6 percent less energy was available for sediment transport whereas in 1964 already 39 percent less energy was available, compared with the average potential energy 1945—1965 of the annual precipitation. If we assume an average specific degradation of $150 \text{ mm} \cdot 1000 \text{ year}^{-1}$ (see 2.3) during the period 1945—1965, a volume of 0.4 km^3 has not been transported, that otherwise would have been discharged out of the Valle de Arán. This leads to a progressive filling of the stream system.

Since the maximum intake ($\text{m}^3 \text{ s}^{-1}$) of the hydroelectrical system does not exceed 30 percent of the mean annual flood ($Q_{2.33}$) at any intake for a power station, it is clear that the hydroelectrical system does not work during important floods. No flood reservoirs are present in the Valle de Arán. It can be concluded that the sediment load of future floods will increase due to hydro-power generation, because more sediment remains trapped in the valleys.

The flood of August 3, 1963 for example was only 10 percent greater in magnitude than the flood of June 8, 1922 in the Valarties near Arties but its effect were extremely disastrous. The flood of August 3, 1963 for the Garonne in Arties was only a moderately severe flood which normally occur every five years, but its effects were very disastrous.

TABLE 7.5. Characteristics of fourteen lakes in the Upper Aiguamoix area

Branch	Name of lake	Number of lake	Max. storage elev. (m)	Min. storage elev. (m)	Catchment area (km^2)	Storage $\times 10^6 \text{ m}^3$	Overflow precipitation for catchment area (mm)	Lake equipped with discharge
Aiguamoix East	Ratera	1	2464.95	2453.0	1.15	0.520	453	tunnel
	Pulgar	2	2423.60	2413.0	0.40	0.330	824	tunnel
	Ubago	3	2221.50	2189.0	2.82	4.190	1485	dam + tunnel
	Cavidurnats	4	2165.20	2161.0	0.16	0.160	1000	tunnel
	Llarg	5	2156.50	2142.5	0.60	1.053	1750	dam + tunnel
	Manyera	6	2161.50	2161.5	0.68	0.518	762	dam + tunnel
	Clot	7	2132.00	2112.0	0.44	0.648	1474	dam + tunnel
Aiguamoix West	Gelat	8	2562.75	2558.0	0.46	0.130	283	tunnel
	Occidental Superior	9	2390.90	2385.5	1.15	0.098	85	tunnel
	Occidental Occidental	10	2286.95	2282.0	2.10	0.072	34	tunnel
	Tort Central	11	2417.15	2413.5	0.13	0.070	500	tunnel
	Bergils	12	2178.75	2178.8	0.92	—	—	natural overflow
	Caldes	13	2184.55	2180.5	2.23	0.107	479	tunnel
	Mayor	14	2098.25	2070.3	1.26	2.806	2010	dam + tunnel

7.13 Flood routing through 14 reservoirs in the Upper Aiguamoix

The Upper Aiguamoix catchment area is a severely glaciated granite area which has been utilized by the power station of Arties since 1954. In that area many lakes have been worn out by the former Aiguamoix glacier and the lakes constitute natural reservoirs for the hydroelectrical usage (fig. 7.14). By means of five small arch dams, ranging in altitude from 13 m to 20 m and after the construction of tunnels for a total length of 1.5 km, the system of lakes in the Upper Aiguamoix has been transformed into a hydrologic unit with a regulating capacity of $10.7 \cdot 10^6 \text{ m}^3$.

The Upper Aiguamoix unit consists of two branches, Aiguamoix east and Aiguamoix west, connected by 582 m of tunnels. The lowest reservoir, Lake Mayor, is situated in the Aiguamoix west branch. Lake Mayor discharges into a 1927 m long tunnel, leading to the Valarties river. The adjacent Upper Garona de Ruda river on the other hand discharges into the Aiguamoix east branch through a tunnel with a length of 1270 m. The characteristics of the lakes in the Upper Aiguamoix area are listed in table 7.5.

In order to study the hydrological characteristics of the Upper Aiguamoix unit, the lakes were assumed to be empty and the discharge tunnel closed. In that case, the maximum water storage in Aiguamoix east amounts to $7.419 \cdot 10^6 \text{ m}^3$, whereas the water storage in Aiguamoix west has a value of $3.283 \cdot 10^6 \text{ m}^3$. After a period of inflow (1205 mm for Aiguamoix east and 435 mm for Aiguamoix west), the lakes are filled and the water storage decreases to zero. This is shown graphically in fig. 7.15.

Assuming a 10 year cloudburst of 150 mm in 2 days (fig. 6.2), the 10 year-safety limit for the Upper Aiguamoix system can be evaluated with fig. 7.15. In order to avoid a destructive overflow flood from the Upper Aiguamoix into the Lower Aiguamoix, it is necessary to keep storage space for two days, or 150 mm in the Upper Aiguamoix. Moreover it seems advisable to keep storage space for a constant inflow of $2 \text{ m}^3 \cdot \text{s}^{-1}$ from the Garona de Ruda, and it is essential to keep the discharge tunnel ($7.5 \text{ m}^3 \cdot \text{s}^{-1}$) from the Aiguamoix to the Valarties closed (fig. 7.14). This implies that the level of lake Ubago under normal conditions of exploitation should never exceed the elevation of 2214 m (7.50 m under the crest of the

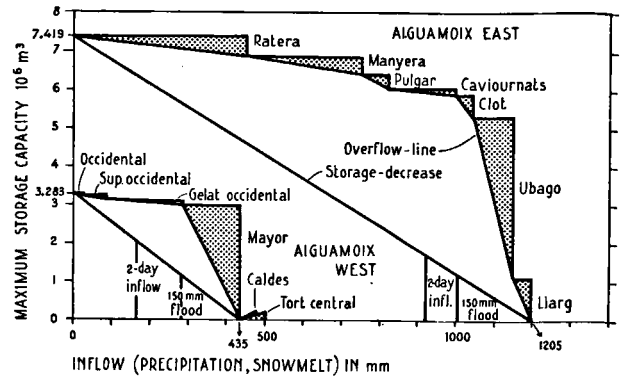


Fig. 7.15 Relation of the inflow and storage in the Upper Aiguamoix area.

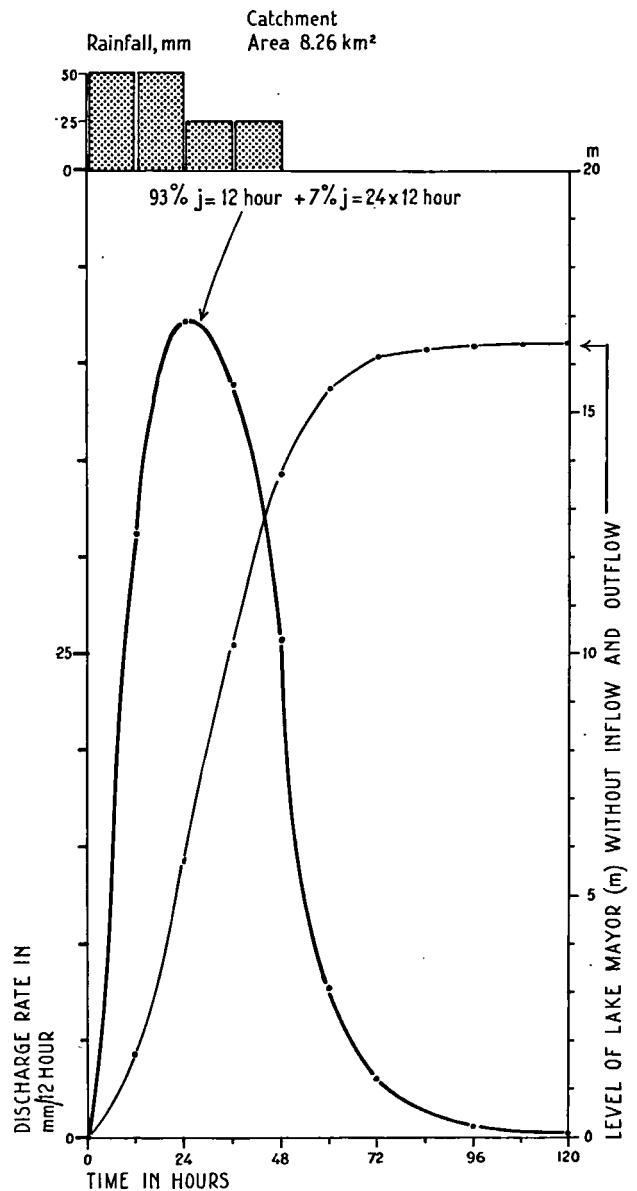


Fig. 7.16 Flood routing through the Aiguamoix west branch.

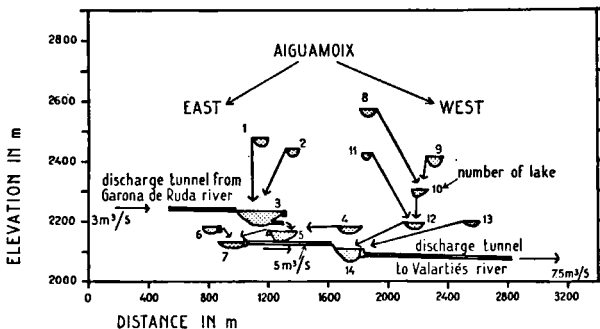


Fig. 7.14 Reservoirs of the Upper Aiguamoix area.

dam). A similar reasoning for the Aiguamoix west branch shows, that the level of lake Mayor should never exceed the elevation of 2082 m (16 m under the crest of the dam).

It should be emphasized that the relation storage-precipitation, in the Aiguamoix-west branch, is much more critical than in Aiguamoix-east (fig. 7.16). This is dangerous, since lake Mayor is the lowest storage reservoir of the system. Any inflow into the Aiguamoix west system, exceeding 130 mm, implies certain risks. Using the data of the enclosed land classification map and applying the results of section 7.8 a two day pre-

cipitation of 150 mm has been routed through the Aiguamoix-west branch. Barren rocks constitute 87 % of the area, scree 7 % and lakes 6 %; therefore the runoff characteristic is 93 % $j = 12$ hours + 7 % $j = 24.12$ hours. The results are shown in fig. 7.17 and the rise of the level of lake Mayor without inflow from Aiguamoix-east nor outflow into the Valarties is shown in the same figure. The ratio lake surface to catchment surface has a value of 1:110. No base-flow has been assumed in this figure. The results of the flood routing correspond with the observations of August 3, 1963.

8. EVAPORATION

8.1 Introduction

The evaporation in the Valle de Arán from 1955—1965 was estimated with a Penman-type formula. During the winter months an important part of the Valle de Arán is covered with snow. The evaporation from a snow surface was estimated with a Dalton-type formula. The evaporation was also estimated with the formulas of Thornthwaite (1948-1955-1957) and Turc (1953).

8.2 Evaporation estimations from meteorological data

A Penman-type formula (3) with a reflection of 25 % could be used for the estimations of the average monthly evaporation at the stations Cledes, Viella, Arties, Restanca and Bonaigua.

$$E = \frac{\frac{\Delta H_{ra}^{ne}}{L\rho} + \gamma Eq}{\Delta + \gamma} \quad (3) \quad (\text{see list of symbols}).$$

The data from tables 22, 31, 40 and 5.4 and from fig. 8.1, 8.2 were used. The results are shown in table 8.1 and figure 8.3. The water vapour pressures of Viella resemble the measured values of Arties if multiplied by 0.75 (see also 5.6). Therefore the more reliable unadjusted values of Viella were used for the evaporation estimations (table 5.4). The measured values of the meteorological station Viella were assumed to be representative for the entire air mass in the Valle de

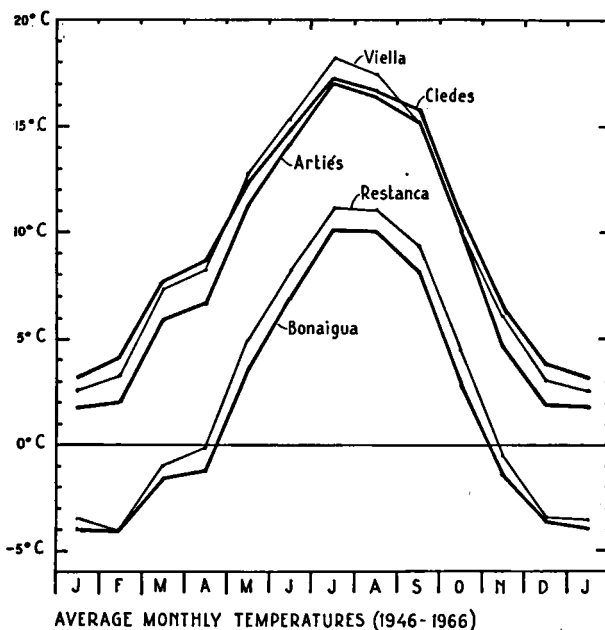


Fig. 8.1 Average monthly temperatures during the period 1955—1965.

Arán. The wind velocity in the Garonne valley is determined as the arithmetic mean of the monthly readings at the stations Cledes, Viella and Arties (fig. 8.2).

TABLE 8.1. Penman monthly evaporation values (mm) during the period 1955—1965

Station	J	F	M	A	M	J	J	A	S	O	N	D
Cledes	29	43	82	106	126	130	136	152	98	59	40	41
Viella	25	35	80	108	130	140	146	151	96	60	39	40
Arties	24	37	73	93	127	137	142	147	99	55	33	31
Restanca	1	17	41	61	86	108	114	122	75	27	8	13
Bonaigua	4	19	13	53	79	104	104	106	62	28	9	1

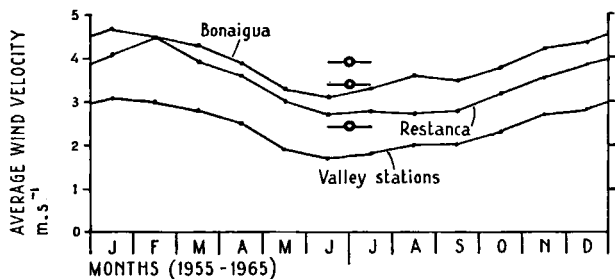


Fig. 8.2 Average monthly wind velocity during the period 1955—1965.

8.3 *Evaporation estimations from the snow cover*

The evaporation from the snow cover during the years 1955—1965 was estimated with a Dalton-type formula (4) for the stations Restanca and Bonaigua (Dalton, 1802).

$E = f(u_2) (P_z w_a] sa - P_z w_a)$ (4) (see list of symbols). For the months with an average air temperature below 0° C., the air temperature at an elevation of 1.50 m above the earth surface was assumed to equal the mean snow surface temperature. The Penman wind function $f(u_2)$ was used, although it has not yet been adapted to mountainous terrains. Measurements of Williams (1963) and Priestley (1963) seem to justify the use of that function. The snow surface temperature was assumed to be 0° C. during the months with a mean air temperature above 0° C., according to Martinec, Wartena, Brugman & Zeilmaker, (1966). The combined Penman-Dalton evaporation estima-

tions for Restanca (elev. 1982 m) and Bonaigua (elev. 2072 m) are shown in figure 8.3.

Thornthwaite's (1948, 1955, 1957) and Turc's (1953) formulas were used for the estimations of the average annual evaporation during the period 1955—1965. The obtained values were compared with the Penman and Penman-Dalton values in table 8.2.

8.4 *Mountain shadow and orientation of the valleys*

Brugman (internal report, 1966) calculated the monthly decrease in outer atmosphere shortwave radiation ($o_a H_{sh}$) on a glacial valley bottom at Lago Mar in order to determine the shadowing effect of the surrounding mountains (fig. 8.4). The percent error in the monthly evaporation (Penman) is shown in figure 8.4. In the case of Lago Mar, the error in the total annual evaporation amounted to 16 percent during the water

TABLE 8.2. Comparison of Penman-, Penman-Dalton-, Thornthwaite- and Turc- annual evaporation values (mm) during the period 1955—1965

Station	Penman	Penman-Dalton	Thornthwaite	Turc
Cledes	1042	1042	646	512
Viella	1050	1050	653	520
Arties	998	998	607	467
Restanca	673	456	337	366
Bonaigua	582	402	288	302

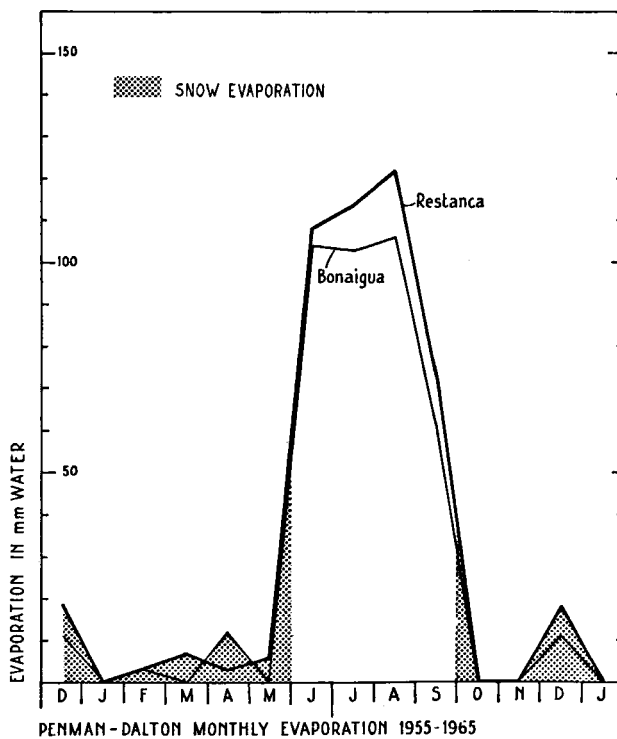
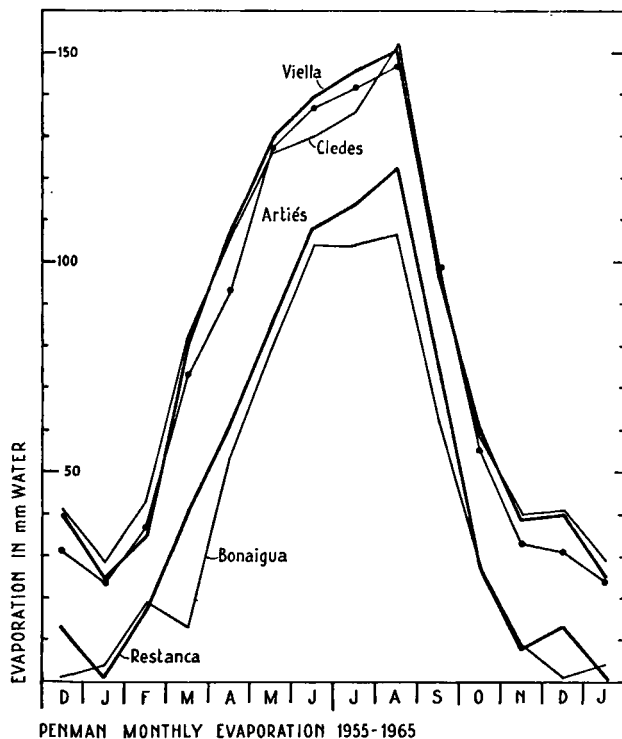


Fig. 8.3 Average monthly Penman-evaporation values and combined Penman-Dalton evaporation values.

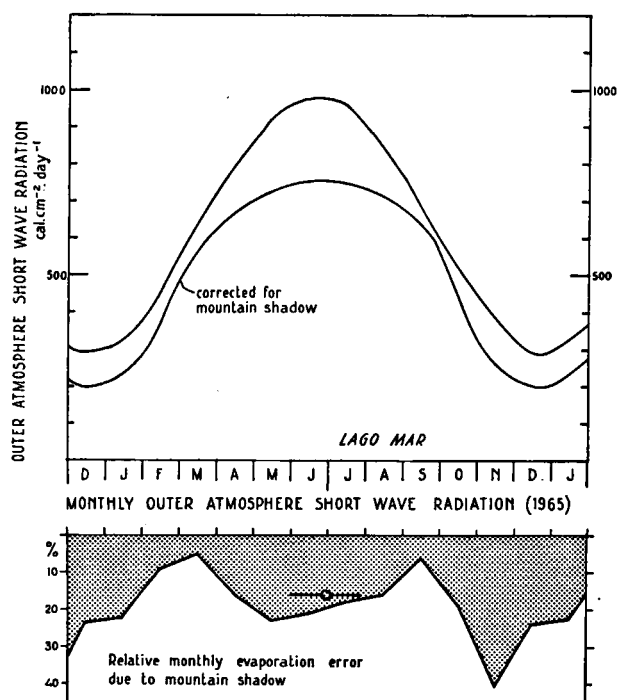


Fig. 8.4 Monthly decrease in outer atmosphere shortwave radiation (${}_{oa}H_{sh}$) on a valley bottom and error in the monthly Penman evaporation values due to mountain shadow (1965).

balance year 1964—1965. This error is typical for nearly all glacial valley bottoms in the Valle de Arán because the average slope of the Lago Mar area has only a moderate value of 26°.

The effect of the orientation of the valleys on shadow patterns was studied and the results are shown in figure 8.5. It shows the percentage of shadowed areas in the Valle de Arán during the winter solstice at 12 hour (17 %). The relation of the percentage shadowed area and the average slope of 31 basins seems to be independent of the orientation of those basins (fig. 8.6).

8.5 Short wave radiation measurements

During the summer of 1965 daily shortwave radiation (H_{sh}) measurements were carried out at Restanca (elev. 1982 m) and Viella (elev. 931 m) with Gun Bellani solarimeters. The results generally indicate higher values than those from the tables of Penman (1960) and Slatyer & Mc Ilroy (1961) which we used for the calculation of the evaporation as listed in table 8.1. The measured H_{sh} values are compared with the calculated H_{sh} values in figure 8.7.

Recent net radiation measurements (H_{ra}^{nc}) by Schröder & van Rooyen (internal report, 1967) carried out with a Kipp solarimeter in the High Pyrenees near Andorra confirm the results obtained in the Valle de Arán. According to Martinec, Wartena, Brugman & Zeilmaker (1966) this is probably due to the high transparency of the atmosphere in this area. The Penman evaporation values, estimated from the measured H_{sh} values of table 8.3 are 23 percent higher for Restanca and as much as 52 % higher for Viella, if compared with the evaporation values of table 8.1.

TABLE 8.3. Short wave radiation measurements in Restanca and Viella during 1965 with Gun Bellani pyranometers (in cal. cm⁻².day⁻¹)

10-day period	Restanca cal.cm ⁻² .day ⁻¹	Viella cal.cm ⁻² .day ⁻¹
11-6/20-6	535	—
21-6/30-6	550	636
1-7/10-7	516	625
11-7/20-7	422	558
21-7/31-7	476	600
1-8/10-8	470	628
11-8/20-8	360	527
	—	476

TABLE 8.4. Average monthly percentage of the Valle de Aran, covered with snow during the period 1955—1965

	J	F	M	A	M	J	J	A	S	O	N	D
%	75	75	45	45	13	3	0.5	0.5	3	13	45	75

TABLE 8.5. Dalton monthly evaporation values (mm) from a snow cover at Restanca and Bonaigua

Station	J	F	M	A	M	J	J	A	S	O	N	D
Restanca	0	3	7	3	6	—	—	—	—	0	0	18
Bonaigua	0	3	0	12	0	—	—	—	—	0	0	11

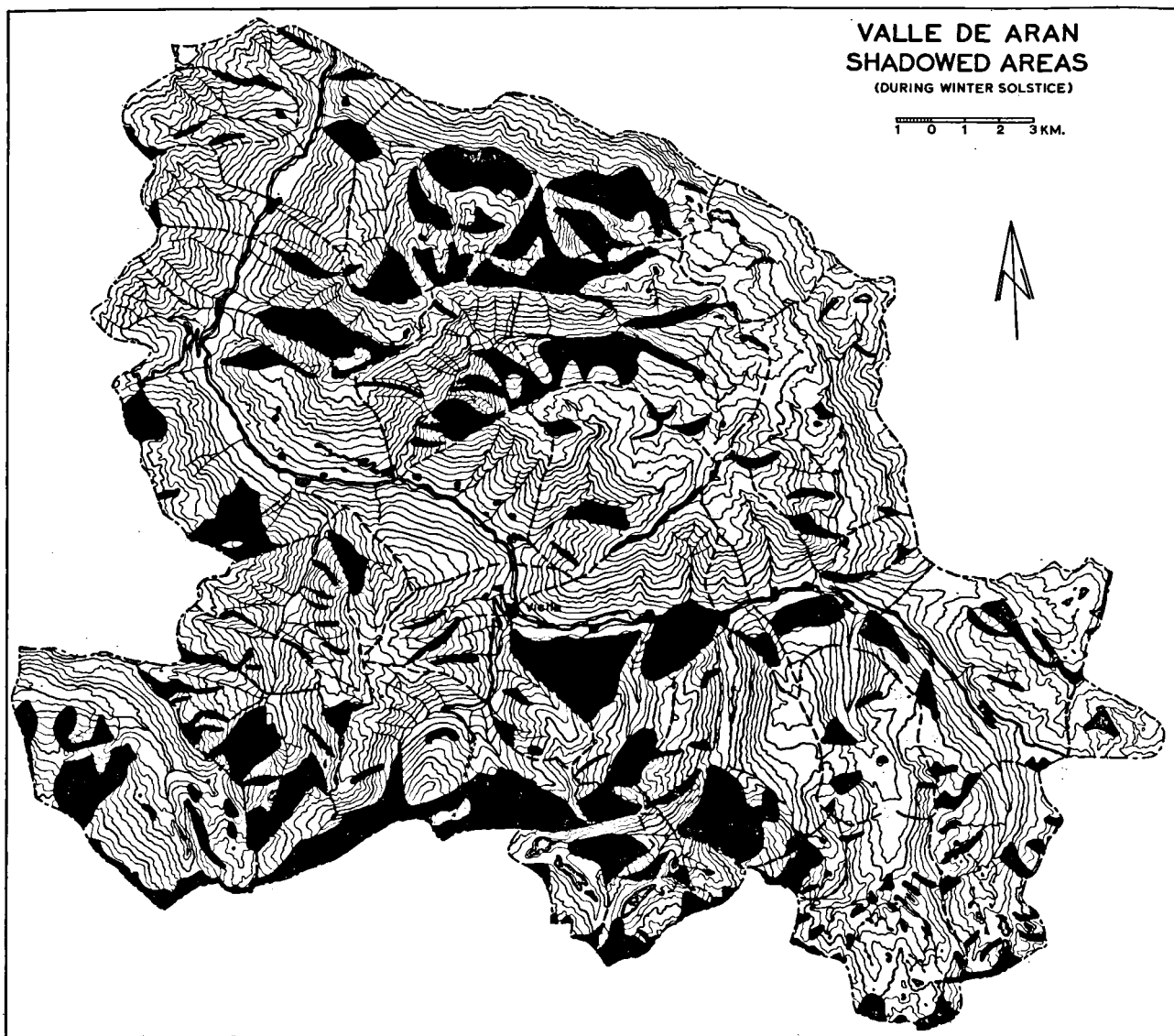


Fig. 8.5 Shadowed areas in the Valle de Arán during the winter solstice at 12.00 h.

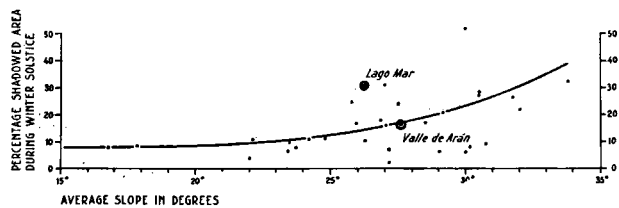


Fig. 8.6 Relation of the percentage shadowed area during the winter solstice and the average weighted slope of 31 basins.

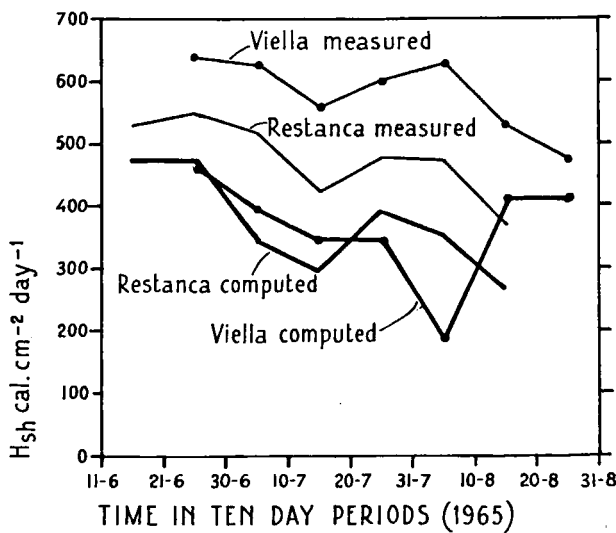


Fig. 8.7 Comparison of calculated and measured short-wave radiation (H_{sh}).

8.6 Actual evaporation estimations

In figure 8.8 the average elevation of the monthly 0° C-isotherm during the years 1955—1965 is shown. The percentage of the Valle de Arán, covered with snow, is listed in table 8.4.

The Dalton monthly evaporation values of table 8.5 can be applied to the areas above the 0°-isotherm. In the areas, which lie below the 0°-isotherm, the monthly Penman evaporation values (E_0) of table 8.1 can be used. On the land classification map, the area of the units below a certain 0°-isotherm can be determined. The actual evaporation (E_{ac}) was estimated, by multiplying the E_0 values by the α -values of table 8.6.

It should be emphasized, that the Penman evaporation values can only be applied to wet surfaces. Hence during the summer period, the actual evaporation in the Valle de Arán is always less than indicated. The relation of the evaporation from barren rocks to runoff measurements is reported by Martinec, Wartena, Brugman and Zeilmaker (1966).

The average annual E_{ac} for the valley is estimated to be 500—550 mm during the period 1955—1965.

TABLE 8.6. α -values, estimated for the Valle de Arán

land classification units	M, J, J, A summer	N, D, J, F winter	M, A, S, O
Barren rocks	1.0—1.1	1.0—1.1	1.0—1.1
Scree	1.0—1.1	1.0—1.1	1.0—1.1
Barren rocks and scattered small groups of trees	1.0—1.1	1.0—1.1	1.0—1.1
Arable land	1.1	—	—
Deciduous trees and brushwood	1.2	0.7	1.1
Conifers	1.1—1.2	1.7	1.5
Grass and scattered small groups of trees	1.1	0.9	1.0
Grassland	1.0	0.8	0.9

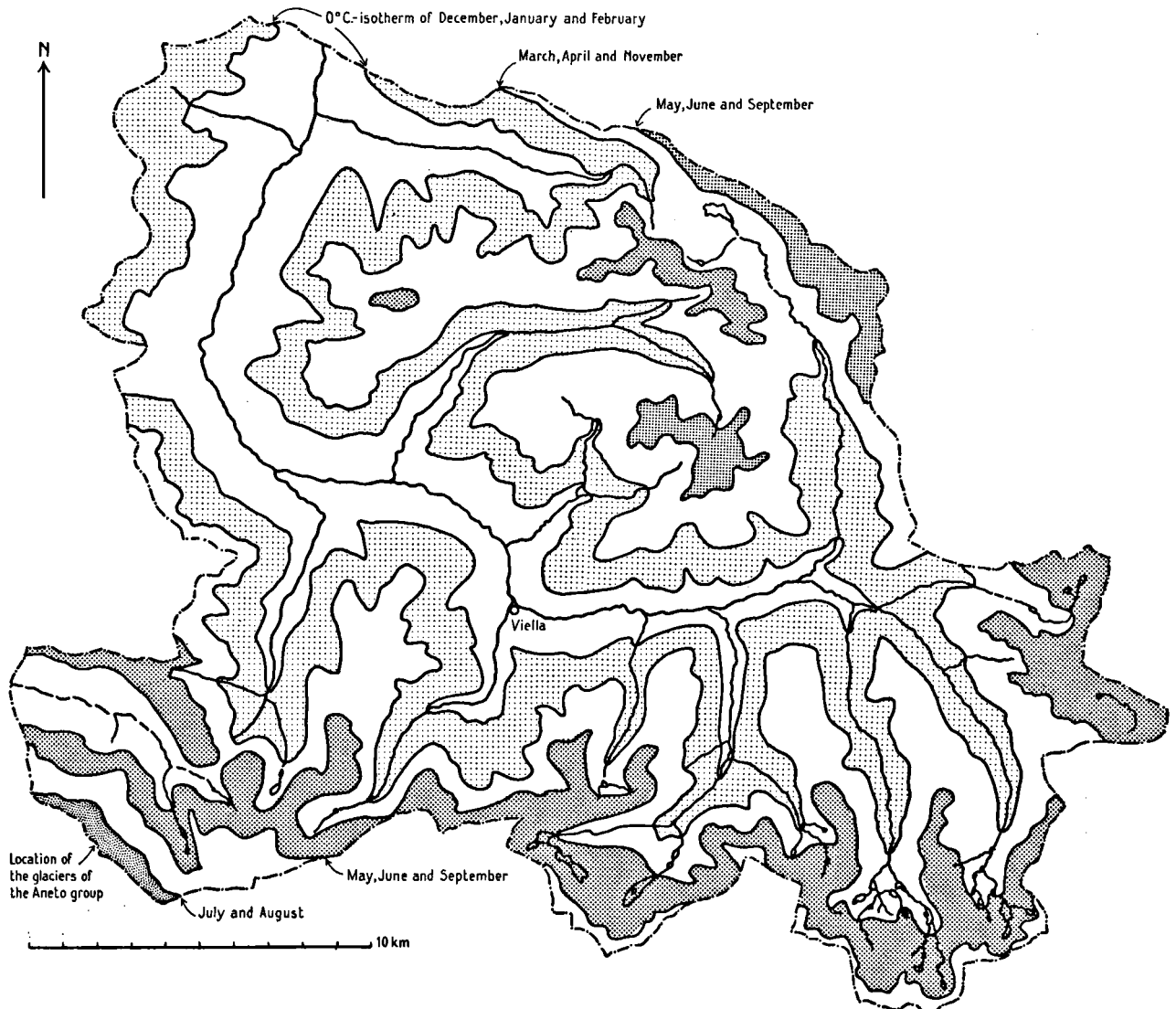
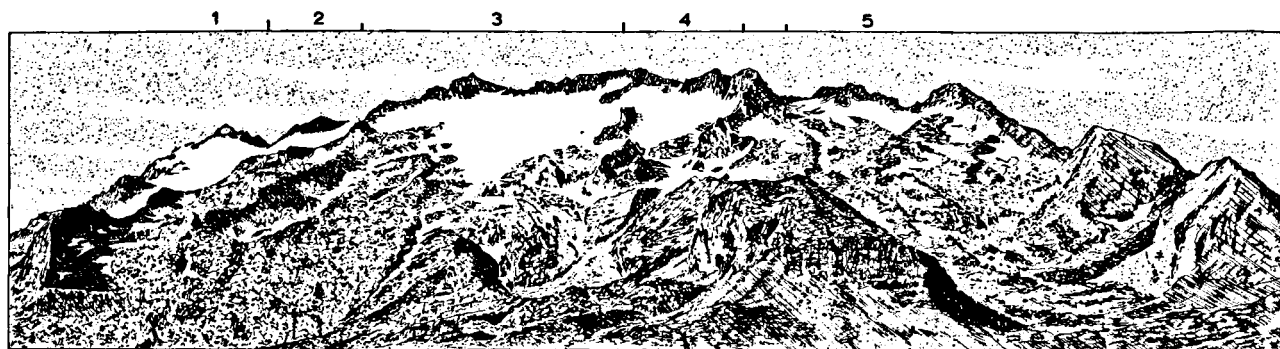


Fig. 8.8 Average height of the monthly 0°C-isotherm during the period 1955—1965.

9. GLACIERS OF THE ANETO GROUP



1: Salenques glacier. 2: Tempestats glacier. 3: Aneto glacier. 4: Maladeta glacier. 5: Alba glacier.

Fig. 9.1 Position of the glaciers of the Aneto group during the summer of 1958.

9.1 Introduction

The purpose of this chapter is to estimate the precipitation and evaporation from the glaciers and to evaluate the snowmelting processes although only sparse data are available.

The six glaciers of the Aneto group are situated at the base of the highest mountain peaks in the Pyrenees. Their location is indicated in fig. 8.8. Their names have been derived from the six steep glacial horns, which rise above the ice masses. The Aneto group is composed of the Alba-, the Maladeta-, Aneto-, Tempestats-, Salenques-, and Russell-glaciers (fig. 9.1). The Russell glacier flows into the Ribagorzana River and is therefore not considered. It is remarkable, that the melting water of the glaciers flows through karst systems into the Garonne River on its way to the Atlantic Ocean, rather than into the Esera River which discharges into the Mediterranean Sea.

Trails which lead across the glaciers, provide access to the highest Pyrenean peak, the Aneto (elev. 3404 m). Some people have lost their lives in efforts to ascend the mountain. One of them, the French mountain guide Barrau, died in the upper part of the glacier, and his remains were recovered near the base after 107 years. This permitted an estimation of the average annual velocity of about 12—14 meters for the Aneto glacier. It is also possible to estimate the retreat movement of the glaciers from publications by mountaineers.

9.2 Precipitation on the glaciers

The average annual precipitation on the glaciers, which have a mean elevation of 3000 m, amounts to 2500 mm during the period 1946—1966 (fig. 9.2). If we apply the precipitation coefficients of the nearest meteorological station, Restanca (elev. 1982 m), to the Aneto area, it is possible to estimate the average monthly precipitation.

An important part (43 percent) of the measured precipitation on the glaciers is snow. However, according to figure 6.7, the assumed snow drifting (see also section 6.10) decreases the effective snow versus rain ratio from 43 to 32 percent (Higashi, 1957). When the average monthly snowfall coefficients of Restanca are applied to the glaciers of the Aneto group, the monthly distribution of snowfall at the 3000 meter level can be estimated (table 9.1).

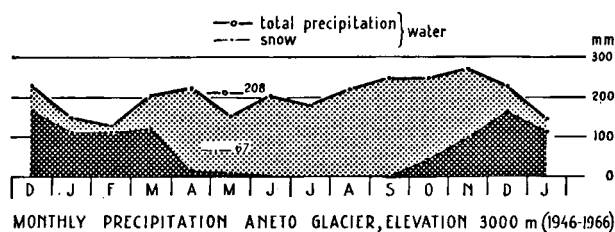


Fig. 9.2 Average monthly rainfall and snowfall in the Aneto area.

TABLE 9.1. Average monthly snowfall (cm) on the glaciers of the Aneto group during the period 1955—1965

J	F	M	A	M	J	J	A	S	O	N	D
112	122	114	120	17	9	—	—	1	42	100	165

TABLE 9.2. Estimated vertical monthly temperature gradients (°C/100 m) and average monthly temperatures (°C) at an elevation of 3000 m

	J	F	M	A	M	J	J	A	S	O	N	D
Average monthly gradient in (°C/100 m)	0.56	0.71	0.89	1.00	1.45	1.45	1.22	1.11	1.45	1.89	1.00	0.64
temperatures, (°C)	-9.1	-11.1	-9.9	-10.2	-9.6	-6.3	-1.1	-0.1	-5.1	-14.4	-10.5	-9.9

As a result of lower temperatures at the elevation of 3000 meters, the monthly snowfall coefficients of the glaciers are not equal to the coefficients of Restanca. The areal variation of the rain-snow ratio (in percent) in the Aneto area and in the Upper Esera valley is shown in fig. 6.9. A significant increase of snow precipitation in a downslope direction from the glaciers is indicated.

9.3 Monthly increase of the 0° C-isotherms

From 1955—1965 the average increase of the monthly 0° C isotherm has been estimated from the temperature readings of the meteorological station Restanca, which is situated 17 km east of the Aneto glaciers. Table 9.2 shows the applied vertical temperature gradients, as well as the estimated average monthly temperature at an elevation of 3000 meters. In general, the vertical temperature gradients from Restanca to Bonaigua (1955—1965) have been used, except for February and December. The position of the 0° C-isotherms in the summer is shown in figure 9.3. The 0° C-isotherm for the warmest month does not reach the 3000 meter level. The maximum elevation of the warmest month is 2790 meters. Therefore this isotherm outlines roughly the region of snow accumulation. An impression of the snow cover in June between the elevations 2200 m—3000 m can be obtained from fig. 9.4, which shows the high mountains of Lago Mar.

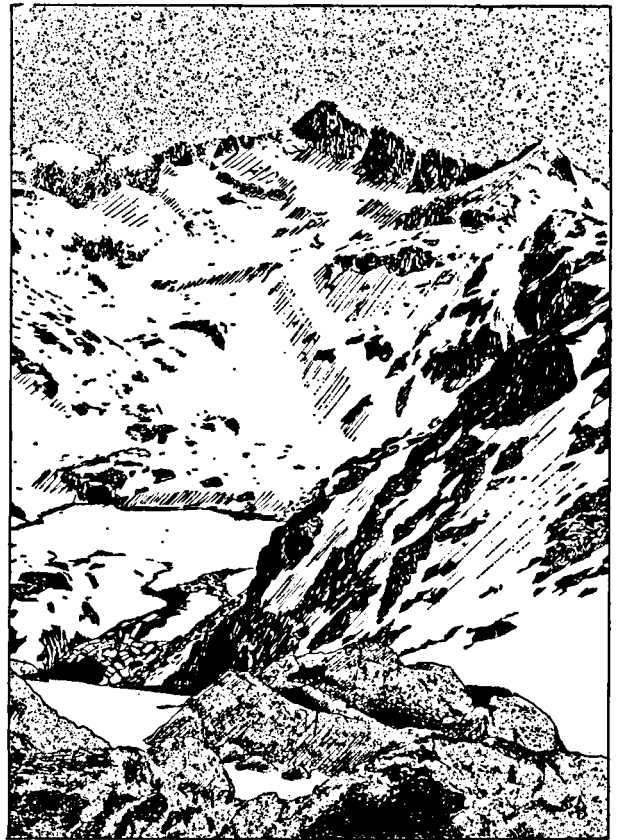


Fig. 9.4 Snow cover in the Lago Mar area (elev. 2200—3000 m) in June 1965.

9.4 Snow depth and snow density

The Martinec equation has been used to estimate the snow depth and snow density on the glaciers.

$$h_t = h_0 \cdot t^{-0.3} \text{ (Martinec, 1965).}$$

h_t = snow depth after the elapse of t days.

h_0 = original snow depth.

The results are shown in figure 9.5. They indicate an average annual snow accumulation of 1.60 m. Since no actual snow depth data are available from the Aneto glaciers, it is not possible to check the results. Faura (1932) measured the annual snow depth during the winter 1923—1924 and found a value of 1.50 m near the elevation of 3000 meters.

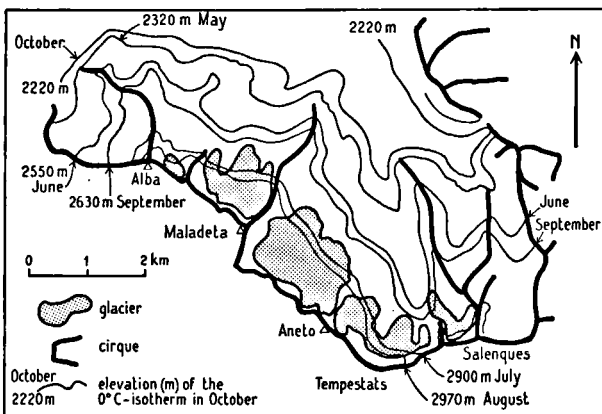


Fig. 9.3 Position of the 0°C-isotherm in the Aneto area during the summer months.

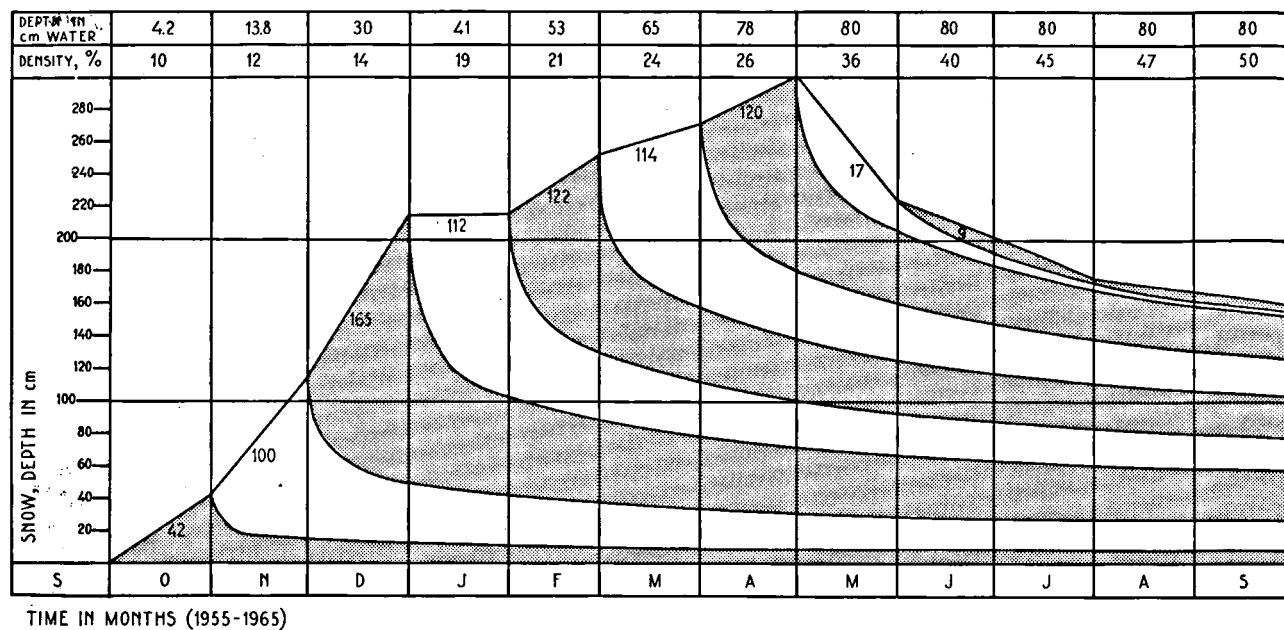


Fig. 9.5 Estimation of the average annual snow accumulation on the Aneto glacier.

The snow melting processes cannot be evaluated due to lack of accurate temperature data. However, the present position of the glacier indicates that the melting of snow above the 3000 m elevation is not very significant, perhaps about 10–20 cm.

The average ice depth of the glaciers of the Aneto group has been estimated, from aerial photographs, to be 65 meters in 1948, which corresponds to an accumulation of the precipitation for 35–40 years, with a snow density of fifty percent (fig. 9.5). The average snow density of glacier ice however, is eighty percent, which corresponds to an accumulation of the precipitation of 80 years. This value corresponds very well with the observed value of 107 years (see 9.1).

9.5 *Evaporation from the glaciers*

The average monthly evaporation, at an elevation of 3000 meters, has been estimated with a Dalton-type formula, applying the average monthly temperatures of table 9.2 and the Penman wind function $f(u_g)$ values from Restanca, (chapter 8.3). In the Dalton formula the uncorrected water vapour pressures from Viella (elev. 932 m) was not used for the Aneto

area, because the difference in elevation is too high. During the summer months a continuous flow of water vapour from the air to the snow surface was assumed and a correction factor of 0.5 was applied to the vapour pressures of Viella.

Martinec, Wartena, Brugman & Zeilmaker (1966) applied a measured correction factor of 0.68 to Viella data in order to obtain the vapour pressures for Lago Mar (elev. 2234 m). The results of the evaporation- and sublimation-estimations for the Aneto area are listed in table 9.3. It can be concluded that the sublimation is much more important than the evaporation from the glaciers in the Aneto area.

9.6 *Long term variations of the glaciers*

Eydoux & Maury (1907), Faura y Sans (1932), Forel (1900), Garcia Sainz (1930, 1935), Hess (1904), Heybrock (1933), Llopis Llado (1946), Michelier (1885), Nussbaum (1933, 1956), Penck (1883), Solé Sabaris (1957), Soler y Santalo (1933), Trutat (1877) and Vallot (1887) give information about the glaciers of the Aneto group and the long term variations in size of the glaciers in the Pyrenees.

TABLE 9.3. *Average monthly evaporation- and sublimation values (mm) for the Aneto area*

	J	F	M	A	M	J	J	A	S	O	N	D	Year
evaporation (mm)	17	10	4	0	0	0	0	5	0	0	0	20	56
sublimation (mm)	0	0	0	5	23	22	13	0	14	32	9	0	118

From all those data it can be concluded, that the glaciers of the Aneto group probably reached a maximal areal extent between 1780 to 1790. We could not obtain information earlier than 1780. The glaciers retreated from 1790—1850, advanced from 1850—1860, but retreated until 1890. An advance was observed in 1890, but since that year the glaciers are retreating. The Maladeta glacier retreated from an elevation of 2286 m (in 1809) to 2550 m (in 1870), indicating an average annual retreat of four meters. Data of the FECSA over 30 years confirm those measurements.

In figure 9.6 the areal extent of the Aneto glaciers in various years is shown. The small Russell glacier which flows into the Ribagorzana River and the small transfluencing Aneto-South or Coronas glacier, which flows into the Vallibierna River, are not shown. The position of the glaciers around 1810 has been deduced from an old picture (Solé Sabaris, 1962), whereas the position in the years 1928, 1948 and 1958 has been derived from topographical maps (scale 1:50.000). The situation in 1948, which is partly indicated on the enclosed land classification map, indicates an advance, whereas in 1958 an important retreat is evident. Long term precipitation measurements in the Valle de Arán are available from a Mougin rain gauge in Lés (elev. 630 m). The data from 43 years are shown in figure 9.6, which indicates no significant decrease in precipitation during the period 1922—1966.

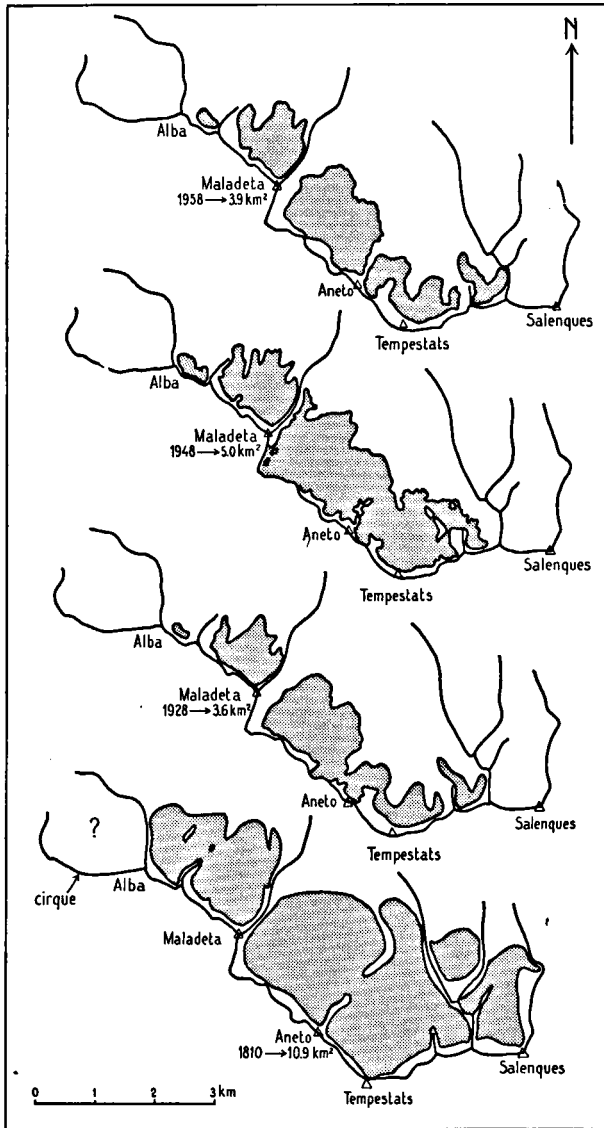


Fig. 9.6 Areal extent of the Aneto glaciers in various periods (1810, 1928, 1948 and 1958).

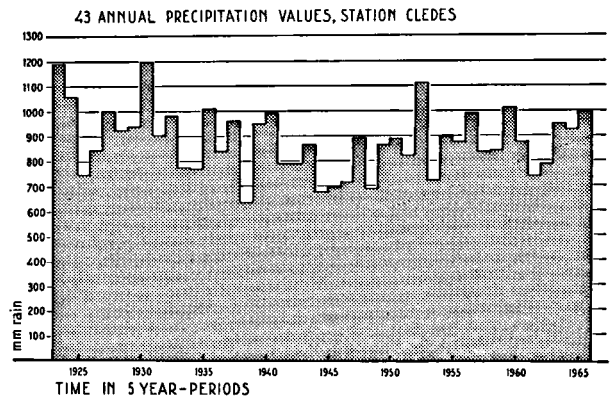


Fig. 9.7 Long term precipitation measurements (1922—1965) from Lés.

10. THE AIGUAMOIX DAM

10.1 Introduction

The Aiguamoix dam and reservoir have been designed for the regulation of the water flow to the Arties power station. The Aiguamoix rock-fill dam is 30 meters high and the Aiguamoix reservoir has a capacity of 500.000 m³. The reservoir can control a maximum water depth fluctuation of 12 meters. The construction of the dam began in 1963 and it was completed in 1966. The Aiguamoix dam and its reservoir form now part of the "Salto del Aiguamoix" system, which comprises 14.000 meters of tunnels and four small rockfill dams.

The system is indicated on the enclosed land classification map. The system uses water from the lower Iñola, Garona de Ruda, Aiguamoix and Valarties Rivers. The maximum permitted waterflow of the system amounts to 12 m³.s⁻¹ and its hydraulic head at Arties reaches a value of 247 m. However, no permission has been given yet to fill the Aiguamoix reservoir, which is probably due to the Vajont disaster in October 1963. The following study may contribute to a better understanding of the construction of the Aiguamoix dam (fig. 10.1).

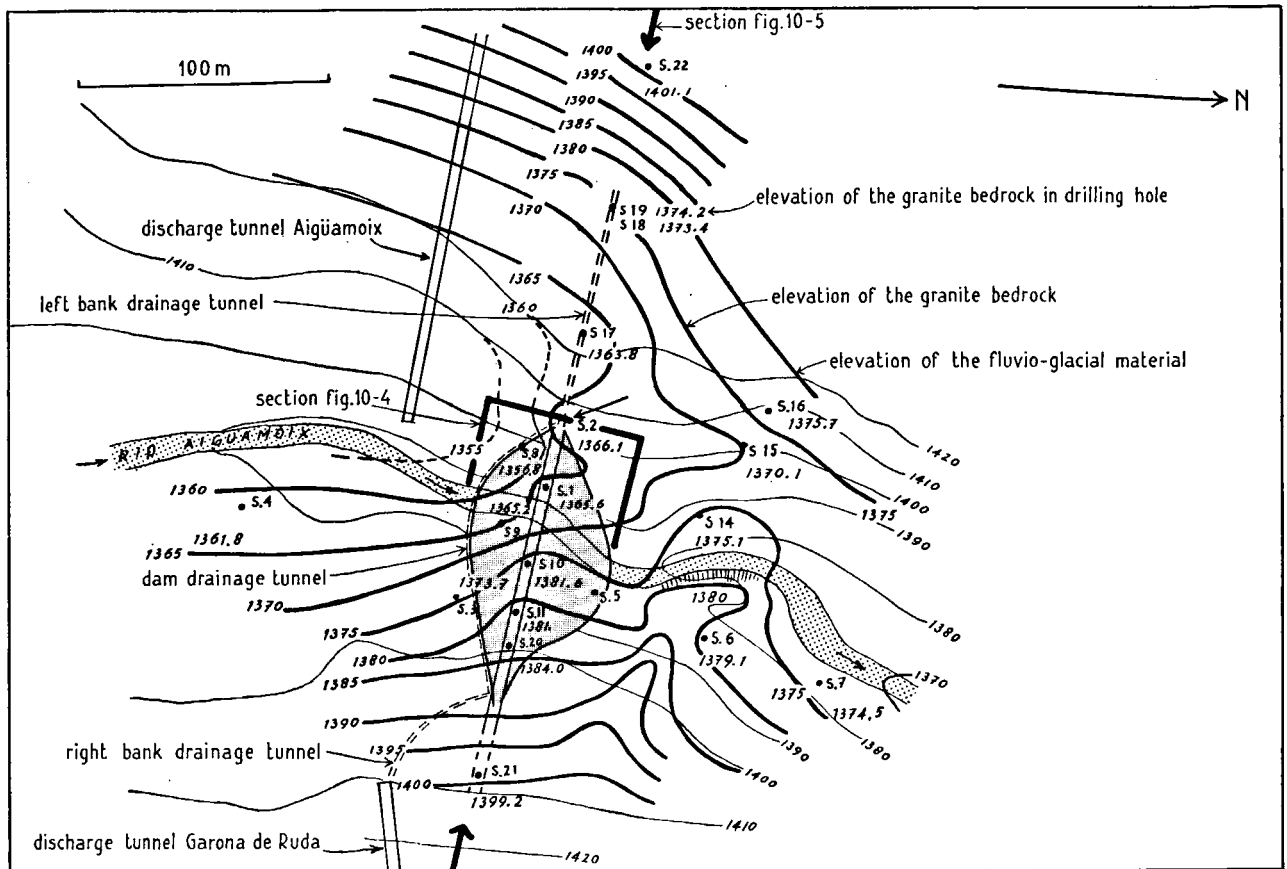


Fig. 10.1 Topographical map of the Aiguamoix dam.

10.2 Topography and geology

The entire footing of the Aiguamoix dam consists of granodiorite rubble and it was shaped by torrential and glacial erosion. The reservoir, south from the dam site, is situated in the so-called "llano" Aiguamoix. The "llano" forms a part of the flat glacial valley bottom and it has the characteristics of a lacustrine depression in glacial material, which developed after the final withdrawal of the Pleistocene Aiguamoix glacier. The depression contained a lake, which had a high water elevation of 1415 meters. It was 400 m wide, 860 m long, and 25 m deep and it was rapidly filled up by glacial material. The lake sediments could be observed during the dam excavations. The downstream end of the lake was situated 50 meters north from the present Aiguamoix dam.

Later deformations of the lake sediment have been observed in the right bank of the Aiguamoix River, 140 meters south from the dam, which indicates a later advance of the glacier. The lacustrine- and glacial-material is, over a depth of 40 meters, dissected by the Aiguamoix River (Fig. 10.2 and 10.3).

The foundations of the Aiguamoix dam could be studied during the excavations. Figure 10.4 shows profiles of the left bank. The alluvial materials on which the dam has been built, rest on a bottle-neck-

shaped granodiorite mass (fig. 10.1). The axis of the bottle neck is situated 40 meters west of the present Aiguamoix River, whereas its highest point is exposed 40 meters north of the dam.

The bed rock at the dam site has been investigated by 700 meters of diamond-drilling and three shafts.

10.3 Development of the project

The reconnaissance survey showed, that the overburden was too thick, to make excavation feasible. A rock fill dam rather than one founded on bedrock was therefore selected.

Since abundant granodiorite scree masses of high quality were available at a distance of only 800 meters, it was decided to fill the dam with scree and to seal the upstream face with a nylon-concrete cover.

Three drainage tunnels were designed, involving a total length of 370 meters. The left bank-, the dam- and the right-bank-tunnel have also been used for grouting. The tunnels discharge into the bottom drainage of the Aiguamoix dam.

10.4 Watertight screen and drainage of the foundations

The principal watertight screen (12.800 m²) consists of a total of 2140 meters of grouted diamond drill holes. The initial spacing of the diamond drill holes



Fig. 10.2 Fluvio-glacial material in the left Aiguamoix bank at the dam axis (elev. 1400 m).

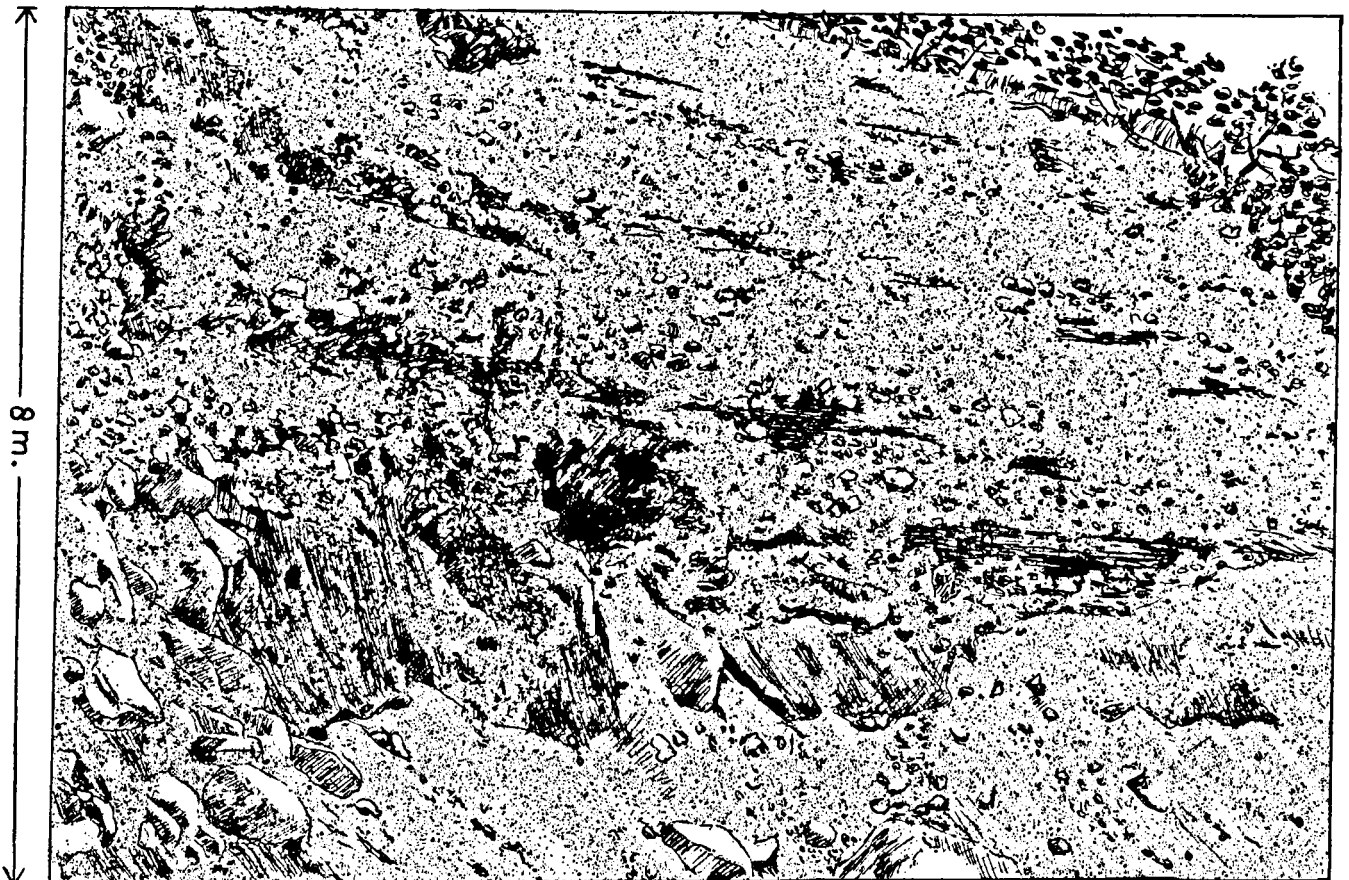


Fig. 10.3 Fluvio-glacial material in the left Aiguamoix bank, 700 m south from the dam

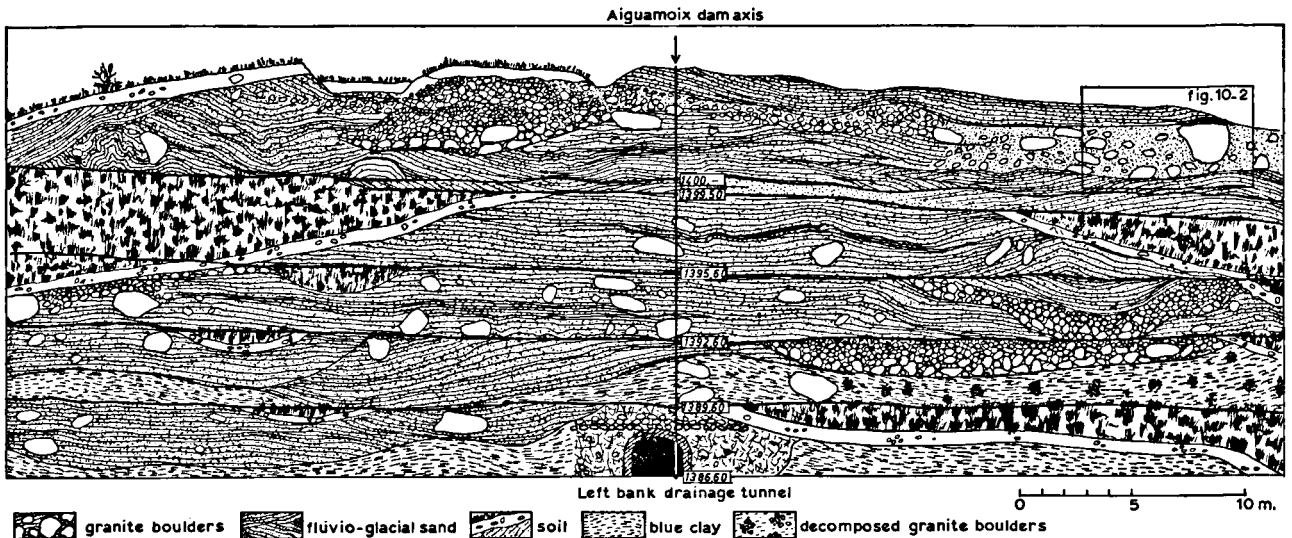


Fig. 10.4 Geological profile of the left Aiguamoix bank at the damsite.

was 6 meters, whereas the secondary holes were placed at intermediate positions.

The maximum injection pressures were fixed at 10 kg.cm^{-2} between 0 and 10 m depth, increasing by 5 kg.cm^{-2} per 5 meters of depth. Pressures were limited to 20 kg.cm^{-2} below 25 meters in depth in order to avoid any possible risks of unwanted breaking out into the ground. The injection was normally carried out in five meter sections, starting from the bottom of the hole. The entire watertight screen involved the injection of 93 m^3 cement, which means an average absorption per metre of 95 kg. The average cement absorption per m^2 screen amounted to 16 kg. Maximum cement losses during the grouting procedure amounted to 2760 kg.m^{-1} . The height of the watertight screen varies between 5 and 45 meters, averaging 16 meters.

A uniform grouting procedure was used during the dam construction. The cement quality was tested continuously. A rough test demonstrated, that the increase in cohesion of the screen was considerable after the grouting.

Since no precise information about the heterogeneous glacial deposits and the arrangements of the different strata in the supporting banks could be obtained, the grouting program met with a success largely because of the great skill and experience of the operators.

The quality of the granitic rock under the fluvial glacial deposits is excellent. The granite is an almost unaltered compact rock with a NW-SE and NE-SW joint system. The zone of slight chemical weathering on the top of the granite reached a maximum depth of 10 meters. The average percentage of core recovery remained at about 80 percent. The first 5 m of the granite was considerably jointed and permeable. The absorptions of cement per meter drilling length varied from 0—25 kg.

The drainage of the dam foundations involved 4.5

inch drilled filter drains under the dam and in the left and right bank. They were drilled from the drainage tunnels and equipped with special filters. No drains have been drilled on the downstream face of the dam.

10.5 Water permeability tests

Water permeability tests at the Aiguamoix dam have been carried out in 22 reconnaissance drillings by means of a pumping-in method with one obturator. The method comprised a closing of the upper end of a drill hole with that obturator. Water was pumped into the hole under a pressure of 5 kg.cm^{-2} and water losses in 10 minutes over the entire open sounding under the obturator were measured. Those losses were calculated in $\text{liter.min}^{-1}\text{meter}^{-1}$. The obturator was then dropped 3.50 m and the same procedure repeated until the bottom of the drill hole was reached. Heitfeld (1965) describes the errors inherent in this method. At the Aiguamoix dam some of the errors have been reduced by decreasing the interval by 50 percent. The pumping pressures had to be rectified using the Heitfeld (1965) — graphs. After correcting the water loss measurements, it was found that 45 % of the foundations have water losses below 3 Lugeons ($= 3 \text{ liter.min}^{-1}\text{meter}^{-1}$ at 10 kg.cm^{-2}), which is acceptable. The remaining 55 %, however, appeared to be very permeable and occasionally water losses of $250 \text{ liter.min}^{-1}\text{meter}^{-1}$ at 5 kg.cm^{-2} were measured. By applying the analysis of Heitfeld (1965) to the water loss values, a permeability pattern of the foundations could be obtained. The results of the study of the reconnaissance drillings, water permeability tests and cement losses are shown in fig. 10.5, which represents a hydrogeological section along the Aiguamoix dam axis. It shows an approximate permeability pattern, since the errors in the interpretation of the data concerning the extreme heterogeneous glacial material do not allow

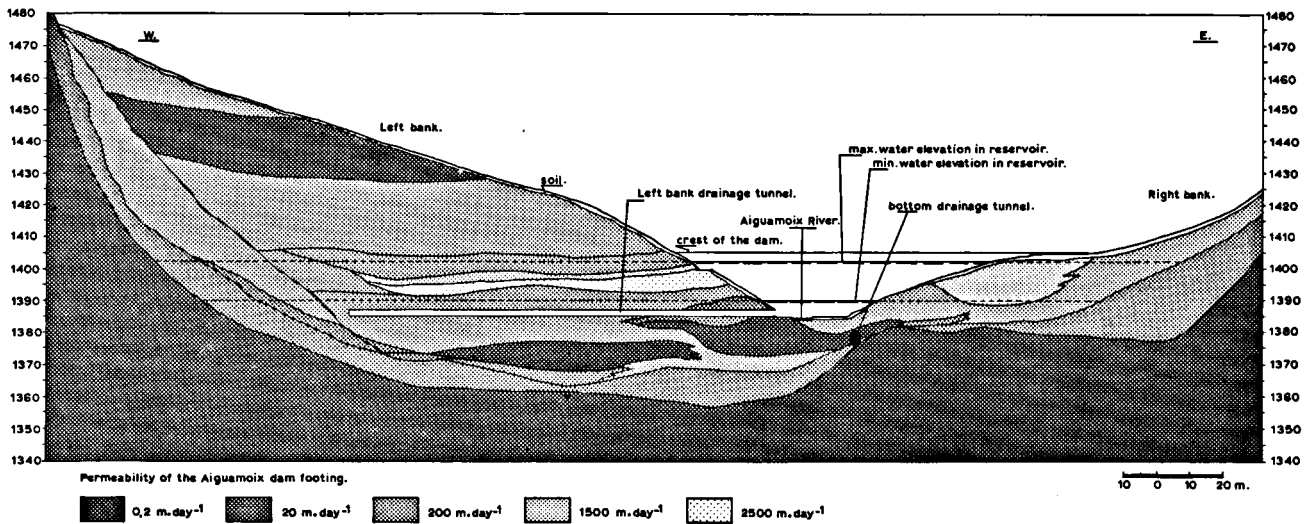


Fig. 10.5 Hydrogeological section along the Aiguamoix dam axis.

a more precise interpretation. Figure 10.5 has been used to compute the groundwater flow through the section along the dam axis.

10.6 Groundwater flow through the ungrouted Aiguamoix dam foundations

This subject is more a purely academic question rather than a practical one, although it probably might have an application to an analysis of grouting procedures. The construction of the Aiguamoix dam has fundamentally changed the groundwater flow in the Aiguamoix valley. Under normal circumstances, groundwater flow in the glacial valleys of the Valle de Arán is very restricted, because of the hummocky-shaped profiles of these valleys.

For the calculation of the laminar groundwater flow from the Aiguamoix reservoir through the ungrouted dam foundations figure 10.5 and a Darcy type formula (5) has been used:

$$Q_t = \sum_{i=1}^n A_i K_i \frac{\Phi_0 - Z_i}{L_i} \quad (5)$$

- Q_t = daily groundwater flow, ($m^3 \cdot day^{-1}$).
- A_i = cross section of horizontal layer (m^2).
- K_i = permeability coefficient, ($m \cdot day^{-1}$).
- Φ_0 = head of the filled reservoir, (m).

Z_i = vertical distance of the centre of gravity of the horizontal layer to the impermeable bedrock, (m).

L_i = length of the horizontal layer (m). See list of symbols

For the computation of the groundwater flow through the supporting banks the same equation was applied with

$$A_i = \frac{(B_{i1} + B_{i2})}{6} D_i. \quad (\text{Van Ouwkerk \& Pette, 1966}). \quad (6)$$

B_{i1} = average horizontal distance from the reservoir to bedrock. (m)

B_{i2} = average horizontal distance from the downstream exposure of the horizontal layer to bedrock. (m)

D_i = average thickness of the horizontal layer. (m)

Water losses from the maximum filled Aiguamoix reservoir under the ungrouted dam would have amounted to $13.000 \text{ m}^3 \cdot \text{day}^{-1}$, whereas the losses through the left bank would have been $57.000 \text{ m}^3 \cdot \text{day}^{-1}$ and through the right bank $24.000 \text{ m}^3 \cdot \text{day}^{-1}$. After the grouting, water losses seem to be largely reduced. This corroborates the opinion of the construction engineers, that the heterogeneous glacial material in the Aiguamoix dam foundations could be made impermeable by applying cement grouting.

11. KARST SYSTEMS

11.1 Introduction

In the Cambro-Ordovician and Devonian limestones, which occupy twelve percent of the Valle de Arán, extensive karst systems have developed (fig. 11.2). They were described by numerous authors throughout the nineteenth century. The karst phenomena prod-

uce profound changes in the various catchment areas. For a hydrological study it was therefore a requirement to delimit the karst systems as exactly as possible. From the geological map and profiles of Kleinsmiede (1960) the connections of sinkholes (forats) and springs were interpreted and checked by

means of a color tracer. The hydrological characteristics of the important Güells del Jueu karst system were studied by applying the method of De Jager (1965).

11.2 Geology

The structural geology of the five karst systems has been described by Kleinsmiede (1960). Some of the karst systems were mapped on a more detailed scale by Mey (internal report, 1963) and Leniger (1965). The five investigated karst systems, which were expected to affect the catchment areas, comprise the Güells del Jueu-, Estua-, Ruda-, Bó-, and Pila-systems. Each system is characterized by the name of its karst spring. In the Valle de Arán, sinkholes are determined by faults, joints and contact planes of limestones and slates or sandstones. The sinkholes have especially been well developed in the glacial depressions between 1900 m and 2300 m. because much cold water was available there during the Pleistocene.

11.3 The Güells del Jueu system

Figure 11.1 shows the complicated structures of the Devonian limestones in which the Güells del Jueu ("Jupiter's eye") system developed. The important

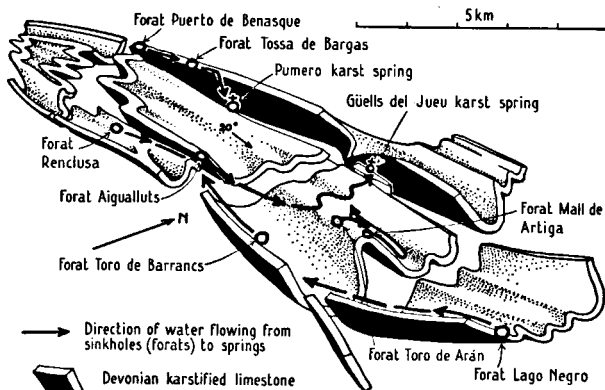


Fig. 11.1 Structures of the Devonian limestones related to the Güells del Jueu system.

sinkholes (forats) are indicated. The forat de la Renclusa,- Aigualluts,- Toro de Barrancs,- Puerto de Benasque are situated in the Upper Esera Valley. The forat del Toro de Arán and forat Mall Artiga are situated in the Jueu valley, whereas the forat Lago Negro is situated in the Negro valley.

Except the Puerto de Benasque sinkholes, which discharge into the Pumero springs, all others drain into the great Güells del Jueu spring. The Devonian limestone cuts three surficial water divides, including the main one of the Pyrenees between France and Spain (fig. 11.2). In table 11.1 some data about the Güells del Jueu system are compiled. Leniger

TABLE 11.2. *Results of color tracer experiments in the Karst systems*

Name of sinkhole and karst spring	Travel time of color tracer (hour)	Water velocity of fast runoff (m/hour) and year of measurement
Renclusa—Güells	13	385 (1947)
Renclusa—Güells	5.2	960 (1948)
Renclusa—Güells	17.2	280 (1948)
Aigualluts—Güells	12	300 (1947)
Toro de Arán—Güells	14	150 (1965)
Mall Artiga—Güells	14	140 (1965)
Toro de Barrancs—Güells	9	360 (1965)
Lago Negro—Güells	72	57 (1964)
Bargadera—Estua	288	14 (1965)
Liat—Pila	327	8 (1965)
Liat—Pila	150	57 (1950)
Liat—Pila	285	11 (1948)
Liat—Pila	300	11 (1949)
Liat—Pila	360	12 (1949)
Liat—Pila	260	10 (1949)
Liat—Terme	480	12.5 (1965)
Arcos—Bó	2.5	240 (1965)

TABLE 11.1. *Sinkholes in the karst systems*

Sinkhole (forat)	elevation (m) of sinkhole	horizontal distance to karst spring (m)	difference in elevation of sinkhole and karst spring (m)	slope in degrees	karst spring
Renclusa	2,225	5,000	745	9°	Güells del Jueu
Aigualluts	2,100	3,950	620	10°	Güells del Jueu
Toro de Arán	2,060	2,125	580	15°	Güells del Jueu
Mall Artiga	2,060	2,000	600	17°	Güells del Jueu
Toro de Barrancs	2,300	3,250	820	14°	Güells del Jueu
Lago Negro	1,980	4,125	500	9°	Güells del Jueu
Bargadera	2,020	3,350	470	8°	Estua
Liat	2,120	2,650—5,970	340—400	7°—4°	Pila—Terme
Arcos	1,960	1,200	160	8°	Bo
Pudo	2,250	6,750	830	8°	Alguaire-Ruda

1965) carried out tracer experiments in order to determine the connections of the Toro de Arán-, Toro de Barrancs- and Mall Artiga sinkholes with the Güells del Jueu spring. The results are listed in table 11.2.

Belloc (1896), Casteret (1931), Lizaur y Roldan (1951) and the F.E.C.S.A. company carried out earlier tracer experiment in the Renclusa-, Aigualluts- and Lago Negro sinkholes. Their results are shown in table 11.2. The Güells del Jueu system was studied by Belloc (1896), Escher (1953), Jeanbernat and others (1873), Lambron & Lezat (1859), Nerée-Boubée (1842), Reclus (1875) and Trutat (1877).

11.4 *The Estua system*

The Estua system occurs in a rather simple Devonian limestone structure and it cuts the surficial drainage divide of the Bargadera- and Valarties-Rivers. The Devonian structure is described by Kleinsmiede (1960). Only one major sinkhole, the forat de Bargadera was investigated. The forat is situated near the shore of a lake and the waters flow into the Estua spring. Results are listed in table 11.2.

11.5 *The Ruda system*

In the valley of the Garona de Ruda River the Ruda-karst system developed in the complicated structures

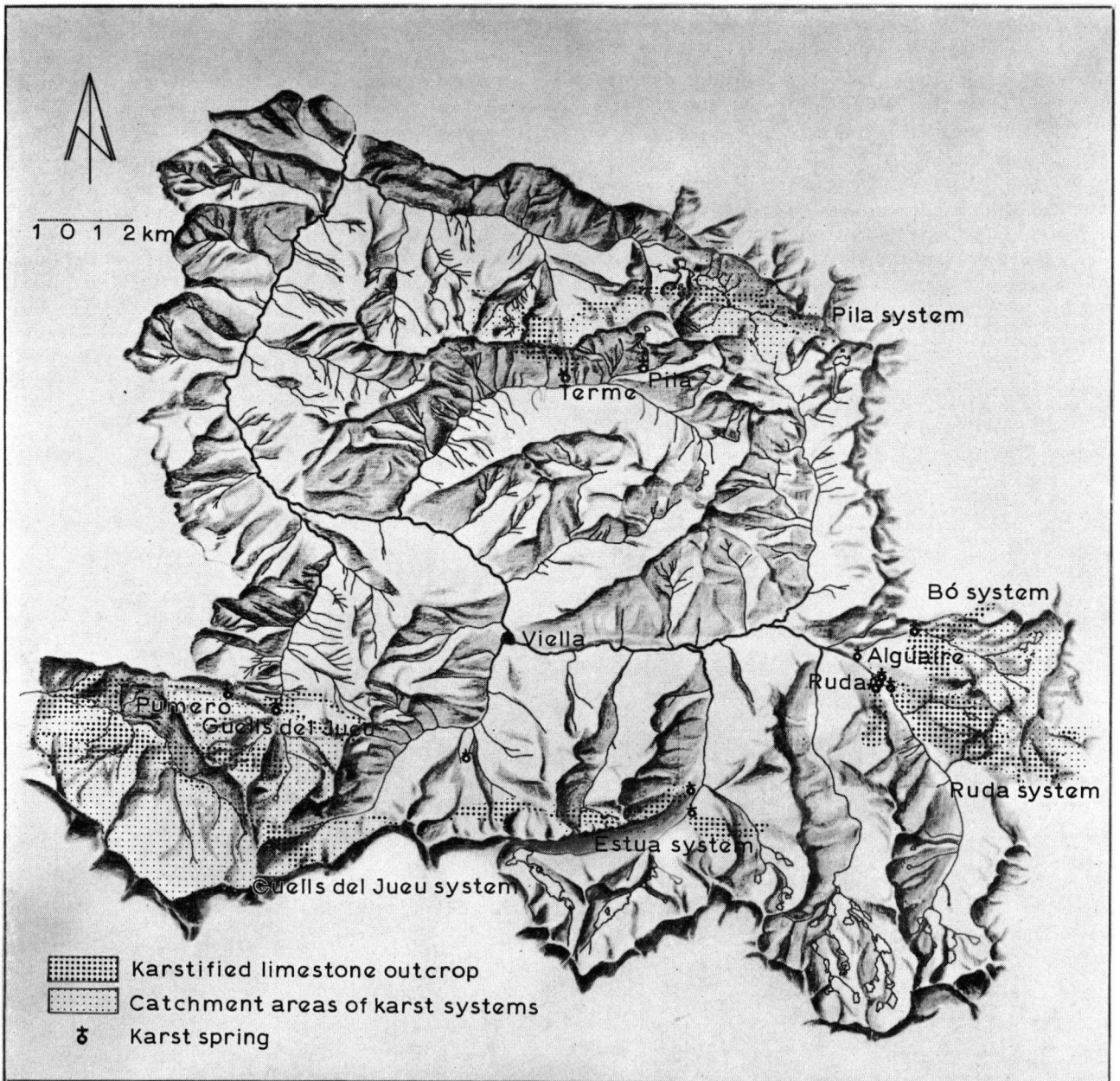


Fig. 11.2 Outcrops of karstified limestones, catchment areas of karst systems and surficial water divides in the Valle de Arán.

of the Cambro-Ordovician. The structure, which is described by Kleinsmiede (1960) as a Cambro-Ordovician anticline, does only partly explain the results of our tracer experiments. Apparently there exists no karst system in the limestones which connects the Rio Malo with the Ruda springs, as could be expected from Kleinsmiede's profiles. Therefore the Rio Malo system is considered as an independent unit, the Bó system. The Ruda system is situated in a severely karstified limestone mass which is intersected by numerous faults. It is drained by the four Ruda springs and the Algüaire spring (fig. 11.2). The Cambro-Ordovician limestones cut the surficial drainage divide of the Garona de Ruda- and the Pallaresa-Rivers. The Lago Pudo sinkhole drains probably water into the Ruda- and Algüaire springs. In the summer of 1965, no water entered the Lago Pudo sinkhole and therefore no tracer experiments could be carried out. The water of Lago Pudo discharges into the Garonne River, rather than into the Mediterranean Sea as otherwise would be expected.

11.6 *The Bó system*

The Rio Malo River is crossed by Cambro-Ordovician limestone in which the Bó system has developed. It was expected, that the Bó system drained into the Algüaire spring and thus was part of the Ruda system, but this has been proven not to be true. Tracer experiments were carried out three times in order to assure

accuracy. The results are shown in table 11.2. The Bó system produces no change in the catchment areas.

11.7 *The Pila system*

A complicated structure in the Cambro-Ordovician limestones in the Upper Toran-, Upper Iñola- and Upper Barrados-Rivers has been mapped by Kleinsmiede (1960) and Mey (internal report, 1963). Mey (1963) mapped the area in much detail. Two of his profiles are shown in fig. 11.3. The Liat sinkhole and the Pila- and Terme-springs are shown in fig. 11.2. The Pila karst system is developed in the Cambro-Ordovician limestones. A tracer experiment showed that water, entering the forat de Liat sinkhole, flows to the Pila- and Terme-springs. The Pila karst spring (fig. 11.4) is most important and it discharges at least three times as much as the Terme spring. It has not been proved that a connection exists between the Plà de l'Ana sinkholes and the Pila spring, but it is quite reasonable to expect this to be true (fig. 11.2). Results of recent and former experiments are listed in table 11.2.

11.8 *Tracer experiments*

Baeyer (1871-a), Bogomolov & Silin Bektchourine (1959), Castany (1963), Casteret (1931), Föster (1951), Kaufman & Orlob (1956), Käss (1964), Keller (1961), Knop (1875—1878), Lehmann (1934), Lizaur y

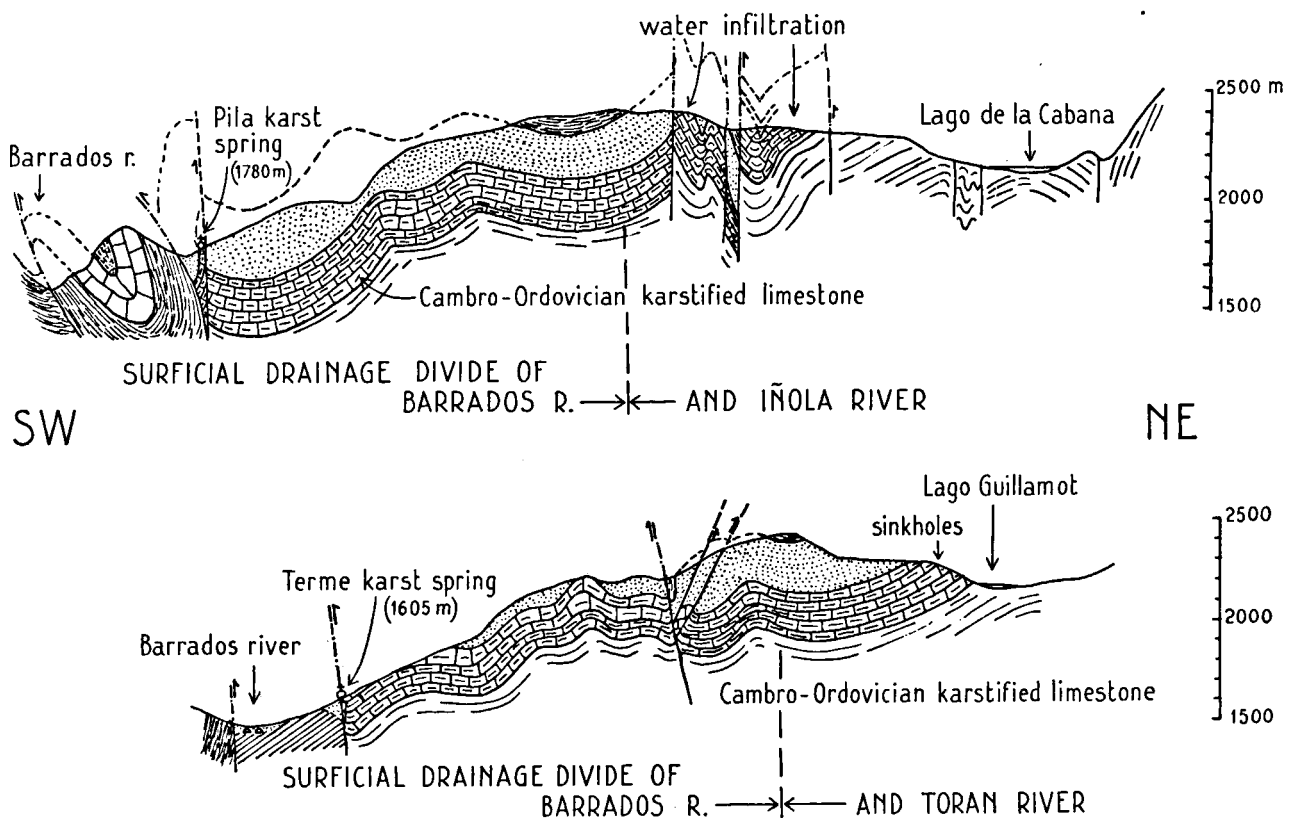


Fig. 11.3 Two geological profiles of the Pila-karst system.



Fig. 11.4 Discharge measurement of the Pila-karst spring.

Roldan (1957), Maurin & Zötl (1959), Schlichter (1902—1905) and Wilson & Thomas (1964) described tracers for a karst system, and fluoresceine appears to be the best. Therefore, this tracer was used during the experiments in 1965. The concentration of the fluoresceine was measured by comparing a sample in a test tube with standard solutions in closed test tubes. An inexpensive field apparatus was designed by J. Hogendoorn with four 1,5 V penlight cells, two wolfram lense lamps, two Kodak light source filters 47 B and two Kodak 58 observation filters. The parts were fixed in a black varnished wooden block and the unit was fastened in a small box. It appeared possible to reach an accuracy of 0.5 ppm. fluoresceine. The preparation of standard solutions requires much attention (see also Käss, 1964). The purpose of the tracer concentration measurements was to determine the average water velocity of the peak runoff in the karst system. A Gaussian distribution of the velocity was assumed and the distance sinkhole to spring was multiplied by $\sqrt{2}$. The average discharge, multiplied by the average velocity is a measure of the water storage capacity in the system. Thus for instance in the Bó system, the water storage reached a value of 900 m³ after a period

of ten dry days. The total cave volume was estimated to be 36.000 m³ by multiplying the water storage with a factor 40. This factor was the average ratio of the cross section of the caves and the cross section of the karst river.

11.9 Chemical analyses

Karst water chemical tests were carried out with the Houseman Palin test kit No. 6. Since the waters in the Valle de Arán appeared to be chemically very pure, the results of the tests could not be interpreted. The specific conductance values, measured in August 1965 showed a more reliable pattern. The conductance values of the karst waters ranged from 30—160 micro-mhos (25° C). Waters, entering the karst systems, had in general lower conductance values than those discharged by the karst springs. As could be expected however, a great variance of the chemical quality of the waters, entering the karst systems, was observed. This indicates an active mixing corrosion (Bögli, 1964) or limestone solution, throughout the karst systems.

Representative samples of the Devonian and Cambro-Ordovician limestones were chemically analyzed

(table 11.3). The results indicate that the Cambro-Ordovician limestone is very pure, whereas the Devonian limestone contains more insoluble material. Thin sections of both limestones show considerable porosity in the sparitic recrystallisation texture.

TABLE 11.3. *Chemical analyses of the Cambro-Ordovician- and Devonian-limestones (weight-percentage).*

Karstified limestone	Fe ₂ O ₃	MnO	MgO	CaO	H ₂ O+CO ₂
Cambro—Ordovician	0.3	—	—	55	44.4
Devonian	2.0	0.3	8.2	42.6	43.8

11.10 *Runoff analysis*

The outflow of the Güells del Jueu spring is continually measured in the tunnel to the Benos power station. A weir and tunnel constitute the intake for this power station (fig. 11.5). The water stage recorder (station

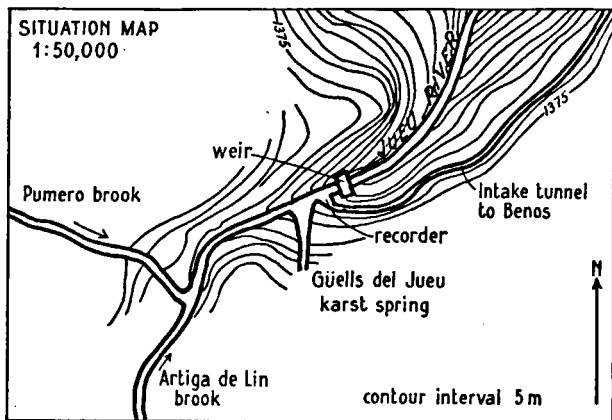


Fig. 11.5 Map, showing the situation of the Güells del Jueu karst spring.

25) is situated in such a way that the outflows of the small Pumero- and Artiga de Lin brooks are also registered. In order to obtain the real outflow of the Güells del Jueu karst system, it was necessary to subtract the runoff values of those brooks. It was difficult to study the hydraulic characteristics of the weir and intake tunnel in the Upper Jueu. The weir has been built so that the inflow into the tunnel can never exceed the maximum tunnel capacity of 5.0 m³s⁻¹. The maximum outflow of the Güells del Jueu spring, is estimated to be 15 m³s⁻¹. Therefore a reservoir analysis of karst system could only be carried out for low outflows, not exceeding 5 m³ s⁻¹.

From fourteen selected depletion curves recorded in the period August-December 1962—1965, a relation of j-values of the fast runoff and the baseflow of the karst system was obtained (fig. 11.6). The j-values of the fast runoff decrease if the related baseflow increases because the system is filled with water. During the winter, the snow cover can produce a j-value, resulting in a greater j-value of the karst system. In order to evaluate the peak storage volume, the inflow into the karst system has been calculated from the outflow of the karst spring. Three runoff peaks were analyzed (fig. 11.7) using j-values, which were derived from the recorded depletion curves. A con-

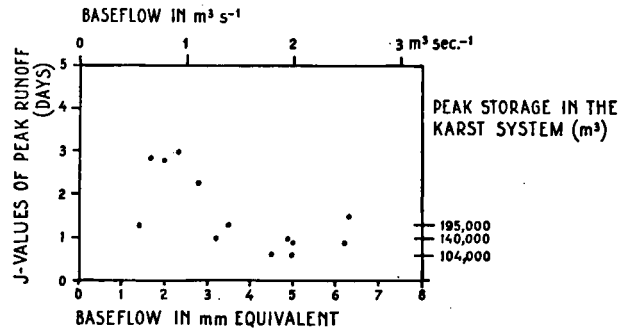


Fig. 11.6 Relation of the fast runoff and baseflow of the Güells del Jueu karst system.

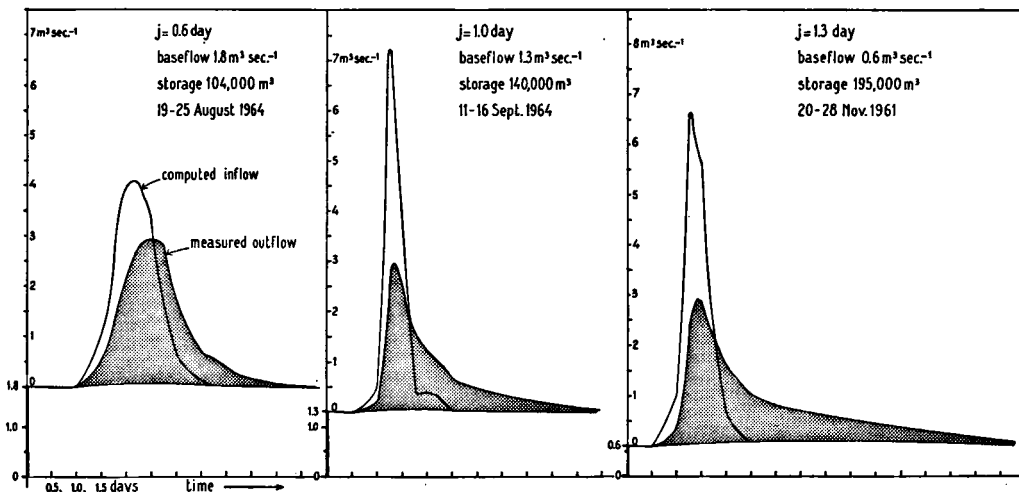


Fig. 11.7 Runoff analysis of three hydrographs of the Güells del Jueu karst system.

stant inflow during twelve hour periods was assumed. The inflow into the Güells del Jueu system is largely the result of rainfall in the Upper Esera basin. Since 39 percent of the Upper Esera basin consists of barren rocks, (see enclosed land classification map and table 7.2) an important fast runoff can be expected as inflow into the karst system. This agrees with the computed inflow curves of fig. 11.7. It was not possible to obtain a complete runoff characteristic of the Upper Esera due to lack of rainfall and runoff data.

The sinkholes (forats) of the Güells del Jueu system have been observed to overflow with a constant inflow of $20 \text{ m}^3 \cdot \text{s}^{-1}$ after a rainy period. This corresponds to a daily precipitation of 125 mm, if 40 percent of the Upper Esera has a fast runoff.

Since the maximum velocity of the water in the karst system (measured with a tracer) has a value of only $0.14 \text{ m} \cdot \text{s}^{-1}$, the system is a superposition of lakes and cascades. Apparently there are narrow tubes in the karst system, which permit the passage of only $20 \text{ m}^3 \cdot \text{s}^{-1}$. Those narrow tubes must be situated not far under the forats. If a storage of $20 \text{ m}^3 \cdot \text{s}^{-1}$ during one day is assumed, the minimum volume of the Güells del Jueu karst system can be estimated to be at least $1.7 \times 10^6 \text{ m}^3$, but it is certainly much more.

11.11 Infiltration into limestones

Measurements, carried out during July and August 1965 on karst systems in the Valle de Arán, indicate that practically no fast surface runoff is possible on these karstified limestones. The baseflow of limestone areas reached therefore values which exceeded the baseflow of little permeable glaciated high mountain basins (granite, sandstones and slates) by 50 to 100

percent. Moreover the evaporation of retention water on limestones after rainfall was very low in the summer months of 1965 as measured for the Estua system. The evaporation had values of only 0.5—1.0 mm after rainfall, whereas the evaporation of retention water of the adjacent Pontet de Rius granite area reached a value of 3.0 mm after rainfall. The total average annual infiltration on limestones could be estimated from measurements on the Pila system. A value of 3.0 mm day^{-1} was computed during 1955 and 1956. The infiltration is greatest during the snowmelt period (6.3 mm day^{-1}) and minimal during the winter ($1.9 \text{ mm} \cdot \text{day}^{-1}$).

As stated previously, the baseflow of karst systems in the Valle de Arán is very important. It was possible for the Güells del Jueu system, to analyze the baseflow from the depletion curves for the winter months from December-March 1962—1965. In the winter period the entire Upper Esera area is covered with snow and infiltration is at a minimum. The baseflow is characterized by j-values of 30 days, 90 days, 450 days and even 750 days. This indicates, that an important part of the karst reservoir empties extremely slowly. The outflow of the karst system, even in February, exceeds always $0.3 \text{ m}^3 \cdot \text{s}^{-1}$. This is equivalent to a water depth of $0.8 \text{ mm} \cdot \text{day}^{-1}$ on the Upper Esera basin (34 km^2). Since the total area of the limestones of the karst system is about 12.7 km^2 , the baseflow of $0.8 \text{ mm} \cdot \text{day}^{-1}$ corresponds to an infiltration of $2 \text{ mm} \cdot \text{day}^{-1}$. According to De Zeeuw (1966), this type of baseflow can be defined as the seepage flow of the karst system. The seepage flow of the Pila karst system corresponds with j-values of 30, 50, 100 and 180 days. In the Ruda system, j-values of 60, 90 and 240 days were computed for the seepage flow.

12. WATER BALANCE

12.1 Water balance of two selected basins

The method of Searcy (1960) has been applied for the correlation of the runoff of the Pontet de Rius and the Aigüestortes basin in order to fill gaps in the records (fig. 12.1). The runoff for both stations (number 20 and 3) has been derived from the recorded water stage heights from 1959—1963. The correlation coefficient has a value of 0.90. The average annual runoff of stations 20 and 3 amounted to 1735 mm and 1643 mm respectively. The higher runoff value of the Pontet de Rius basin is the result of more precipitation (fig. 6.3), which can be evaluated at both basins, since their average altitudes are known (fig. 7.4). By using fig. 6.6, precipitation values of 1720 mm and 1560 mm can be derived. The water balance (table 12.1) shows errors in the precipitation and runoff. The actual evaporation in the Pontet de Rius basin is greater than in the Aigüestortes area. This is probably due to a more extensive scree area and a greater "rouche moutonnée" landscape in the Pontet de Rius basin (fig. 12.2).

TABLE 12.1. Water balance of the Pontet de Rius- and Aigüestortes-basin (1959—1963)

Basin and number of gauging station	Precipitation (mm)	Runoff (mm)	Difference Precipitation-Runoff (mm)
Pontet de Rius (20)	1720	1735	—15
Aigüestortes (3)	1560	1643	—83

12.2 Water balance of eight basins

Table 12.2 shows the water balance of eight basins which have been analyzed in chapter seven. It is clear, that the errors in the terms precipitation and runoff are significant. Only the water balance of the Upper Valarties-, Upper Aiguamoix- and Lower Negro-basins show differences between precipitation and runoff, which correspond to the estimated evaporation values of chapter eight. Precipitation values were

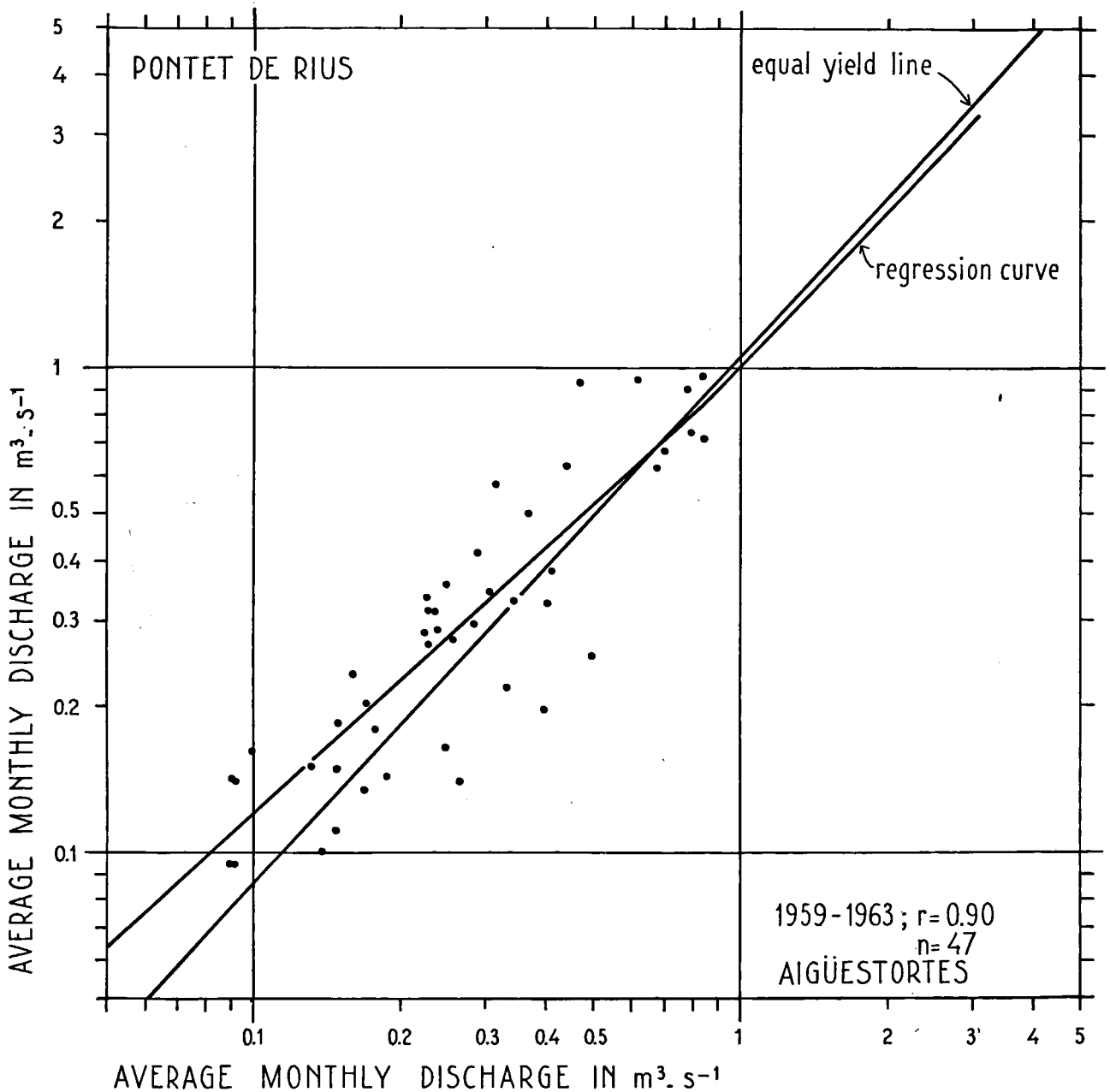


Fig. 12.1 Graphical correlation of the runoff of the Pontet de Rius- and Aigüestortes-basin.

determined with fig. 12.3 and fig. 6.6, and runoff values were derived from appendix tables 41, 42, 43 and 44.

12.3 *Water balance of the Valle de Arán*

A water balance of the Valle de Arán can be set up for the years 1956, 1957, 1962 and 1963. During those years the runoff at station 29, Pont de Rey, is known. The runoff data of 1962 and 1963 are very reliable, because they have been registered in the power station of Pont de Rey.

The precipitation during the four years was estimated with the method, as explained in chapter 6. The water balance is shown in table 12.3. It indicates, that

the term precipitation minus runoff is too small. In chapter 8 the actual evaporation in the Valle de Arán has been estimated to be 500–550 mm (1955–1965). If during the years 1962 and 1963, with very reliable runoff data, a precipitation error of ten to fifteen percent is assumed, which is very probable due to the high position of the rain gauges above ground level, the term evaporation in the water balance (table 12.3) corresponds very well with the calculated Penman evaporation values. It can be concluded, that the errors, which were found in the previous ten water balances were produced by too low precipitation values and inaccurate runoff measurements.



Fig. 12.2 The "roche moutonnée" landscape in the Pontet de Rius basin.

TABLE 12.2. Ten-year water balance of eight basins (1946—1956)

Basin and number of runoff gauging station	Precipitation (mm)	Runoff (mm)	Difference Precipitation-Runoff (mm)
Iñola (6)	1420	1419	1
Negro (13)	1790	1672	118
Barrados (16)	1570	1676	-106
Garona de Ruda (2)	1450	1537	-87
Upper Valarties (20)	1931	1422	509
Upper Aiguamoix (3)	1816	1463	353
Upper Negro (12)	1890	2017	-127
Lower Negro (13-12)	1700	1052	648

12.4 Runoff of the Valle de Arán

The runoff of the Valle de Arán (station 29) during the calendar year 1956 is shown in fig. 12.4. The slow runoff or baseflow is extremely important. It exceeds always 1.5 mm day^{-1} , which corresponds to 30—35

percent of the annual precipitation. During August and September 1956 the valley was free of snow, and runoff characteristics were calculated: $10\% j = 1.5 \text{ day} + 2.0 \text{ mm day}^{-1}$ (August) and $15\% j = 1.5 \text{ day} + 1.5 \text{ mm day}^{-1}$ (September). See also 7.5 for runoff characteristics. For the entire Valle de Arán the percentage of the precipitation, which contributes to the fast runoff corresponds also to the area of barren rocks.

It can be concluded that in the Valle de Arán huge quantities of water are stored, which leave the Upper Garonne basin only after six months (snow) or after a period ranging from 15—60 days (rain). Fast runoff is only a minor phenomena.

TABLE 12.3. Water balance of the Valle de Aran of 1956, 1957, 1962 and 1963

Year	Precipitation (mm)	Runoff (mm)	Precipitation—Runoff (mm)
1956	1300	1360	-60
1957	1120	985	135
1962	1260	1140	120
1963	1650	1400	250

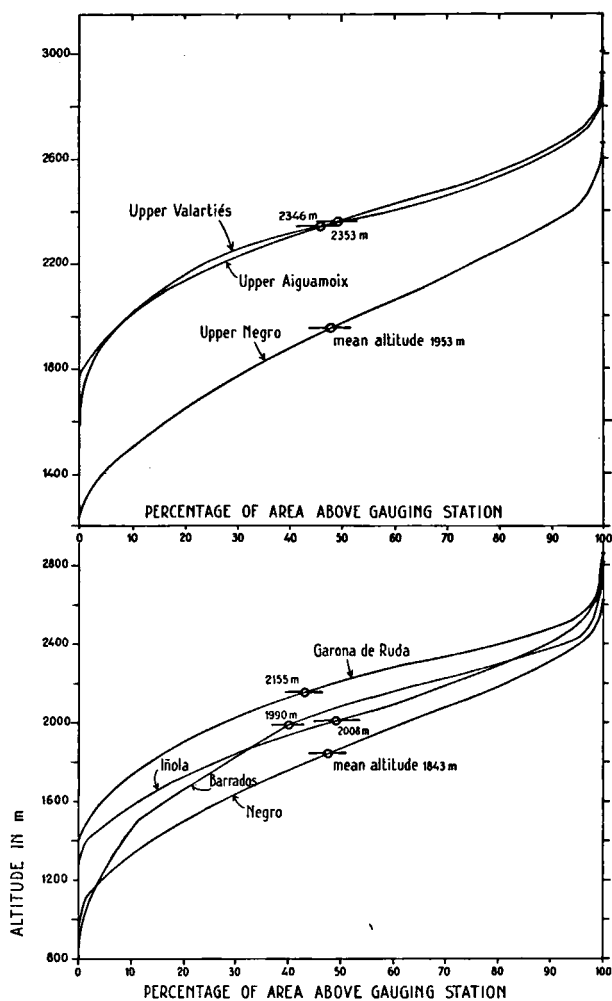


Fig. 12.3 Hypsometric integrals for eight basins.

CONCLUSIONS

1. The runoff in the Valle de Arán consists essentially of baseflow.
2. The baseflow is related to the areas covered by scree and forest.
3. Fast runoff is only a minor phenomenon.
4. The percentage of the precipitation which contributes to the fast runoff is related to the area of barren rocks.
5. Orographic precipitation is induced by the slopes and general trend of the mountain ranges.
6. Broad valleys with steep slopes are characterized by a homogeneous precipitation pattern.
7. Rainfall measurements at 1.50 m above ground level give about 50 percent higher results than those simultaneously recorded from 4.40 m above ground level.
8. The Penman evaporation values give reliable results in this mountainous terrain.
9. The annual actual evaporation (500—550 mm) decreases with altitude.
10. On the glaciers, at an elevation of 3000 m, sublimation exceeds evaporation.
11. The storage coefficient of the fast runoff in karst systems decreases rapidly when the systems reach the saturation stage.
12. Water infiltration into karstified limestones during the snow melt period is highly significant (6 mm/day).
13. A morphometric analysis demonstrated that the planation level from elevations 2500—2000 m constitutes the remains of a Miocene landscape, with a relief of at least 1000 meters.
14. Specific degradation in a section of the axial zone of the Pyrenees during part of the Tertiary was only 33 mm/1000 year.

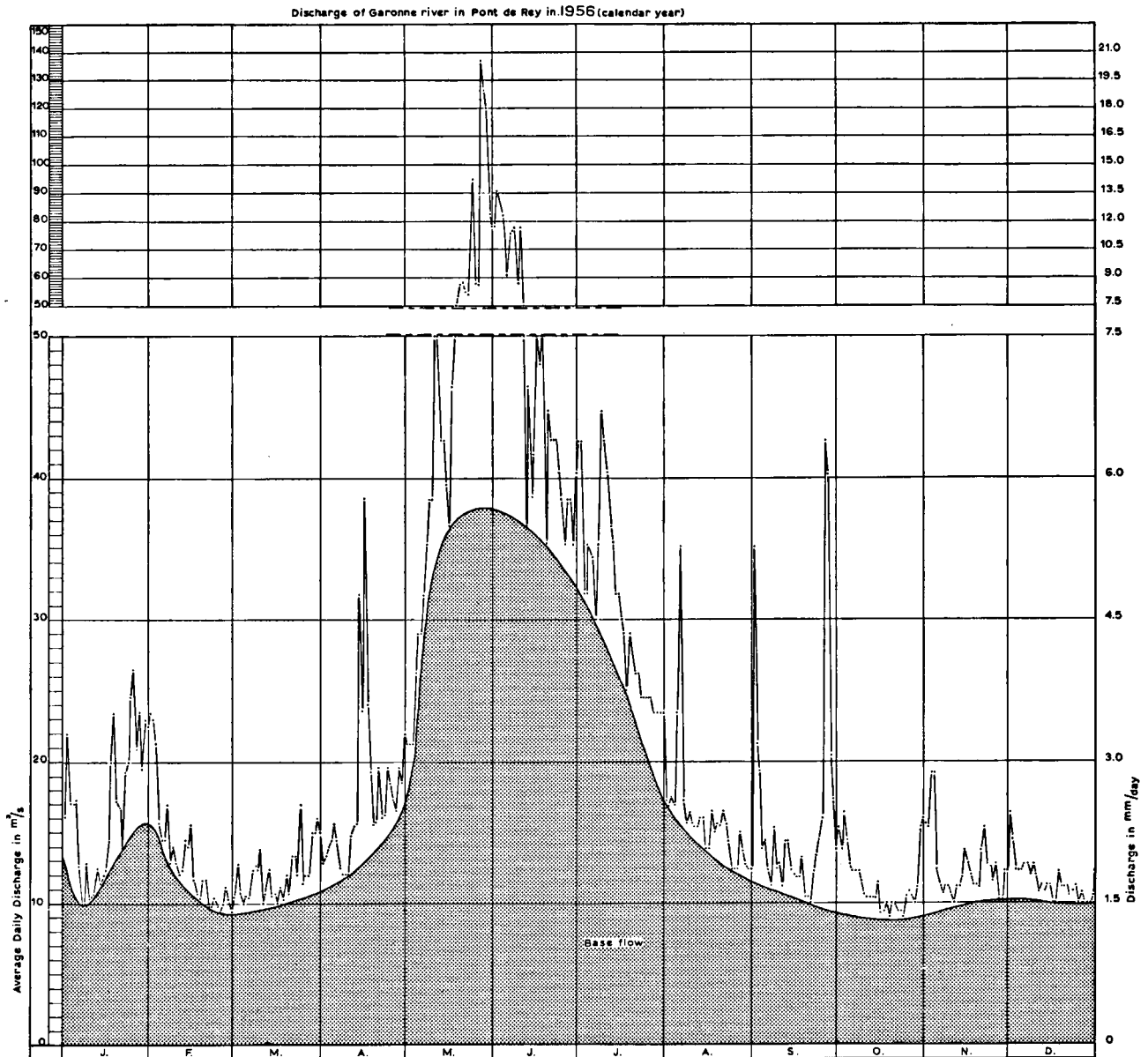


Fig. 12.4 Runoff of the entire Valle de Arán during the calendar year 1956.

REFERENCES

- Atlas reducido de nubes, 1943. Publ. C, 12, Serv. Met. Nac. Madrid, 21 p.
- Baeyer, A. v., 1871a. Über eine neue Klasse von Farbstoffen. Ber. Chem. Ges. Berlin, 4, p. 555—558.
- Belloc, E., 1894. Nouvelles recherches lacustres faites au port de Venasque, dans le Haut-Aragon et dans la Haute-Catalogne (Pyrénées centrales). Assoc. Franc. Avanc. Sci. Congr. Besançon. Vol. 2, p. 415—442.
- Benson, M. A., 1962a. Evolution of methods, for evaluating the occurrence of floods. U.S. Geol. Survey, Water-Supply Paper 1580-A, 30 p.
- 1962b. Factors influencing the occurrence of floods in a humid region of diverse terrain. Geol. Survey Water-Supply Paper 1580-B, 64 p.
- Bleasdale, A., 1959. The measurement of rainfall. *Weather*, 14, p. 12—18.
- Bögli, A., 1964. Die Kalkkorrosion, das zentral Problem der unterirdischen Verkarstung. *Steirische Beitr. Hydrogeol. N.F.* 1963/1964, p. 68—75.
- Bogomolov, G. V. & Silin-Bektchourine, A. I., 1959. *Hydrogéologie spécialisée*. B.R.G.M. publ. 37, Paris, 235 p.
- Braak, C., 1945. Invloed van de wind op regenwaarnemingen. *Kon. Ned. Meteor. Inst. Med. en Verh.* 48, 74 p.
- Bruce, P. & Potter, J. G., 1957. The accuracy of precipitation measurements. *Proc. R. Met. Soc. Canad. Branch*, 8, p. 1—15.

- Brugman, A. J. M., 1965. Lago Mar, onderzoek ter bepaling van de meerverdamping. M.Sc. thesis Geol. Inst. Leiden, 39 p.
- California Department of Public Works, 1923. Flow of California streams. Div. Eng. and Irrigation, Bull. 5, chap. 5.
- Campistol, J. R., 1951. Francia, la corona de Aragon y la frontera pirenaica. C.S.I.C., Est. Medievales 18, Madrid, 331 p.
- Caro Baroja, J., 1946. Los pueblos de España, Barcelona.
- Castany, G., 1963. Traité pratique des eaux souterraines. Paris, 648 p.
- Casteret, N., 1931. Le problème du Trou du Toro, détermination des sources du Rio Esera et de la Garonne Occidentale. Bull. Soc. Hist. Nat. Toulouse, t. 61, fasc. I, p. 89—132.
- Cenac, P. & Moncaut, J., 1873. Histoire des peuples et des états pyrénéennes depuis l'époque celtibérique jusqu'au nos jours. 3ième ed. Paris.
- Colenbrander, H. J., 1965. The Research Watershed "Leerinkbeek", Netherlands. Symposium Budapest I.A.S.H. 66, p. 558—563.
- Dalrymple, T., 1960. Flood frequency analysis. U.S. Geol. Survey Water-Supply Paper 1543-A, 80 p.
- Dalton, J., 1892. Experimental essays on the constitution of mixed gases; on the force of steam or vapor from water and other liquids in different temperatures, both in a Torricelli vacuum and in air; on evaporation; and on the expansion of gases by heat. Manchester Lit. Phil. Soc. Mem. Proc., vol. 5, p. 536—602.
- De Jager, A. W., 1965. Hoge afvoeren van enige Nederlandse stroomgebieden, 167 p., Centr. Landb. Publ. Doc. Wageningen.
- De Lizaur y Roldan, J., 1951. Estudio sobre las conexiones subterráneas de las cabeceras de los rios Esera y Garona. Libro Jubilar 1848—1948, t. II, Madrid, p. 381—425.
- De Sitter, L. U., 1953. Note préliminaire sur la géologie du Val d'Aran. Leidse Geol. Med. 18, p. 272—280.
- 1956. A cross section through the Central Pyrenees. Geol. Rundschau, B. 45, p. 214—233.
- De Zeeuw, J. W., 1966. Analyses van het afvoerregime van gebieden met hoofdzakelijk grondwaterafvoer, Wageningen, 139 p.
- Dominy, F. E., 1965. Water resources developments in Spain. Rept. Bur. of Reclamation, Dept. of the Interior, Washington, p. 7.
- Escher, B. G., 1953. Une perspective-relief de la région du Trou du Toro et des Gouëils de Jouéou (Pyrénées centrales). Prem. Congr. Int. Spel., Paris, t. II, 1, p. 1—2.
- Eydoux, D. & Maury, L., 1907. Les glaciers orientaux du Pic Long (Pyrénées centrales).
- Fairbridge, R. W., 1965. Eiszeitklima in Nordafrika. Geol. Rundschau, B. 54, H. 1, p. 299—414.
- Faura y Sans, M., 1932. Origenes del Garona o del Esera. Rev. Ciencia, 7, Barcelona.
- Flohn, H., 1965. Grundfragen der Paläoklimatologie im Lichte einer theoretischen Klimatologie. Geol. Rundschau, B. 54, H. 1, p. 504—515.
- Forel, J., 1900. Les variations périodiques des glaciers. Extr. Sci. Phys. Nat. Genève.
- Föster, Th., 1951. Fluoreszenz organischer Verbindungen. Göttingen, 312 p.
- Garcia Sainz, L., 1930. Les phénomènes d'époque glaciaire et d'évolution karstique dans le Val du Haut-Esera (Espagne). Geogr. Anales, Stockholm, 12, p. 323—339.
- 1935. Morfologia glaciär y preglaciär de la region de la Noguera (Cuenca, Cinca, Segre). Boll. Soc. Geogr. Nac., t. 75, p. 64—110.
- Gold, E., 1931. The splashing of rain. Meteor. Mag., 66, p. 153—158.
- Haver, A., 1951. A new recording rain gauge. Jour. Sci. Instrum. 28, p. 84—85.
- Heybrock, W., 1933. A note on the Aneto glacier. Geol. Jour., 82.
- Heitfeld, K. H., 1965. Hydro- und baugeologische Untersuchungen über die Durchlässigkeit des Untergrundes an Talsperren des Sauerlandes. Geol. Mitt. 5, H. 1—2, 210 p.
- Hess, H., 1904. Die Gletscher, Braunschweig, p. 85—290.
- Higashi, A., 1957. Snow survey in Hokaido, Japan, I.A.S.H. Gen. Ass. Toronto, 4, p. 22—39.
- Hoor, B. v., 1965. Foto-morfologische analyse van het Valle de Aran. M.Sc. thesis Geol. Inst., Leiden, 32 p.
- Jarvis, C. S. and others, 1936. Floods in the United States, magnitude and frequency, U.S. Geol. Survey Water-Supply Paper 771, p. 497.
- Jeanbernat, D., Peyre, A., Timbal-Lagrave, E. & Filhol, E., 1873. Une excursion scientifique aux sources de la Garonne et de la Noguera-Pallaresa (Catalogne); topographie, botanique, mineralogie. Bull. Soc. Sci. Phys. Nat. Toulouse, t. 1, p. 46.
- Jelgersma, S., 1957. Investigaciones palinologica de lignitos terciarios procedentes de Cerdaña y del Valle de Aran. C.S.I.C. Inst. Lucas Mallada, fasc. 4, p. 159—162.
- Kaufman, W. J. & Orlob, G. T., 1956. Measuring ground water movement with radioactive and chemical tracers. Jour. Am. Water Works Assoc., vol. 48, nr. 5, p. 559—572.
- Käss, W., 1964. Die unmittelbare Bestimmung von Uranin-Spuren bei Farbversuchen. Steirische Beitr. Hydrogeol. N.F. 1963/1964, p. 38—67.
- Keller, R., 1961. Gewässer und Wasserhaushalt des Festlandes, Berlin, p. 239—245.
- Kleinsmiede, W. F. J., 1960. Geology of the Valle de Aran (Central Pyrenees). Leidse Geol. Med. 25, p. 131—241.
- Knop, A., 1875. Über die hydrographischen Beziehungen zwischen der Donau und der Aach quelle im Badischen Oberlande. N.Jb. Min. p. 942—958.
- Köppen, W. & Geiger, R., 1936. Handbuch der Klimatologie, Vol. 1, Pt. C, Borntraeger, Berlin.
- Kurtyka, J. C., 1953. Precipitation measurements study. Illinois State Water Survey Division, Urbana, 178 p.
- Krayenhoff van de Leur, A. D., 1958. A study of non-steady groundwater flow with special reference to a reservoir coefficient. De Ingenieur 70B, p. 88—94.
- 1962. A study of non-steady groundwater flow II. De Ingenieur 74B, p. 285—292.
- 1965. In: De Jager, A. W.: Hoge afvoeren van enige Nederlandse stroomgebieden. Centr. Landb. Publ. Doc. Wageningen, p. 20—22.
- Lacy, R. E., 1951. Observations with a directional rain gauge. Quart. Jour. R. Met. Soc. 77, p. 283—292.
- Lamborn, E. & Lezat, T., 1859—1860. Les Pyrénées et les eaux thermales de Bagnères de Luchon, 2 vol., Paris, 976 p.

- Langbein, W. B., 1949. Annual floods and the partial duration series. *Am. Geophys. Union Trans.* v. 30, p. 879—881.
- Lautensach, H., 1964. Die iberische Halbinsel. p. 337—354.
- Lehmann, O., 1932. Hydrographie des Karstes. *Enzykl. d. Erdk.* p. 122—124
- Leniger, H. D. F., 1965. Karsthydrogeologie van het Valle de Aran. M.Sc. thesis Geol. Inst., Leiden, 32 p.
- Lizop, R., 1931. Histoire des deux cités gallo-romaines: les Convenae et les Consoranni, Toulouse.
- Llopis Llado, N., 1946. Los movimientos corticales intra-cuaternarios del NE de España. *Est Geol.* 3, Madrid, p. 181—236.
- Meinzer, O. E., 1942. *Hydrology*, London. p. 93—113
- Martinez, J., Wartena, L., Brugman, A. J. M. & Zeilmaker, D. A., 1966. Water balance assessment of Lago Mar in the Pyrenees. *Symposium of Garda. I.A.S.H.*, 70, p. 59—76.
- Martinez, J., 1965. Snow cover density changes in an experimental watershed. *Symposium A.I.S.H. Davos*, p. 127—134.
- Mattauer, M. & Seguret, M., 1966. Sur le style des déformations tertiaires de la zone axiale hercynienne des Pyrénées. *C.R. Somm. Soc. Géol. France*, fasc. 1, p. 10—13.
- Maurin, V. & Zött, J., 1964. Die Hydrogeologie der Kykladeninsel, Amorgas. *Steirische Beitr. Hydrogeol. N.F.* 1963—1964, p. 107—154.
- Mey, P. H. W., 1963. Rapport sur la mise en carte géologique d'une région entre le Rio Barrados et l'Etang de Liat. *Internal report*, Geol. Inst., Leiden, 6 p.
- Michelier, F., 1885. Etude sur les variations des glaciers des Pyrénées. *Ann. Bur. Centr. Met. France*, 1, p. 37—235.
- Moner y de Siscar, J. M., 1898. Historia de Rivagorzana desde su origen hasta nuestros dias. Ribagorzana-Fonz.
- Nagel, J. F., 1954. New recording rain gauges. *Jour. Sci. Instrum.*, 31, p. 158—162.
- Nérée-Boubée, M., 1842. Sur les traces d'anciens glaciers dans les Pyrénées. *C.R. Ac. Sci.*, t. 14, p. 528.
- Nussbaum, F., 1938. Die eiszeitlichen Schneegrenze in den Pyrenäen. *Comm. 3rd Int. Quart. Congr. Vienna*, p. 182—211.
- 1956. Observations morphologiques dans la région de la Noguera Pallaresa. *Pirineos, Rev. Est. Pyrenaicos, Zaragoza*, 12, p. 57—98.
- Nye, J. F., 1965. The flow of a glacier in a channel of rectangular elliptic or parabolic cross section. *Jour. Glac.*, vol. 5, 41, p. 661—689.
- Penck, A., 1883. Die Eiszeit in den Pyrenäen. *Mitt. d. Vereins für Erdkunde, Leipzig*, 69 p.
- Penman, H. L., 1960. *Vegetation and hydrology*. *Techn. comm.* 53, Harpenden, 124 p.
- Pericot, L., 1934. *Historia de España*, Barcelona.
- Poncelet, L., 1959. Sur le comportement des pluviomètres. *Inst. R. Met. de Belgique, Bruxelles*, 58 p.
- Powell, R. W., 1943. A simple method of estimating flood frequencies. *Civil Eng.* vol. 13, 2, p. 105—106.
- Priestley, C. H. B., 1959. Turbulent transfer in the lower atmosphere, Chicago, 130 p.
- Reclus, J. J. E., 1875. *Nouvelle géographie universelle*, t. 2, La France, p. 113.
- Riesbol, H. S., 1940. Report on exploratory study of rain gauge shields and enclosures at Coshocton, Ohio. *Trans. Am. Geophys. Union*, 21, p. 474—482.
- Rubinstein, E. S., Allisow, B. P. & Drosdow, O. A., 1956. *Lehrbuch der Klimatologie*, Berlin, 536 p.
- Scheidegger, A. E., 1961. *Theoretical geomorphology*. Springer Verlag, Berlin, 333 p.
- Schröder, M. & van Rooyen, P., 1967. De verdamping van het Certescansmeer. M.Sc. thesis Geol. Inst. Leiden, 46 p.
- Schlichter, C. S., 1902. The motion of underground waters. *U.S. Geol. Survey Water-Supply Paper* 67, 106 p.
- 1905. Field measurement of the rate of movement of underground water. *U.S. Geol. Survey Water-Supply Paper* 140, 122 p.
- Searcy, J. K., 1960. Graphical correlation of gaging-records. *Geol. Survey Water-Supply Paper* 1541-C, 100 p.
- Slatyer, R. O. & McIlroy, I. C., 1961. *Practical micro climatology*, Canberra, 175 p.
- Smithsonian Institution, 1951. *Smithsonian meteorological tables* *Smiths. Misc. Colln.*, vol. 114, 527 p.
- Solé Sabaris, J., 1951. *Los Pirineos, el medio y el hombre. El mundo y los hombres* 8, Barcelona, 624 p.
- 1962. *Geografia de Catalunya*. Ed. Aedos, Barcelona, 665 p.
- Soler y Santalo, J., 1933. *La Vall d'Aran*, 2nd ed., C.E.C., Barcelona.
- Stanhill, G., 1958. Rainfall measurements at ground level. *Weather*, 13, p. 33—34.
- Taillefer, F., 1951. *Le piemont des Pyrénées françaises*, Toulouse, 383 p.
- Thorntwaite, C. W., 1948. An approach toward a rational classification of climate. *The Geogr. Rev.* 38, 55.
- Thorntwaite, C. W. & Mather, J. R., 1955. The water balance. *Publ. in climatology*, vol. 8, 1, 104 p.
- Thorntwaite, C. W. & Mather, J. R., 1957. Instructions and tables for computing potential evapotranspiration and the water balance. *Publ. in climatology*, vol. 10, 3, 311 p.
- Trutat, E., 1877. Des glaciers des Pyrénées, station de la dent de la Maladetta. *Ann. Club Alpin Franç.* 3, p. 408—486.
- Turc, L., 1953. *Le bilan d'eau des sols*. *Inst. Nat. Rech. U.S. Agron, Paris*.
- U.S. Geol. Survey Water-Supply Paper 1251, 1957. *Quality of surface waters of the U.S. 1952*, parts 5 & 6, 478 p.
- 1351, 1958. *Quality of surface waters of the U.S. 1954*, parts 5 & 6, 283 p.
- 1401, 1959. *Quality of surface waters of the U.S. 1955*, parts 5 & 6, 305 p.
- 1450, 1960. *Quality of surface waters of the U.S. 1956*, parts 1—4, 603 p.
- 1451, 1960. *Quality of surface waters of the U.S. 1956*, parts 5 & 6, 349 p.
- 1520, 1960. *Quality of surface waters in the U.S. 1957*, parts 1—4, 641 p.
- 1547, 1962. *Inventory of published and unpublished sediment-load data, U.S. and Puerto Rico, 1950—1960*, 117 p.
- U.S. Weather Bureau, 1952. *Interpretation of missing precipitation records*. *Monthly Weather Rev.* vol. 80
- Vallot, J., 1887. *Oscillations des glaciers pyrénéens. Etudes pyrénéennes* 3, 16 p.

- Van Ouwerkerk, J. H. & Pette, D., 1965. Een berekeningsmethode voor stationaire en verzadigde grondwaterstromingen. Tijdschr. Kon. Ned. Heide Mij., p. 337—348.
- Williams, G. P., 1963. Evaporation from water, snow and ice. Techn. Paper 164 of the Div. of Building Research, Ottawa.
- Wilson, M. T. & Thomas, H. E., 1964. Hydrology and hydrogeology of Navajo Lake, Kane Country, Utah. Geol. Survey Prof. Paper 417-C, 26 p.
- Winter, E. J., 1962. Simple lysimeters and unusual rain gauges for horticultural research. Special Rept. SR 2, Water Res. Assoc.
- Zeilmaker, D. A., 1966. Hydrologische en meteorologische aspecten van het Valle de Aran (Hoge Pyreneeën). M.Sc. thesis, Geol. Inst., Leiden, pt. I & II, 96 + 40 p.

APPENDIX

TABLES 1—45

Table 2. Monthly precipitation (mm) at Viella (st. 2)

	jan.	febr.	march	april	may	june	July	aug.	sept.	oct.	nov.	dec.	year
'45									52.4	19.8	30.2	210.6	
'46	10.4	16.6	28.6	128.6	96.4	85.6	25.8	47.8	44.6	64.0	23.6	183.0	780.2
'47	37.6	68.6	69.3	15.3	174.2	21.8	72.8	71.6	67.8	85.0	61.0	101.0	846.0
'48	94.0	11.6	13.0	79.9	107.6	54.7	66.8	40.6	81.5	38.0	12.6	34.4	634.7
'49	49.7	12.1	87.0	44.2	66.2	96.3	60.2	57.2	82.7	29.7	142.1	107.1	834.5
'50	39.9	88.1	54.3	111.5	27.3	21.7	77.0	65.4	106.8	31.0	54.8	122.6	800.4
'51	98.3	68.1	107.2	44.0	216.5	118.5	29.0	121.5	67.0	59.6	171.5	82.5	1183.1
'52	65.0	141.4	60.1	88.6	41.3	56.4	86.6	61.6	31.6	88.0	107.2	123.8	951.6
'53	42.9	32.4	14.0	43.5	30.0	177.5	47.0	71.6	75.0	55.3	51.0	36.9	677.1
'54	60.5	71.0	73.0	44.0	115.5	84.0	53.0	62.0	88.0	60.0	48.0	106.0	865.-
'55	125.0	32.1	43.0	4.0	28.6	98.1	81.2	50.0	101.5	67.3	40.7	95.0	766.5
'56	88.4	32.6	44.6	70.6	171.8	77.6	105.5	118.9	90.1	23.7	84.0	19.0	926.8
'57	53.8	27.1	41.5	117.0	67.4	169.8	20.7	106.7	45.6	41.0	62.9	47.7	801.2
'58	58.2	38.9	119.5	66.3	73.4	67.1	65.7	73.1	53.1	59.2	78.7	147.7	927.9
'59	32.5	33.0	111.6	170.4	62.7	71.4	126.9	74.9	70.2	111.8	72.8	103.2	1041.4
'60	50.4	34.6	66.2	60.1	48.5	84.5	111.2	43.6	72.0	176.4	95.9	172.1	1015.5
'61	101.5	26.5	1.0	88.6	96.2	73.1	77.5	71.0	72.0	60.4	69.6	40.0	777.4
'62	85.7	101.8	52.0	84.7	87.6	28.5	54.5	25.3	74.8	41.5	125.0	97.5	858.9
'63	76.5	24.1	50.9	126.9	49.6	68.5	108.6	247.7	103.6	27.5	137.0	95.0	1115.9
'64	10.5	79.8	86.2	120.5	86.0	134.0	50.5	79.0	102.6	102.7	40.5	75.0	967.3
'65	76.5	40.0	47.0	71.6	84.5	52.0	44.5	67.6	177.0	63.7	164.6	177.0	1065.9

Table 3. Monthly precipitation (mm) at Artes (st. 3)

	jan.	febr.	march	april	may	june	july	aug.	sept.	oct.	nov.	dec.	year
'45									45.7	57.5	26.5	135.6	
'46	51.4	78.6	65.3	13.8	155.4	16.6	100.0	71.6	58.3	23.1	68.3	127.9	805.3
'47	96.7	19.8	14.0	82.0	100.0	70.6	49.2	38.1	117.5	46.4	6.2	21.0	661.6
'48	51.7	17.1	89.0	41.2	69.2	80.7	59.6	71.6	86.8	38.2	185.5	104.3	893.9
'49	43.0	97.9	63.0	166.0	38.8	29.8	81.7	83.8	121.6	41.8	70.3	189.1	1026.8
'50	122.1	100.5	125.2	45.9	221.1	128.0	31.0	158.0	42.0	68.8	183.1	89.0	1272.7
'51	88.5	200.0	55.0	95.3	58.0	76.0	122.8	92.2	36.5	119.5	136.0	138.0	1217.8
'52	54.8	60.0	9.0	42.7	52.0	167.3	27.4	93.0	91.2	67.0	81.0	48.0	793.3
'53	66.4	70.0	71.0	39.7	101.5	94.3	47.0	90.5	37.9	48.8	47.7	125.0	839.8
'54	120.0	41.0	44.0	10.0	32.8	98.0	68.0	53.0	104.0	64.0	37.0	112.5	760.4
'55	78.0	26.0	54.0	68.6	152.0	79.0	83.0	118.0	152.2	19.1	56.0	13.6	899.5
'56	47.8	37.1	39.7	111.3	69.6	168.9	19.1	104.9	35.0	48.2	63.1	37.3	782.0
'57	46.5	40.6	93.2	55.9	62.8	41.0	76.4	80.3	48.1	40.5	78.2	145.6	809.1
'58	23.9	30.4	92.2	192.8	40.1	80.8	103.1	72.4	76.4	105.4	49.1	118.3	984.9
'59	50.7	36.6	83.3	56.7	42.1	83.6	99.8	51.2	71.0	149.0	74.9	137.7	936.6
'60	79.2	29.5	0.5	87.0	75.8	76.2	46.6	79.2	91.0	103.6	74.0	32.0	774.6
'61	80.5	91.2	89.7	105.3	51.1	122.9	61.3	25.2	115.6	40.8	112.8	106.1	1002.5
'62	82.9	27.9	76.8	103.2	54.9	72.0	89.2	221.6	83.4	54.5	179.6	172.5	1218.5
'63	13.1	71.6	80.6	132.0	91.9	162.6	96.6	87.9	109.4	84.4	42.7	77.7	1106.3
'64	67.6	37.1	37.5	83.9	64.1	49.3	26.7	57.4	111.2	45.8	114.3	158.7	853.6

Table 4.

Monthly precipitation (mm) at Puerto de Bonaigua (st. 4)

	jan.	febr.	march	april	may	june	july	aug.	sept.	oct.	nov.	dec.	year
'49	44.5	27.4	89.6	68.0	154.1	115.5	43.5	85.7	138.2	51.5	205.8	131.0	1154.8
'50	54.0	62.3	52.8	176.5	60.2	44.2	96.1	112.6	114.1				
'51					218.5	121.0	49.0	152.6	112.1	121.0	200.5	59.5	
'52	101.6	155.0	111.5	124.1	57.5	87.0	65.0	109.0	38.5	155.0	192.0	150.5	1336.7
'53	74.6	40.0	24.0	71.5	64.5	221.5	44.0	138.0	104.6	98.0	86.0	71.5	1038.2
'54	39.0	84.5	139.0	109.6	202.0	155.0	88.0	92.5	95.5	83.5	65.0	180.1	1333.7
'55	94.1	75.1	61.0	12.0	41.1	160.1	91.5	72.0	129.0	175.0	39.2	154.0	1104.1
'56	216.0	63.0	126.0	155.0	152.0	116.5	54.0	124.0	134.0	65.0	85.5	23.0	1314.-
'57	99.0	48.0	38.0	188.0	143.0	214.0	47.0	141.0	57.0	68.0	71.0	47.1	1161.-
'58	60.5	35.0	202.0	154.0	60.2	92.0	72.0	57.5	44.5	60.5	155.6	179.0	1172.8
'59	36.5	80.0	180.0	146.0	99.0	116.5	87.0	120.0	93.5	125.6	72.0	115.0	1271.-
'60	96.0	71.0	106.0	101.0	65.0	123.0	145.6	82.4	120.4	305.4	137.4	209.0	1562.2
'61	98.0	28.0	4.0	175.0	128.0	165.0	60.6	71.8	78.0	112.5	100.8	49.0	1070.7
'62	102.0	211.0	92.0	110.0	79.0	124.0	36.0	35.0	114.0	69.0	185.0	237.0	1394.-
'63	106.6	69.0	101.0	154.0	97.0	105.3	153.0	210.0	121.0	75.0	181.2	86.0	1459.1
'64	35.0	83.0	103.0	110.4	103.4	124.2	86.1	76.1	137.3	81.0	93.6	80.0	1113.1
'65	70.7	61.8	57.2	183.6	94.7	62.8	61.0	65.4	171.9	106.9	175.2	166.4	1277.6

Table 5.

Monthly precipitation (mm) at Benos (st. 5)

	jan.	febr.	march	april	may	june	july	aug.	sept.	oct.	nov.	dec.	year
'55									124.7	62.2	42.0	112.8	
'56	89.1	38.5	51.6	78.3	175.5	66.4	65.5	80.5	80.0	31.4	79.7	19.4	855.9
'57	43.8	37.6	29.7	128.7	85.5	172.7	27.3	64.8	41.6	49.9	70.8	42.4	751.0
'58	74.2	31.6	120.4	76.2	68.0	51.3	58.8	59.5	54.0	55.3	92.5	128.9	870.7
'59	43.8	20.0	105.7	212.6	79.6	68.5	94.6	72.4	61.0	126.5	77.6	183.1	1145.4
'60	55.7	26.5	63.2	69.4	48.7	64.8	86.8	46.8	58.0	158.0	105.7	121.5	915.1
'61	116.9	38.5	1.5	100.6	74.5	93.3	69.6	55.5	39.0	108.7	59.8	31.3	789.2
'62	59.9	66.2	47.2	112.8	44.4	69.0	45.0	16.8	68.6	36.6	125.5	111.7	803.7
'63	37.5	24.2	89.5	89.5	53.1	71.6	85.9	164.9	69.0	25.5	102.5	68.5	881.7
'64	24.0	78.0	88.2	102.5	86.8	92.0	99.1	96.0	85.3	87.7	41.8	98.7	980.1
'65	93.0	31.7	57.5	104.2	83.9	35.3	36.0	66.0	111.8	57.7	137.5	193.0	833.9

Table 6.

Monthly precipitation (mm) at Camara Barrados (st. 6)

'56											103.0	25.4	
'57	56.3	37.8	35.2	138.5	128.0	202.4	41.5	92.7	60.9	53.1	80.5	36.6	963.5
'58	84.7	57.1	165.2	106.1	68.1	74.2	84.6	86.8	62.9	79.3	149.9	150.4	1169.3
'59	68.7	29.0	134.7	168.7	110.8	94.0	108.5	102.4	68.5	151.0	94.2	190.5	1321.-
'60	79.6	30.7	69.7	109.0	70.3	84.3	98.7	65.0	75.9	177.4	110.2	208.5	1179.3
'61	171.0	57.1	1.5	134.3	101.8	135.0	102.9	64.5	50.2	99.4	64.1	27.0	1008.8
'62	77.5	148.8	72.8	115.2	56.0	80.0							

Table 7.

Monthly precipitation (mm) at Tunnel Viella North (st. 7)

'55					43.8	179.7	99.4	72.1	116.1	144.7	66.3	182.2	
'56	133.0	59.1	142.4	159.8	206.1	123.2	140.0	192.7	161.2	42.8	100.5	27.4	1489.1
'57	52.7	46.5	81.1	148.0	102.4	252.9	34.3	94.1	58.0	70.6	93.1	87.9	1121.6
'58	64.8	79.1	230.4	109.1	97.1	100.3	81.3	138.0	90.1	78.9	88.2	226.3	1383.6
'59	71.3	34.8	282.0	201.0	89.7	121.8	113.0	110.2	87.1	122.5	127.4	150.3	1257.3
'60	113.4	121.6	135.3	81.6	106.5	142.9	157.4	69.3	130.5	541.5	182.0	184.0	1966.-
'61	108.0												

Table 8.

Monthly precipitation (mm) at Restanca (st. 8)

	jan.	febr.	march	april	may	june	july	aug.	sept.	oct.	nov.	dec.	year
'55							134.7	118.2	154.7	147.5	88.1	295.2	
'56	131.1	76.6	97.3	197.4	140.5	122.9	78.1	228.0	327.9	31.3	87.5	48.3	1566.9
'57	51.2	70.9	75.0	124.4	92.1	259.8	57.0	144.7	77.3	85.0	106.3	72.8	1216.5
'58	77.7	109.7	236.4	129.8	82.9	140.3	91.5	165.8	78.8	102.2	95.2	320.0	1630.3
'59	38.9	52.3	348.3	264.6	102.4	120.7	186.6	152.5	94.2	132.5	81.3	139.8	1714.1
'60	175.5	183.7	111.4	73.7	107.1	125.2	197.9	119.7	249.2	657.2	178.5	168.2	2347.3
'61	66.0	22.6	2.4	194.1	221.8	153.1	97.4	101.3	122.9	169.8	164.0	64.5	1379.9
'62	220.9	126.6	222.5	132.0	63.6	116.1	62.6	54.7	160.7	97.5	223.3	150.5	1631.0
'63	127.5	73.6	115.3	194.0	67.1	152.8	199.5	327.8	167.5	81.3	568.2	80.0	2154.6
'64	31.1	111.0	134.8	180.5	97.0	182.5	183.5	92.0	185.3	106.6	82.1	98.7	1485.1
'65	110.1	63.2	71.6	73.5	92.0	42.6	38.8	31.5	308.4	121.2	220.4	170.2	1343.5

Table 9.

Monthly precipitation (mm) at Camara Arties (st. 9)

'56		34.8	66.9	119.7	137.4	58.5	61.6	132.0	155.4	30.8	69.2	19.8	950.8
'57	69.0	38.4	34.9	118.0	80.2	172.2	16.9	110.4	37.6	57.5	64.2	40.5	839.8
'58	66.9	61.6	104.6	84.3	69.9	54.1	67.8	82.6	29.5	46.8	66.8	121.4	856.3
'59	37.1	27.8	150.6	134.1	57.6	81.9	129.5	85.0	84.2	89.4			

Table 10.

Monthly precipitation (mm) at Moncasau (st. 10)

'55								117.4	129.1	150.8	132.3	78.7	167.7
'56	112.0	81.0	62.3	166.1	117.1	96.0	93.9	193.6	210.9	36.2	113.5	40.8	1323.4
'57	91.5	43.5	44.3	129.6	107.7	241.9	53.8	140.8	54.0	60.4	98.9	73.4	1139.8
'58	99.6	114.1	139.9	119.2	90.3	141.0	93.5	130.2	86.9	93.3	108.1	152.1	1368.2
'59	38.5	29.1	207.2	247.0	92.1	113.6	150.6	122.7	133.2	125.7	66.7	99.3	1429.7
'60	108.1	155.6	88.2	58.2	88.7	183.2	198.4	121.7	186.1	467.1	127.0	157.8	1940.1
'61	59.1	22.8	1.0	140.8									

Table 11.

Monthly snowfall (cm) at Cledes (st. 1)

winter sept. oct. nov. dec. jan. febr. march april may june july aug. year

'47/48				18	14	1							33
'48/49							24	9					33
'49/50				9	26	23	7	15					80
'50/51													
'51/52		6		9	48	55		5					123
'52/53			6	25	60	38	1						130
'53/54					57	13							70
'54/55					10	7	3						20
'55/56				2		51	8						61
'56/57			16	1	47	1							65
'57/58			10	1	9	8	26	2					56
'58/59				8									8
'59/60				2	26	1							29
'60/61				75	21								96
'61/62		1	2			29	1	8					41
'62/63			2	5	1	3	3	1					57
'63/64				3	9		3						15
'64/65				23	22	24							69

Table 12.

Monthly snowfall (cm) at Viella (st. 2)

'46/47			63	35	38							136
'47/48			5									5
'48/49				7		7	5	1				20
'49/50		6	30	45	19	3	7					110
'50/51												
'51/52	4		18	42	73		2					139
'52/53		21	57	61	38		2	5				181
'53/54			12	72	32	3	4	5				128
'54/55				33	12	8						53
'55/56			11	16	45	1	18	7				98
'56/57	20	27	6	49	5		5					107
'57/58		24	3	50	33	30	24					164
'58/59		4	20	4	17	1	1					47
'59/60	4		28	32	2		2					68
'60/61		2	182	80								264
'61/62	20	7	2	8	88	4	23					152
'62/63		13	45	14	16	34	16					138
'63/64		3	9	10	3	18						43
'64/65		3	52	60	49	13						177

Table 13.

Monthly snowfall (cm) at Arties (st. 3)

winter sept. oct. nov. dec. jan. febr. march april may june july aug. year

'52/53			36	70	52	47	3		1				209
'53/54				13	86	51	7	2	8				165
'54/55					40	10							50
'55/56				3	29	51	5	30	20				138
'56/57	10	61	7	63	11			20					172
'57/58		64	16	82	44	36	44						286
'58/59		13	44	27	33	17	2						136
'59/60	18	3	92	40	11	4	26						194
'60/61		6	182	82	6								276
'61/62	20	17	9	27	117	10	30	1					231
'62/63		5	45	59	32	40	71	8					260
'63/64			8	39	17	7	28	2					101
'64/65		2	2	11	12	7	5	3					270

Table 14.

Monthly snowfall (cm) at Puerto de Bonaigua (st. 4)

'48/49		10	5	40	85	28	123	29	33	7			410
'49/50			82	145	46	79	43	115	4				514
'50/51													
'51/52		85	88	83	147	120	13	95	15				646
'52/53		16	136	186	135	84	27	26	15	17			642
'53/54		12	10	73	184	82	89	52	92				594
'54/55		23	21	63	138	112	35	4					396
'55/56		12	38	94	158	175	97	136	100	36			846
'56/57		42	161	34	124	48	25	144	29	24			631
'57/58		32	82	72	117	32	180	141	4	3	4		707
'58/59		16	93	163	59	80	116	129	12				668
'59/60		85	94	283	137	76	105	117	1				898
'60/61	6	45	72	356	115	17	3	83	12	16			725
'61/62		59	57	53	122	266	69	90	20	29			765
'62/63	2	36	156	189	101	92	170	86	25				857
'63/64	3	25	119	131	105	116	142	45					686
'64/65		96	44	179	146	117	75	124	24	3			808

Table 15.

Monthly snowfall (cm) at Bonos (st. 5)

winter sept. oct. nov. dec. jan. febr. march april may june july aug. year

'52/53			10	51	66	37	2						166
'53/54				2	61	28							91
'54/55					10	7	5						22
'55/56				12	17	63		6					98
'56/57		1	29	2	42	5		1					80
'57/58			36	4	53	20	20	16					149
'58/59			6	12	9	7							34
'59/60				32	34	2							68
'60/61				110	70								180
'61/62		3	8	2	5	68	28						114
'62/63			13	40	7	21	24	1					106
'63/64			1	7	7	1	7						23
'64/65		7	2	46	47	49	5	1					157

Table 16.

Monthly snowfall (cm) at Camara Barrados (st. 6)

'56/57		22	105	15	61	38		53					294
'57/58			94	17	117	58	34	75	1				396
'58/59			20	73	29	22	16	47					207
'59/60		40	5	132	46	10	20	37					290
'60/61		1	16	152	97	18							284
'61/62		20	20	12	37	158	13	20	3				283

Table 17.

Monthly snowfall (cm) at Tunnel Viella North (st. 7)

'56/57		15	91	13	68	42		45					274
'57/58			77	50	87	35	57	53					349
'58/59			26	69	45	45	45	15					245
'59/60		16	11	106	33	29	32	37					264
'60/61			12	142	130	33							317

Table 18.

Monthly snowfall (cm) at Restanca (st. 8)

winter	sept.	oct.	nov.	dec.	jan.	febr.	march	april	may	june	july	aug.	year
'55/56		3	26	115	71	188	128	124	10	45			710
'56/57		40	124	54	72	80	37	145	26	12			590
'57/58		23	115	96	124	78	152	154	18				760
'58/59		2	55	146	70	69	106	121	3				572
'59/60		55	86	177	103	73	96	79					669
'60/61	1	25	48	260	115	20	3	33	13	4			552
'61/62		47	44	54	84	193	81	136	10	7			656
'62/63	2	12	155	164	68	98	114	67	20				700
'63/64	2	10	104	109	51	90	116	50					532
'64/65		108	37	139	140	90	69	42	29	1			655

Table 19.

Monthly snowfall (cm) at Camara Arties (st. 9)

'55/56	*		12/1/56*	92	110	74	95	88	22			481*
'56/57	29	137	40	149	31	7	122	11	7			533
'57/58	20	110	81	137	80	121	100	6				655
'58/59		41	112	82	54	112	100	12				523

Table 20.

Monthly snowfall (cm) at Moncasau (st. 10)

'55/56		4	22	122	110	203	65	121	84	44		775
'56/57		56	173	72	144	68	19	164	34	31		761
'57/58		34	132	106	155	125	160	142	16			860
'58/59		8	75	153	77	58	124	172	8			675
'59/60		76	62	177	143	119	63	78	2			720
'60/61	5	25	59	267	96	18	1	30	8			509

Table 21.

Monthly snowfall (cm) at Bosost (st. 11)

'56/57		1	16	2	44	2		1				66
'57/58			25	1	23	14	31	4				98
'58/59			3	5	2	3						13
'59/60				11	26	1						38
'60/61				93	27							120
'61/62		1	4			37	1	10				53
'62/63			4	40	3	11	20	1				79
'63/64				3	7		6					16
'64/65				26	32	34	2					94

Table 22. Average monthly temperatures in °C (1955-1965)

station	jan.	febr.	march	april	may	june	july	aug.	sept.	oct.	nov.	dec.	year
Cledes	3.2	4.1	7.7	8.7	12.4	14.8	17.3	16.7	15.8	11.1	6.5	3.8	10.2
Viella	2.6	3.3	7.3	8.2	12.7	15.3	18.2	17.5	15.2	11.0	6.1	3.1	10.2
Arties	1.8	2.0	5.9	6.6	11.3	14.2	17.0	16.4	15.2	10.1	4.7	1.9	9.0
Restanca	-3.5	-4.0	-1.0	-0.2	4.9	8.2	11.1	11.0	9.4	4.5	-0.5	-3.5	3.1
Bonaigua	-4.0	-4.0	-1.6	-1.3	3.6	6.9	10.1	10.0	8.1	2.8	-1.4	-3.6	2.2

Table 23. Average monthly maximum temperatures in °C (1955-1965)

Cledes	8.7	10.4	14.2	14.4	18.8	21.0	23.4	23.4	22.4	17.6	12.0	9.0	16.3
Viella	7.6	9.3	13.4	13.8	19.3	21.8	25.0	24.7	22.9	17.2	11.2	7.6	16.2
Arties	5.9	7.0	11.1	11.3	16.7	19.4	22.7	22.1	20.9	15.3	8.9	5.8	14.0
Restanca	0.3	0.2	3.2	3.9	9.2	12.4	15.7	15.5	13.5	8.3	2.9	-0.2	7.1
Bonaigua	0.3	0.5	3.0	2.4	7.3	10.9	14.6	14.5	12.2	6.2	2.0	0.1	6.2

Table 24. Average monthly minimum temperatures in °C (1955-1965)

Cledes	2.3	2.3	1.1	2.9	5.9	8.6	11.1	10.0	9.2	4.6	0.9	1.4	4.0
Viella	2.3	2.6	1.2	2.5	6.1	8.8	11.3	10.5	7.4	4.8	1.0	1.4	4.1
Arties	2.4	3.1	0.7	1.9	5.9	9.0	11.2	10.6	9.4	4.8	0.5	2.1	3.9
Restanca	-7.2	-8.2	-5.2	-4.3	0.6	3.9	6.5	6.4	5.2	0.6	-3.9	-6.7	-1.0
Bonaigua	-8.2	-8.5	-6.3	-5.1	-0.2	2.9	5.6	5.4	4.0	-0.6	-4.8	-7.3	-1.9

Table 25. Average monthly temperature amplitudes in °C (1955-1965)

	jan.	febr.	march	april	may	june	july	aug.	sept.	oct.	nov.	dec.	year
Cledes	11.0	12.7	13.1	11.1	12.9	12.4	12.3	13.4	13.2	13.0	11.1	10.4	12.3
Viella	9.9	11.9	12.2	11.3	13.2	13.0	13.7	14.2	15.5	12.4	10.2	9.0	12.1
Arties	8.3	10.1	10.4	9.4	10.8	10.4	11.5	11.5	11.5	10.5	8.4	7.9	10.1
Restanca	7.5	8.4	8.4	8.2	8.6	8.5	9.2	9.1	8.3	7.7	6.8	6.5	8.1
Bonaigua	8.5	9.0	9.3	7.5	7.5	8.0	9.0	9.1	8.2	6.8	6.8	7.4	8.1

Table 26. Average monthly temperature gradients in °C/100 m (1955-1965)

station	jan.	febr.	march	april	may	june	july	aug.	sept.	oct.	nov.	dec.	year
Cledes/Viella	0.21	0.28	0.14	0.18	-0.11	-0.18	-0.32	0.28	0.21	0.04	0.14	0.25	-
Viella/Arties	0.39	0.63	0.68	0.78	0.68	0.53	0.58	0.53	~	0.53	0.68	0.58	0.58
Arties/Rest.	0.63	0.71	0.82	0.80	0.76	0.71	0.70	0.64	0.69	0.60	0.62	0.64	0.70
Rest./Bon.	0.56	-	0.89	1.00	1.45	1.45	1.22	1.11	1.45	1.89	1.00	0.11	1.00
Arties/Bon.	0.62	0.64	0.80	0.84	0.82	0.78	0.74	0.69	0.76	0.78	0.65	0.59	0.73

Table 27. Average monthly number of frost days, with minimum temperatures below 0°C (1955-1965)

station	sept.	oct.	nov.	dec.	jan.	febr.	march	april	may	june	july	aug.	year
Cledes		1.6	11.0	17.7	19.5	18.5	9.1	2.9	0.4				80.7 (22%)
Viella		1.5	10.0	15.3	18.3	17.1	8.7	4.8	0.4				76.1 (21%)
Arties		2.4	11.1	17.8	18.9	17.9	9.7	5.6	0.3				83.7 (23%)
Restanca	4.2	12.7	23.6	28.7	28.7	26.2	27.0	24.9	11.3	4.2	0.7	1.6	193.8 (53%)
Bonaigua	2.9	14.7	26.0	29.6	30.6	27.3	29.2	26.8	15.7	6.1	0.7	0.8	210.4 (58%)

Table 28. Average monthly number of ice days, with maximum temperatures below 0°C (1955-1965)

	jan.	febr.	march	april	may	june	july	aug.	sept.	oct.	nov.	dec.	year
Cledes					0.9	1.3	1.4	0.1					3.7
Viella					1.5	1.8	2.1	0.3					5.7
Arties				0.3	2.5	2.6	3.8	0.7					10.0
Restanca	0.2	2.1	6.6	13.7	13.2	12.2	7.2	5.9	0.4	0.1			61.6
Bonaigua	0.1	3.7	9.3	13.2	13.2	13.2	7.5	9.7	1.7	0.2			71.0

Table 29. Average monthly number of precipitation days (1955-1965)

station	jan.	febr.	march	april	may	june	july	aug.	sept.	oct.	nov.	dec.	year
Cledes	10.3	7.3	9.8	15.7	11.7	12.2	9.9	9.2	10.0	9.1	11.3	11.3	127.8 (35,0%)
Viella	11.0	7.9	10.8	15.6	11.1	12.1	9.2	9.9	10.3	9.8	11.9	12.3	131.9 (36,2%)
Arties	10.9	8.6	11.5	15.0	11.3	12.0	10.1	10.0	11.3	10.3	11.8	13.6	136.4 (37,4%)
Restanca	11.5	9.9	12.9	15.6	12.8	15.1	11.8	10.9	12.4	11.6	12.1	13.7	150.3 (41,2%)
Bonaigua	12.1	10.0	12.5	16.0	11.7	13.4	10.1	9.8	11.3	11.1	13.1	13.7	144.8 (39,6%)

Table 30. Average monthly number of snow days (1955-1965)

	jan.	febr.	march	april	may	june	july	aug.	sept.	oct.	nov.	dec.	year
Cledes	2.7	2.2	1.1	0.6	0.1					0.1	0.6	2.9	10.3
Viella	4.2	4.5	1.9	1.8	0.5					0.5	1.5	4.6	19.5
Arties	6.6	5.2	3.4	2.6	0.2					0.8	3.1	6.3	28.2
Restanca	10.3	9.1	9.7	10.3	2.4	0.9			0.2	3.4	8.1	11.7	66.1
Bonaigua	10.7	9.3	10.1	12.0	3.3	1.5	0.1		0.4	4.6	8.6	11.8	72.4

Table 31. Average monthly cloud cover in percentage (1955-1965)

station	jan.	febr.	march	april	may	June	July	aug.	sept.	oct.	nov.	dec.	year
Cledes	37	38	42	58	47	47	47	42	43	37	44	43	44
Viella	45	40	46	64	46	48	45	41	42	41	48	52	46
Arties	41	43	50	62	49	48	44	44	46	45	49	49	47
Restanca	39	41	51	60	50	45	42	41	45	44	48	47	46
Bonaigua	44	45	54	59	49	45	39	39	48	50	54	51	48

Table 32. Average monthly number of cloudless days (0-1/10) 1955-1965

Cledes	17.5	15.2	14.6	8.8	11.1	10.8	12.1	13.6	13.6	15.3	13.1	14.3	159.1
Viella	15.0	14.5	13.8	7.1	11.0	11.8	14.1	14.9	13.4	15.0	12.6	12.5	155.7
Arties	16.3	14.0	12.0	7.7	11.0	11.2	13.6	14.1	12.7	14.2	12.1	13.9	152.8
Restanca	17.4	15.0	12.4	8.8	11.0	13.2	14.1	14.3	13.0	14.7	12.6	14.6	161.1
Bonaigua	14.3	11.8	8.4	7.4	10.4	11.1	13.8	13.5	10.2	11.5	10.2	12.4	135.0

Table 33. Average monthly number of clouded days (9/10-10/10) 1955-1965

Cledes	9.2	8.3	9.5	13.6	10.3	10.1	10.9	8.4	9.3	8.2	9.6	10.9	118.3
Viella	11.9	9.0	10.8	15.7	10.0	10.7	10.9	9.6	9.6	9.8	11.6	13.4	133.0
Arties	10.9	9.7	12.0	14.9	10.6	10.2	10.1	10.2	10.5	10.8	11.5	13.3	134.7
Restanca	10.3	9.5	12.8	14.9	10.7	9.2	9.4	8.9	10.0	10.8	11.1	12.9	130.5
Bonaigua	10.3	8.3	10.9	11.4	7.4	6.6	5.8	5.2	7.3	9.7	11.6	12.0	106.5

Table 34. Average monthly number of clouded days (1/10-9/10) 1955-1965

Cledes	4.3	4.5	6.9	7.6	9.6	9.1	8.0	9.0	8.0	7.5	7.4	5.8	87.6
Viella	4.1	4.5	6.4	7.2	10.0	7.5	6.0	6.5	7.0	6.2	5.8	5.1	76.3
Arties	3.8	4.3	7.0	7.4	9.4	8.6	7.3	6.7	6.8	6.0	6.4	3.8	77.6
Restanca	3.3	3.5	5.8	6.3	9.3	7.6	7.5	7.8	7.0	5.3	6.3	3.5	73.4
Bonaigua	6.4	7.9	11.7	11.2	12.2	12.3	11.4	12.3	12.5	9.8	8.2	6.6	123.5

Table 35. Average monthly number of days with northern winds (1955-1965)

station	jan.	febr.	march	april	may	june	july	aug.	sept.	oct.	nov.	dec.	year
Cledes	7.0	6.6	7.7	10.2	9.1	9.4	11.5	11.0	9.2	8.5	5.9	6.7	102.8
Viella	6.8	5.6	6.5	9.7	8.8	9.6	12.4	11.4	8.1	7.4	6.9	6.1	99.3
Arties	1.2	1.7	1.8	2.4	3.2	3.2	1.9	2.1	1.7	2.7	2.3	2.1	26.3
Restanca	8.2	5.8	7.4	12.1	8.1	5.5	7.3	5.6	3.8	8.3	8.3	7.6	88.0
Bonaigua	17.7	16.2	16.1	18.8	17.4	15.7	15.0	15.1	14.1	15.3	17.4	18.8	194.6

Table 36. Average monthly number of days with eastern winds (1955-1965)

Cledes	0.1	10.6	12.3	12.0	13.6	11.2	12.0	10.9	0.3	0.1	0.1	0.2	0.8
Viella	9.4	19.9	19.9	13.9	16.4	16.1	17.4	17.4	11.0	12.1	11.2	11.8	138.1
Arties	21.7	4.8	3.2	3.1	5.4	5.8	7.0	5.3	16.3	18.6	19.8	19.9	217.3
Restanca	4.2	10.5	13.0	8.7	10.9	11.2	11.2	11.9	5.6	4.7	4.2	5.6	58.5
Bonaigua	11.1	10.5	13.0	8.7	10.9	11.2	11.2	11.9	11.6	12.5	9.8	11.0	133.4

Table 37. Average monthly number of days with southern winds (1955-1965)

Cledes	11.4	9.7	9.2	4.8	4.3	4.2	3.8	4.5	5.9	6.7	8.7	9.7	82.9
Viella	14.0	11.8	11.9	7.9	7.9	8.7	6.2	8.5	9.9	10.6	11.0	12.1	120.5
Arties	0.3	0.3	0.6	0.1	0.2	0.7	0.2	0.7	0.9	0.4	0.6	0.6	5.
Restanca	18.3	17.4	20.3	14.2	17.7	18.4	16.6	20.0	20.3	17.8	17.3	17.6	215.9
Bonaigua	1.1	0.8	0.8	1.4	1.8	1.5	3.1	2.6	2.7	2.5	1.9	0.5	20.7

Table 38. Average monthly number of days with western winds (1955-1965)

station	jan.	febr.	maarch	april	may	june	july	aug.	sept.	oet.	nov.	dec.	year
Cledes	12.3	10.8	13.6	14.9	17.2	16.2	15.2	15.4	14.5	15.5	15.0	14.0	174.6
Viella	0.8	0.2	0.2	0.4	0.6	0.5	0.4	0.5	0.9	0.8	0.9	0.9	7.1
Arties	7.4	6.0	8.6	13.3	10.8	9.7	11.6	10.3	10.9	8.9	7.8	8.1	113.4
Restanca	0.2			0.2	0.1	0.1			0.1		0.1		0.8
Bonaigua	0.4	0.4	1.0	1.0	0.7	1.5	1.2	1.3	1.5	0.7	0.6	0.2	10.5

Table 39. Average monthly number of days with unknown wind-direction (1955-1965)

Cledes	0.2	0.2	0.5	0.2	0.3	0.1	0.4		0.2	0.2	0.3	0.4	2.9
Viella													
Arties	0.3	0.3	0.2	0.2	0.3	0.3	0.3	0.4	0.2	0.4	0.2	0.3	3.4
Restanca	0.1		0.1	0.4	0.1	0.2	0.1	0.1	0.2	0.2	0.1	0.2	1.8
Bonaigua	0.7	0.3	0.1	0.1	0.2	0.1	0.5	0.1	0.1	0.1	0.3	0.5	3.0

Table 40. Average monthly wind velocity (U_2) during the period 1955-1965.

Station	jan.	febr.	maart	april	mei	juni	juli	aug.	sept.	oet.	nov.	dec.
Cledes	3,1	3,0	2,8	2,5	1,8	1,7	1,8	2,0	2,0	2,3	2,7	2,8
Viella	3,1	3,0	2,8	2,5	1,8	1,7	1,8	2,0	2,0	2,3	2,7	2,8
Arties	3,1	3,0	2,8	2,5	1,8	1,7	1,8	2,0	2,0	2,3	2,7	2,8
Restanca	4,7	4,5	4,3	3,9	3,3	3,1	3,3	3,6	3,5	3,8	4,2	4,3
Bonaigua	4,1	4,5	3,9	3,6	3,0	2,7	2,8	2,7	2,8	3,2	3,5	3,8

Table 41. Average monthly runoff (mm) of the Inola river (st. 6)

	sept.	oct.	nov.	dec.	jan.	febr.	march	april	may	june	july	aug.	year
1947	31	22	32	39	58	50	158	214	271	165	108	165	1313
1948	105	86	107	56	-	-	-	-	-	-	-	-	-
1949	-	-	-	-	29	25	45	157	166	128	52	40	-
1950	35	23	39	31	64	61	83	76	544	332	140	82	1510
1951	81	55	50	38	80	57	126	239	366	391	197	92	1772
1952	83	82	168	79	72	68	262	339	390	356	118	76	2093
1953	55	98	94	85	51	40	115	146	544	291	87	78	1684
1954	45	92	139	50	35	46	113	143	243	126	90	98	1220
1955	78	69	51	216	127	54	53	240	118	115	72	48	1241
1956	51	45	35	58	41	25	27	64	287	217	49	58	957
	63	63	79	73	62	47	109	198	326	236	101	82	1419

Table 42. Average monthly runoff (mm) of the Barrados river (st. 16)

	sept.	oct.	nov.	dec.	jan.	febr.	march	april	may	june	july	aug.	year
1947	50	47	45	48	53	47	75	172	311	217	103	64	1232
1948	54	101	114	75	82	77	137	114	288	204	93	58	1397
1949	129	67	63	53	47	25	62	153	134	87	64	56	940
1950	55	58	148	144	93	91	132	176	362	323	152	76	1810
1951	88	61	160	90	85	79	125	189	324	460	242	185	1988
1952	112	107	172	112	99	157	236	404	434	343	149	88	2413
1953	53	147	131	142	90	84	125	187	424	353	179	97	2012
1954	57	77	130	59	55	63	100	135	359	323	162	65	1585
1955	83	85	84	145	146	101	97	182	243	136	96	65	1463
1956	107	149	90	87	96	59	71	110	357	407	265	129	1927
	79	90	114	95	84	78	116	182	314	285	151	88	1676

Table 43. Average monthly runoff (mm) of the Negro river (st. 13)

	sept.	oct.	nov.	dec.	jan.	febr.	march	april	may	june	july	aug.	year
1947	85	83	65	82	66	69	173	119	251	153	90	78	1314
1948	71	79	76	82	92	83	81	121	297	242	148	79	1454
1949	112	79	62	68	74	50	70	91	98	123	84	70	981
1950	84	73	126	103	69	59	79	107	294	163	77	69	1303
1951	82	76	118	74	95	82	176	219	360	486	321	274	2363
1952	187	168	223	136	119	117	193	295	369	335	206	121	2469
1953	124	147	198	221	93	57	76	134	212	199	182	77	1720
1954	80	84	88	89	93	85	119	136	274	312	249	165	1784
1955	152	120	103	116	121	86	107	161	184	194	112	68	1524
1956	79	124	116	125	150	102	118	157	316	193	191	141	1812
	106	103	117	109	97	79	119	154	266	240	166	114	1672

Table 44. Average monthly runoff (mm) of the Garona de Ruda river (st. 2)

1947	58	58	61	60	57	48	112	144	132	97	73	54	954
1948	48	56	54	53	52	47	71	91	123	85	87	64	831
1949	75	65	49	60	65	57	66	89	114	131	78	89	938
1950	95	78	81	86	82	68	95	113	284	261	133	121	1497
1951	97	80	122	89	80	69	141	193	240	430	246	170	1957
1952	147	139	206	115	81	85	106	168	199	223	133	87	1689
1953	95	134	104	109	78	60	73	121	201	177	139	102	1393
1954	85	93	89	111	65	54	69	98	216	295	204	92	1471
1955	83	75	76	94	97	78	96	133	198	123	88	82	1223
1956	82	91	80	98	78	63	70	96	299	276	182	117	1532
	98	99	108	100	80	68	93	132	234	255	160	110	1537

Table 45.

maand	Precipitation in mm of the stations:					Monthly precipitation coefficients of the stations:				
	Cledes	Viella	Arties	Bonaigua	Restanca	Cledes	Viella	Arties	Bonaigua	Restanca
jan.	66	66	67	83	103	0,86	0,88	0,85	0,80	0,71
febr.	48	51	62	75	89	<u>0,64</u>	<u>0,68</u>	<u>0,79</u>	<u>0,71</u>	<u>0,61</u>
mrt.	56	60	66	94	141	0,73	0,81	0,85	0,90	0,98
apr.	88	76	81	127	156	1,14	1,02	1,04	1,22	1,07
mei	95	86	81	107	107	1,23	1,15	1,04	1,02	0,73
juni	91	82	89	126	142	1,18	1,09	1,14	1,21	0,98
juli	65	71	68	75	132	0,85	0,94	0,87	0,72	0,91
aug.	78	79	87	103	154	1,02	1,06	1,11	0,88	1,06
sept.	83	80	82	106	173	1,07	1,07	1,05	1,01	1,19
okt.	72	64	63	110	173	0,93	0,86	0,81	1,05	1,19
nov.	81	82	84	128	189	1,05	1,10	1,08	<u>1,22</u>	<u>1,30</u>
dec.	102	100	107	121	161	<u>1,33</u>	<u>1,33</u>	<u>1,37</u>	1,21	1,10
jaar-totaal	925	897	937	255	17201					
maand-gem.	77	75	78	105	145	1,-	1,-	1,-	1,-	1,-